Characterisation of a maize mutant deficient in antifungal kauralexin accumulation

Dissertation submitted in fulfilment of the requirements for the degree of

Master of Science

Molecular and Cell Biology

The University of Cape Town

Sara Wighard

March 2017

Supervisor: Dr Shane Murray

Co-supervisor: Dr Jeanne Korsman

Plagiarism Declaration

I, **Sara Wighard**, know that plagiarism is wrong. Plagiarism is to use another's work and pretend that it is one's own. Each contribution to, and quotation in, this project from the work(s) of other people has been attributed, and has been cited and referenced. This is my own work. I have not allowed, and will not allow, anyone to copy my work with the intention of passing it off as his or her own work.

Signature Signed by candidate Date: 13/05/17

Acknowledgments

I would like to thank my supervisor, Dr Shane Murray. We've been down this path for a few years now and I've always felt grateful and, not to mention, supremely lucky to have you as my supervisor. Thank you for always being happy to help out, even when I've popped into the office for a silly question. Your willingness and genuine care doesn't go unnoticed and I will truly miss having you as my primary academic caretaker.

A big thank you to my co-supervisor, Dr Jeanne Korsman, who has always been willing to help out, despite her many, many students. Jeanne, all I can say is: Your weirdness is only matched by your kindness.

And, of course, thanks to all of lab 227 (RIP). Short-lived but never forgotten. Amy, Jean, Nina and Nads. I really enjoyed our lab environment and how everyone is always friendly, helpful and supportive. It's easy to take it for granted, but I appreciate it. I'll try keep stocking the office with Bounty sweets.

I'd like to thank everyone in MCB who was happy to lend a helping hand in bringing this dissertation to fruition, as well as everyone who helped in my education, starting with the techniques course in Honours. Not only did I learn so much, I was lucky enough to be partnered up with 2 people who'd become two of my closest friends. TJ, I'll always cherish our friendship and the trust we share; thanks for being you. Gertrud, through the years we've gradually snuck up a pretty special friendship. You're better at WKOB than anyone else which says it all. Aitäh.

For all their professional help, thanks to the Ac/Ds Tagging Facility for the transposon-seeds and, in particular, Dr Erica Unger-Wallace who not only answered replied to emails from a stranger but really helped me out. Thank you also to Dr Shawn Christensen at the USDA for the metabolite analysis.

I'd also like to acknowledge the NRF-Thutuka and the MCB EDP for the funding.

Finally, I'd like to thank my family who have always supported me and who I know always will. I'm really grateful for it and everyone. If this dissertation is for anyone it's for Cassius, my companion for 11 years. Miss you, boy.

Abstract

Fusarium verticillioides and *Cercospora zeina* are two economically important fungal pathogens of maize in Southern Africa. Phytoalexins are low molecular weight anti-microbial compounds produced in plants in response to pathogen infection. In maize, two classes of non-volatile terpenoid phytoalexins, viz. kauralexins and zealexins, play a role in fungal resistance. It has previously been shown that maize lines inoculated with either *F. verticillioides* or *C. zeina* induces kauralexin and zealexin accumulation. In addition, kauralexin metabolite accumulation and candidate kauralexin biosynthetic gene expression were highly correlated. In this study a mutant line with a *Dissociation* transposon element inserted into *An2* was identified with the goal of stopping *An2* from being expressed. The mutants were maintained in an inbred W22 maize line. Gene expression was compared between transposon-insertion mutants and wild type W22 at the seedling stage. A *F. verticillioides* and *C. zeina* inoculation assay was carried out on a segregating knock-down line. Phytoalexin accumulation, gene expression and disease susceptibility were subsequently examined in the mutants and wild type. *F. verticillioides*-inoculated mutants displayed significantly decreased kauralexin and zealexins accumulation and *An2* gene expression. Fungal load and symptoms was greater in mutants than wild type controls. Kauralexin accumulation and *An2* expression were negatively correlated with the quantified fungal load. *C. zeina*-inoculated mutants did not display significantly reduced kauralexin accumulation and *An2* expression as *An2* did not appear to be up-regulated in the W22 maize line in response to *C. zeina*. This is likely due to a genetically-controlled leaf flecking phenotype in W22 leading to broad-spectrum resistance, as well as potentially impacting the jasmonic acid pathway. Lastly, an attempt was made to clone *An2* towards *A. thaliana* transformation for overexpression analysis. Only a truncated section of *An2* was able to be cloned into the expression vector.

List of Abbreviations

°C	degrees Celcius
Ac	*Activator*
An2	*ent-copalyl diphosphate synthase*
ANOVA	Analysis of Variance
BLAST	Basic Local Alignment Search Tool
bp	base pair(s)
BX	benzoxazinoid
cDNA	complementary deoxyribonucleic acid
cm	centimetre(s)
cpr1	cytochrome P450 reductase 1 gene
DIMBOA	2,4-dihydroxy-7-methoxy-1,4-benzoxazin-3-one
DNA	deoxyribonucleic acid
dpi	days post inoculation
Ds	*Dissociation*
EF1α	*elongation factor 1 α*
ET	ethylene
ETBR	ethidium bromide
ETI	effector-triggered immunity
ETS	effector-triggered susceptibility
FW	fresh weight
g	gram
GA	gibberellin
GC-MS	gas chromatography–mass spectrometry
GLS	grey leaf spot
hr	hour
JA	jasmonic acid
kb	kilobase(s)

KO	*kaurene oxidase*
KS	*kaurene synthase*
L	litre(s)
LB	Luria Bertani
LBA	Luria Bertani Agar
LRR	leucine-rich repeat
m	metre(s)
MAP	mitogen-activated protein
MBOA	6-methxy-benzoxazolin-2-one
ml	millilitre(s)
mM	millimolar
MS	Murashige and Skoog
Mt	metric ton(s)
NB	nucleotide binding
NCBI	National Centre for Biotechnology Information
ng	nanogram(s)
NMR	nuclear magnetic resonance
PAMP	pathogen-associated molecular pattern
PCR	polymerase chain reaction
PRR	pattern recognition receptor
PTI	PAMP-triggered immunity
QDR	quantitative disease resistance
QRL	quantitative resistance loci
QTL	quantitative trait loci
qPCR	quantitative polymerase chain reaction
R	resistance
RIL	recombinant inbred line(s)
RNA	ribonucleic acid
RNAi	RNA interference

RT-qPCR	quantitative reverse transcription polymerase chain reaction
s	second(s)
SA	salicylic acid
SAR	systemic acquired resistance
sd	standard deviation
TBE	tris base, boric acid and EDTA
TPS	terpene synthase
µg	microgram(s)
µl	microliter(s)
µmol	micromole
V3	vegetative stage: leaf three fully developed
w/v	weight per volume

Table of Contents

List of Figures

List of Tables

Chapter 1: Introduction and Literature Review

1.1. Introduction

Food demands are rising worldwide; at the current rate food production would have to increase by 50% to feed the world in 2050 (Chakraborty & Newton, 2011). These food security problems are exacerbated by climate concerns. Undesirable weather conditions such as drought lead to resources being pulled to withstand water stress resistance, thereby increasing susceptibility to other forms of attack, including pathogens. Overall, the cereal crops maize, wheat and rice, provide the bulk of plant food for human consumption (faostat3.fao.org). However, they are at risk to infection by a wide range of pathogens which could reduce yield loss. Approximately 10–16% of global crop preharvest is lost annually to plant diseases (Oerke, 2006), and there are further postharvest losses of around 6-12%, with developing countries in particular losing out (Agrios, 2005).

Maize (*Zea mays* L.) is the prominent cereal crop in Africa, and finding means of increasing production is critical. It is particularly important in South Africa, where it is the largest locally produced field crop with production averaging around 10,2 Mt a year over the past ten years (faostat3.fao.org) and a gross value of R25 000 million (South Africa Yearbook 2015/2016: Agriculture). It is the major food source for most low-income communities (Shiferaw et al., 2011), who would struggle economically to find alternative food sources. Maize is also a major source for animal feed – constituting on average 55% of animal feed produced in South Africa (South Africa Yearbook 2014/2015: Agriculture) - and is increasingly used in biofuel production (Shiferaw et al., 2011). Harmful maize diseases could potentially have devastating impacts on the economy and agriculture in South Africa, as well as limiting affordable and abundant food for the impoverished. Higher temperatures and increased droughts are expected in the coming future with worldwide maize yield expected to be reduced by up to 10% by 2050 (Hellin et al., 2012) – with sub-Saharan Africa particularly vulnerable (Lobell et al., 2011). Approximately a quarter of maize in the region was estimated to be under drought stress already in a 1998 study (Heisey & Edmeades, 1998). Finding means of reducing yield loss is thus of extreme importance.

Fungal pathogen attack on maize is a major contributor to yield loss. Two of the most harmful fungal pathogens, *Fusarium verticillioides* and *Cercospora zeina*, have had damaging impacts

on crops in Sub-Saharan Africa. *F. verticillioides* can be found in nearly every maize harvest (Oren et al., 2003) and is a producer of toxic compounds that are linked to cancer and provide an additional food safety risk (Boutigny et al., 2012), while *C. zeina* has led to yield losses of up to 60% (Ward et al., 1999). Fungicides are often used to control the diseases caused by these pathogens, however, the use of them is costly, particularly for small-scale farmers. The more frequently fungicides are used, the greater the risk of the pathogens becoming resistant. Increased fungicide use has led to increased outbreaks in some areas (Oerke, 2006). Frequent use of fungicides also has a harmful impact on the environment. As a result of this, the need for less toxic fungicides has increased (Agrios, 2005). A cost-effective method of increasing pathogen defence is developing robust host plant resistance (Ward et al., 1999). Examining disease resistance mechanisms used in maize and subsequently implementing these in breeding programmes is a potential solution. Favourable genes or alleles that confer increased resistance and/or higher yield can be used to create new cultivars through conventional breeding (Shiferaw et al., 2011). By improving our knowledge of the host-pathogen interaction and natural plant defensive mechanisms, we can find novel genes and/or alleles in the long-term goal of introducing and potentially up-regulating them in plants to aid disease resistance.

1.2. Disease Resistance

1.2.1 Pathogens

Plant pathogens have different modes of action when it comes to plant attack and can be divided into three groups. Biotrophs reside within plants and exploit their hosts as a source of nutrients without killing them (Agrios, 2005). Necrotrophs, the largest class of plant pathogenic fungi (Bary, 2012), produce toxins and cell-wall degrading enzymes that initiate cell death, before then feeding on the contents. Hemibiotrophs make use of both strategies to optimise their growth. They are initially biotrophic where they establish an infection and proliferate without harming the host, before switching to a necrotrophic lifestyle and killing cells (Dangl & Jones, 2001). Fungi and bacteria can be part of either lifestyle, but viruses are only biotrophic. This puts plants at risk of infection by a wide variety of pathogens, including fungi, bacteria, nematodes and insects. As plants are sessile organisms they also cannot move away from these harmful pathogens. Due to this the plant immune system has evolved to be highly polymorphic in its ability to detect and respond to pathogens. Plants have evolved a number of diverse

defence mechanisms in order to perceive a wide variety of attacks, with each plant cell acting individually in its response (Agrios, 2005).

The first barrier of defence for pathogens is the waxy cuticular outer layer and cell wall of plants. Pathogens often enter through wounds, stomata or hydathodes (pores in the leaf margin) (Bary, 2012) although fungal pathogens can directly enter epidermal cells (Jones & Dangl, 2006). Many fungal pathogens can adhere to the plant surface using adhesive proteins and apply mechanical pressure to penetrate plant tissue. This is done via the fungal hypha forming a bulblike structure called an appressorium which punctures though the cuticle and cell wall. Penetration is usually assisted by cell-wall degrading enzymes secreted by the pathogen (Agrios, 2005; Bary, 2012). Some parasites and nematodes have similar mechanisms of penetrating the cell surface through mechanical pressure. Fungal pathogens often penetrate host membrane tissue with specialised feeding structures called haustoria. The pathogens release a variety of substances, including fatty acids, glycoproteins, carbohydrates and peptides (Agrios, 2005). Some of these are recognised by the host plant as a signal of pathogen attack. Once recognised, a chain of biochemical reactions is set off in what becomes the start of a continuous 'battle' of pathogen attack and plant defence.

1.2.2 'Zigzag' model

The defence mechanisms used by plants are complex and differ according to the pathogen. There is no one model that fits all, however, the currently utilized model of the plant immune system is the 'zigzag' model. This four phase model, which was developed for biotrophs, involves a range of different infection mechanisms by pathogens and subsequent defence responses by plants. During phase one, transmembrane pattern recognition receptors (PRRs) of plants bind to conserved microbial compounds, pathogen- or microbial- associated molecular patterns (PAMPS/MAMPS) (Jones & Dangl, 2006). Common examples of these being chitin in fungi (Felix et al., 1993) and flagellin in bacteria (Felix et al., 1999). Bound PRRs result in PAMP/MAMP-triggered immunity (PTI). This leads to phosphorylation of the receptors' cytoplasmic domains and the triggering of a MAP kinase cascade, leading to the expression of genes encoding defence proteins and pathways. In general, different hormones are used in response to biotrophs and necrotrophs: salicylic acid (SA) for biotrophs and ethylene (ET) and jasmonic acid (JA) for necrotrophs (Bary, 2012). PRRs recognize both biotrophs and necrotrophs, however, the responses to biotrophs is far better understood.

In phase two, successful pathogens produce effectors – often produced by the haustoria in fungi (Dangl & Jones, 2001) - that enhance pathogenicity and suppress host immune responses in effector-triggered susceptibility (ETS). Effectors are transferred from the pathogen cell into the host tissue.

In phase three, plants use Resistance (R) proteins to initiate the next defensive mechanism, termed effector-triggered immunity (ETI). In ETI, R protein receptors recognize pathogen effectors, either directly or indirectly by detecting the products of their action on host targets (Dangl & Jones, 2001), and in response initiate an enhanced immune response. Activation of R proteins can induce production of SA and reactive oxygen species which induce defence response genes and initiate programmed cell death – also known as hypersensitive response - in the affected cells. *R*-genes encode resistance to a wide range of pathogens. R proteins recognize the effects of the effectors on host cell machinery. This latter strategy might be advantageous in that by surveying its own proteins, the plant doesn't need a separate R protein for every effector a pathogen might produce; a single R protein often guards against many different effectors (Bary, 2012). The largest and most well-known class of *R*-genes are the 'nucleotide-binding site plus leucine-rich repeat' (NB-LRR) which usually act inside the cell (Jones & Dangl, 2006). However, NB-LRR-mediated resistance is only deployed against biotrophs. R protein-mediated immunity is normally not involved in necrotroph defence. As R proteins lead to cell death response infection sites, they would only favour a necrotrophic mode of action. Due to this, certain necrotrophs hijack this mechanism to initiate cell death (Jones and Dangl, 2006).

In the fourth and last phase of the 'zigzag' model, pathogens can prevent ETI by removing the effector, or by attaining additional effectors (Jones & Dangl, 2006). Both PTI and ETI can induce systemic acquired resistance (SAR). The SAR pathway is activated in response to the formation of a necrotic lesion, although it can also be induced by the application of exogenous chemicals, including benzothiadiazole S-methyl ester (BTH) and β-aminobutyric acid (BABA). SAR leads to development of broad-spectrum resistance (Ryals et al., 1996). Certain plant cultivars are known to produce necrotic lesion spotting on leaves without any induced stressors. These 'leaf flecking' phenotypes are genetic and lead to increased overall resistance (Olukolu et al., 2016). SAR thus "primes" plants for improved defence (Bary, 2012).

One should note that the signalling events downstream of pathogen attack have been characterised through *Arabidopsis* studies, therefore, there may be difference in signalling

responses in other plant systems. The defence responses by plants are also much more complex than any one model can explain. Plants respond to different integrated signals. For example, those induced by biotrophs can intersect with those produced by necrotrophs and abiotic stress pathways. Plants have to prioritize their responses within this contex (Bary, 2012).

1.2.3 Conferring disease resistance

Plant defence genes are often targeted in order to improve disease resistance. Disease resistance can be separated into two general categories: 1) complete resistance conditioned by a single *R*-gene that confer qualitative effects, and 2) incomplete resistance conditioned by multiple genes of partial effect in quantitative disease resistance (QDR). There are a number of terms for these two categories including major-gene and minor-gene, and narrow-spectrum and broad-spectrum, but the terms that will be used henceforth are qualitative resistance to refer to resistance conferred by *R*-genes, and QDR to refer to resistance conferred by quantitative resistance loci (QRL) (Poland et al., 2009).

The molecular mechanisms underlying QDR still aren't fully understood. Poland et al. (2009) compiled a list of six hypotheses of different mechanisms thought to underlie QDR: 1) Disease resistance genes are involved in plant morphology and development; 2) QRLs represent different alleles of PRR genes acting in basal defence; 3) QRLs represent different alleles of genes involved in regulation of defence signalling pathways such as SA, JA and ET; 4) QRLs are weaker forms of *R*-genes where over time pathogen evolution has eroded the *R*-gene effectiveness; 5) QRLs represent classes of genes not previously reported to function in disease resistance; 6) QDR is involved in toxic deployment (e.g. phytoalexins) against pathogens. Most studies agree that more than one mechanism is likely to be valid and no single hypothesis can fully explain QDR. It is also likely new mechanisms will be suggested in the future.

R-genes usually confer complete resistance to a specific race, while QRLs confer partial resistance to a broad range of pathogens (Poland et al., 2009). *R*-genes are more commonly utilised to increase disease resistance in plants due to the high levels of resistance it provides and as only manipulation of a single gene is required. However, *R*-genes have a number of limitations. Firstly, they can be overcome by natural selection, and in turn subject pathogens to high levels of selection pressure. For example, wheat stem rust, *Puccinia graminis*, used to be a devastating disease until resistant strains carrying an *R*-gene, *Ug99*, were bred in the 1960s and the pathogen was not a noticeable problem for a few decades. However, a line resistant to the *R*-gene again appeared after high selection pressure and has been spreading throughout the

world (Singh et al., 2011). QDR is more durable than *R*-gene mediated resistance as a number of genes or alleles confer resistance (Bary, 2012).

Another major limitation of *R*-genes is that they are usually only a useful mechanism for increased disease resistance against biotrophs. Very few *R*-genes have been identified for necrotrophic pathogens as cell death is in the interest of the necrotroph. QDR, on the other hand, can be an effective method to confer enhanced necrotrophic pathogen resistance. Variation in QDR can be selected for high phenotypic resistance and many QRLs can be combined to produce plants with heightened immunity (Bary, 2012).

1.3. Secondary Metabolites involved in Defence

1.3.1 Phytoalexins and Phytoanticipins

Plants cells contain a large number of secondary metabolites which are involved in disease resistance. They can be split into two groups: phytoanticipins and phytoalexins. These are both classified as "low molecular weight antimicrobial compounds" (Van Etten et al., 1994), however, phytoanticipins are constitutively expressed, while phytoalexins are synthesized *de novo* at areas of pathogen infection (Meyer et al., 2016; Van Etten et al., 1994). A metabolite can act as a phytoanticipin in one plant and as a phytoalexin in another. Phytoanticipins are stored as preformed antimicrobial compounds that are activated in response to pathogens (Meyer et al., 2016). Benzoxazinoids (BXs) are the main phytoanticipin found in most cereal crops, including maize.

The cereal crops, maize and rice (*Oryza sativa),* produce substantial amounts of structurally diverse groups of phytoalexins (Ejike et al., 2013). Pathogen-induced antimicrobial phytoalexins were described in rice decades ago (Cartwright et al., 1977). However, research into the antimicrobial role of these phytoalexins is recent. In rice, pathogen infection induces levels of transcripts encoding key biosynthetic enzymes, namely *ent*-copalyl diphosphate synthase, termed An2. This leads to diterpenoid phytoalexin accumulation that then has a role in fungal pathogen protection. Several families of diterpenoid phytoalexins have recently been discovered in rice (Ejike et al., 2013) - a much wider range than has been characterized in maize. Phytoalexin is a broad term based on how the metabolite is produced. Phytoalexins fall

under a number of chemically diverse classes, including terpenes, stilbenes, steroids, alkaloids and flavonoids (Bary, 2012).

1.3.2 Terpenes

Terpenes are a large and diverse class of organic compounds, produced by a variety of plants as well as by some insects and marine organisms (Gershenzon & Dudareva, 2007). Terpenes constitute the largest and most diverse class of plant chemicals with over 50,000 known structures (Gershenzon & Dudareva, 2007; Langenheim, 1994). These compounds, which are often strong-smelling, are produced by plants in order to attract pollinators, deter herbivores and attract predators and parasites of herbivores (Martin et al., 2003).

Terpenes can act as toxins, growth inhibitors, or deterrents against insects, herbivores and fungi (Gershenzon & Dudareva, 2007). Terpenes have been shown to have a number of roles, including acting in direct and indirect defence and inhibiting seed germination. Terpenes act in indirect defence by attracting predators and parasitoids that attack herbivores above-ground (Dicke et al., 1990) and attract nematodes that prey on insects that feed below-ground (Rasmann et al., 2005). Usually a diverse combination of terpenes is produced in defence and this is thought to achieve protection against a diverse range of pathogens. The mode of action of terpenes is not fully understood, but it is believed they target the cell membrane (Gershenzon & Dudareva, 2007).

When terpenes are modified chemically, such as by oxidation or rearrangement of the carbon skeleton, the resulting compounds are terpenoids, also known as isoprenoids. Terpenoids are a well-characterized family of inducible defence chemicals derived from five-carbon isoprene units. They have been demonstrated to act in direct defence through their antimicrobial activities (Schmelz et al., 2011). Despite their identity having being well-characterized for some few decades, the role terpenoids play in pathogen defence in maize has only recently been discovered. There are two maize phytoalexins whose roles in pathogen defence have been characterized: members of the diterpenoid super-family termed kauralexins and the sequiterpenoids in maize termed zealexins.

1.4. Maize Phytoalexins

1.4.1 Identification of phytoalexins in maize

Phytoalexins in maize were identified decades ago, shortly after the discovery of rice phytoalexins, when diterpene accumulation was elicited in cell-free extracts following *F. verticillioides*, *Rhizopus stolonifer*, *Aspergillus niger* and *Verticillium albo-atrum* infection (Mellon & West, 1979). Maize and rice are the only monocots in which diterpenoid phytoalexins have been identified (Schmelz et al., 2014). Maize phytoalexins have been shown to be accumulated in response to biotic and abiotic stress, including fungal pathogen infection, herbivory, drought stress and salt stress (Huffaker et al., 2011; Schmelz et al., 2011; Vaughan et al., 2014, 2015, 2016). However, maize phytoalexins' active defensive roles were only recently discovered.

Schmelz et al. (2011) detected six diterpene acids in response to herbivorous stem attack by the insect, *Ostrinia nubilalis* and the fungal pathogen, *Rhizopus microsporus* using metabolic profiling. The compounds were isolated by purification from the infected tissue and subsequent structural elucidation of the six compounds. Through nuclear magnetic resonance (NMR) spectroscopy they were revealed to be *ent*-kaurene-related diterpenoids, termed kauralexins. A series of these induced *ent*-kaurene diterpenoid defences were termed kauralexins A1, A2 and A3. A second *ent*-isokaurene series of diterpenoids were identified, termed kauralexins B1, B2 and B3. The kauralexin biosynthesis pathway (Figure 1a) is the focus of this study. The chemical structure of the kauralexins is shown in Figure 1b.

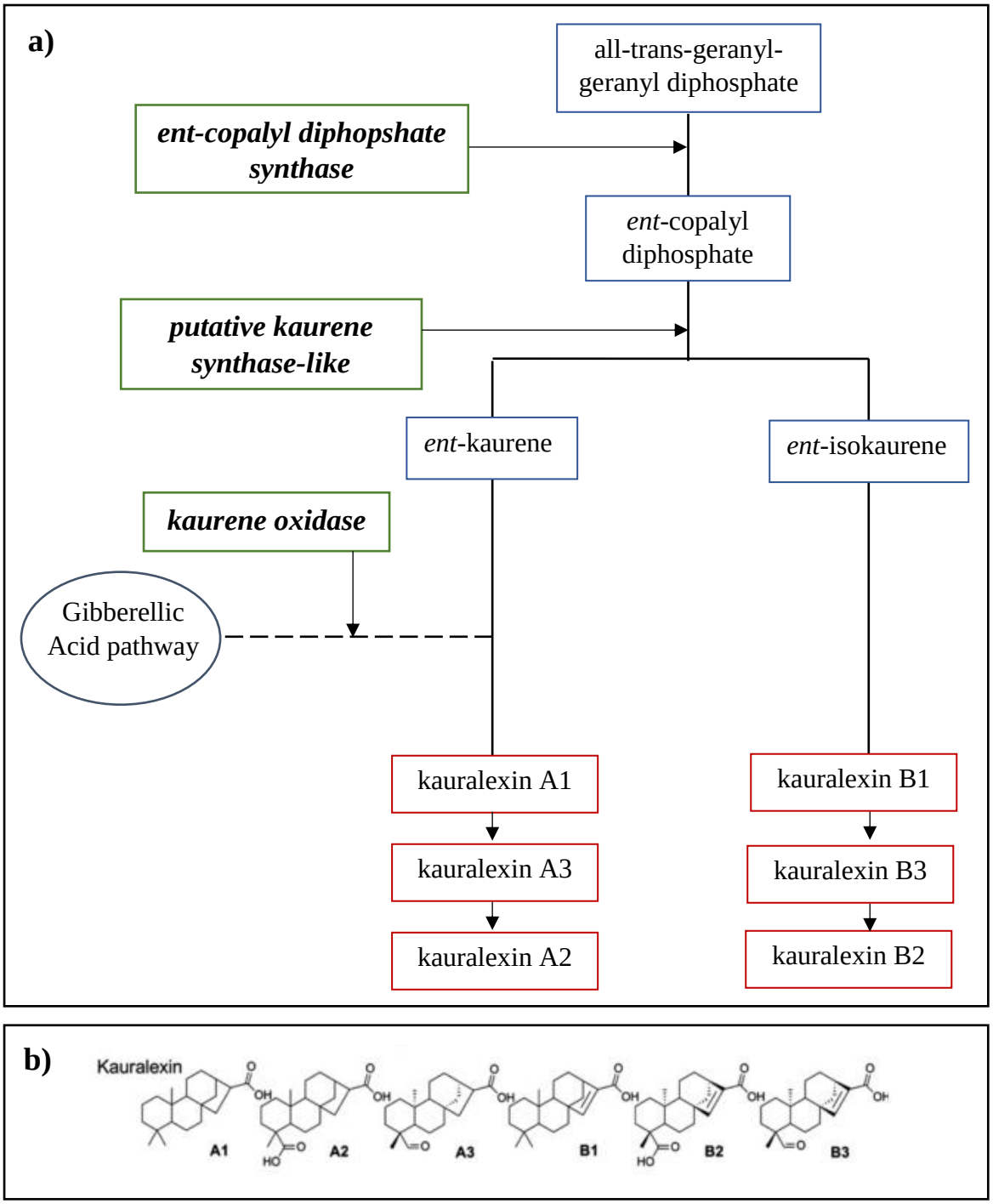

Figure 1: Maize kauralexin biosynthetic pathway leading to kauralexin accumulation.

a) Kauralexin biosynthesis pathway including key biosynthetic enzymes (adapted from http://www.plantcyc.org/). Putative kauralexin biosynthesis genes catalysing the enzymatic reactions are in bold.

b) Structures of known maize kauralexins (Schmelz et al., 2014).

Kauralexins are not the only metabolites induced when maize stems are inoculated with a fungal pathogen. Huffaker et al. (2011) discovered zealexins by purifying *Fusarium graminearum*-infected tissue. Acidic sesquiterpenoid compounds were isolated and structural

elucidation via NMR revealed them all to be closely related to the volatile β-macrocarpene. The series of sequiterpenoids discovered were termed zealexins. They are believed to result from β-macrocarpene via catalysis of enzymes encoded by the gene *terpene synthase 11* (*TPS11*) and/or *terpene synthase 6 (TPS6)*. Zealexins A1, A2, A3 and B1 were all experimentally identified and their chemical structures determined (Figure 2).

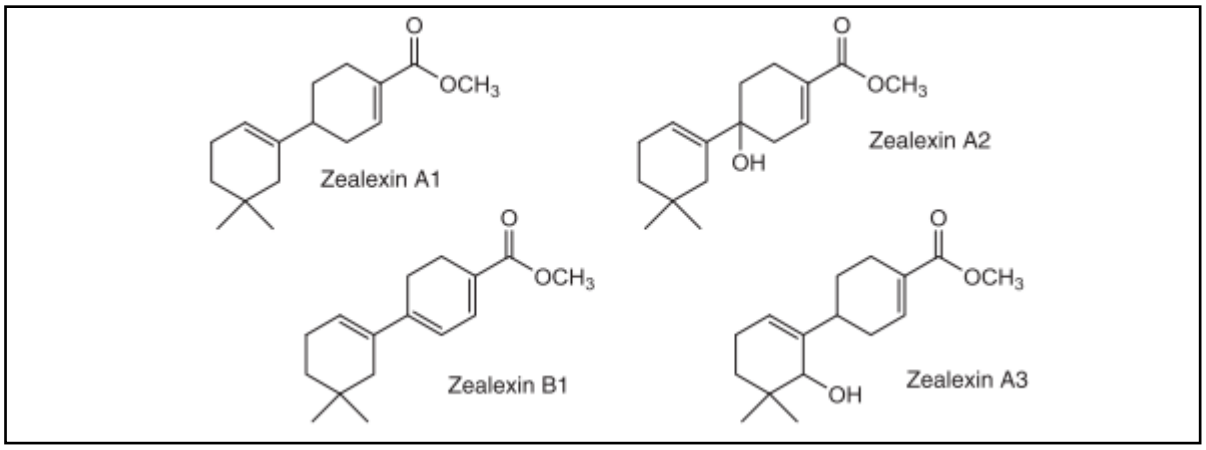

Figure 2: Chemical structures of known maize zealexins (Ejike et al., 2013)

1.4.2 Pathogen induction of phytoalexins

A number of pathogens have been shown to induce maize terpenoid phytoalexins (Huffaker et al., 2011; Ntuli & Murray, 2016; Schmelz et al., 2011; Vaughan et al., 2014). The success of the various insect and fungal pathogens examined in inducing various diterpenoid phytoalexins is summarized in Table 1.

R. microsporus and *F. graminearum* were the only fungal pathogens that significantly induced all of the phytoalexins examined. *C. graminicola* induced kauralexin accumulation, but to a lesser extent than the fungi *R. microsporus* and *F. graminearum* did (Schmelz et al., 2011). Fungal pathogens *F. verticillioides* and *C. zeina* also induced kauralexin accumulation (Ntuli & Murray, 2016; Vaughan et al., 2014), however, it was in separate studies so total accumulation between the pathogens cannot be directly compared. Herbivorous treatment with *O. nubilalis* led to kauralexins A1, B1, B2 and B3 levels that were significantly higher compared to treatment with mechanical damage, however kauralexins A2 and A3 damage-induced levels were lower compared to unwounded controls (Schmelz et al., 2011). Another insect, *Diabrotica balteata* induced all six kauralexins. Only zealexin induction was examined in *Cochliobolus heterostrophus, Aspergillus flavus* and *Colletotrichum sublineolum*. Zealexins were strongly induced by most fungal pathogens, except for *C. zeina* (Ntuli & Murray, 2016)

and *Colletotrichum graminicola* (Huffaker et al., 2011). All zealexins were induced in response to *O. nubilalis* insect herbivory. Overall, the results indicate both kauralexins and zealexins are induced by a wide variety of pathogens. Although not indicated in Table 1, drought has been shown to induce zealexins and, in particular, kauralexins (Vaughan et al., 2015). Elevated CO_2 concentration [CO_2] has also been shown to reduce zealexins and kauralexin accumulation in response to *F. verticillioides*. This indicates both biotic and abiotic stressors affect phytoalexin production.

Table 1: Effects of insect herbivory and fungal infection on accumulation of kauralexins and zealexins.
The green shaded cells indicate there is experimental evidence the pathogen induced significant accumulation of the corresponding diterpenoid phytoalexin. Yellow cells indicate the phytoalexin was shown to not be significantly induced in the corresponding pathogen. Grey cells indicate no experimental work was examined for that particular phytoalexin in the pathogen examined.

	**Ostrinia nubilalis*	**Diabrotica balteata*	*Fusarium verticillioides*	*Fusarium graminearum*	*Cercospora zeina*	*Aspergillus flavus*	*Rhizopus microsporus*	*Colletotrichum graminicola*	*Colletotrichum sublineolum*	*Cochliobolus heterostrophus*
Kauralexin A1										
Kauralexin A2										
Kauralexin A3										
Kauralexin B1										
Kauralexin B2										
Kauralexin B3										
Zealexin A1										
Zealexin A2										
Zealexin A3										
Zealexin B1										

**O. nubilalis* and *D. balteata* are insects while the rest are fungi.

1.4.3 Antifungal activity

Schmelz et al. (2011) examined the biological activity of kauralexins by analysing growth curves of the fungi *R. microsporus* and *C. graminicola* in the presence of either kauralexin A3 or B3 at high (100 $\mu g.ml^{-1}$) and low doses (10 $\mu g.ml^{-1}$). Kauralexin A3 significantly inhibited growth of *C. graminicola* at both doses. However, only a high dose of kauralexin A3 significantly reduced *R. microsporus* growth. Kauralexin B3 greatly inhibited growth of *R. microsporus* and *C. graminicola* at high and low doses at a greater percentage than kauralexin A3 did. Kauralexin B3 has also been shown to reduce *F. verticillioides* growth by 30% (Vaughan et al., 2014). Insect antifeedant activity was also shown by Schmelz et al. (2011) where maize stem surfaces were treated with kauralexins A3 and B3, resulting in significantly reduced tissue consumption by *O. nubilalis*.

A vast number of antimicrobial defence genes are also induced in response to zealexins (Huffaker et al., 2011). The antimicrobial activity of zealexins was examined by growing the fungi *R. microsporus, A. flavus,* and *F. graminearum* in separate nutrient broths containing zealexins A1, A2, and A3 at high (100 $\mu g.L^{-1}$) and low (0,25 $\mu g.L^{-1}$) doses. High doses of zealexin A1 significantly inhibited the growth of the three fungi and at low doses inhibited all except *R. microsporus*. Zealexin A2 showed no significant antifungal activity against the three fungi whatsoever. High doses of zealexin A3 inhibited the growth of *A. flavus* and *F. graminearum,* which was the only significant antifungal activity it displayed. It appears the antifungal activity of zealexins A2 and A3 is far less than that of zealexin A1. A mixture of oxygenated zealexins has also been shown to reduce *F. verticillioides* growth by 14% by Vaughan et al. (2014). These findings all provide evidence for the antifungal activity of both kauralexins and zealexins which likely act in direct defence against pathogens.

1.4.4 Abundance and spatial distribution

Kauralexin accumulation has shown to be nearly exclusive to the top surface of the infected tissue (Schmelz et al., 2011) which is typical of phytoalexins where accumulation is localized at the site of infection to prevent further pathogen entry (Meyer et al., 2016). Kauralexins were detected in the scutella (cotyledons) of 19 diverse maize lines and zealexins were detected in 23 diverse maize inbred lines (19 and 23 were investigated respectively by Schmelz et al. (2011) and Huffaker et al. (2011)). Both kauralexins and zealexins appear widespread in maize

seedlings. This suggests they may act as phytoanticipins initially and be developmentally regulated.

1.4.5. The role of hormones

The phytohormones JA and ET are involved in signalling downstream defensive pathways in response to necrotrophs and hemibiotrophs (Bary, 2012). Schmelz et al. (2011) examined the role of JA and ET in regulating kauralexin production. Damaged stems were inoculated with the fungus *R. microsporus*, with pharmacological applications of both JA and ET on stems significantly inducing kauralexins to a much greater extent than individual applications of the hormones. This implies JA and ET work synergistically to promote kauralexin production. This synergistic application was also shown by Ejike et al. (2013) who demonstrated that inoculation of maize stems with *F. graminearum* induced JA and ET production. This was then followed by an increase in zealexin accumulation. These findings show the phytohormones JA and ET promote accumulation of kauralexins and zealexins after fungal-induction in maize and indicate there may be pathway conservation between kauralexins and zealexins.

Vaughan et al. (2015) demonstrated that SA, which is involved in mediating defence response to biotrophs (Bary, 2012), has no effect on phytoalexin production in the roots of maize. However, treatment with abscisic acid (ABA), a phytohormone also involved in mediating drought stress, was shown to induce phytoalexin accumulation in maize roots (Vaughan et al., 2015)

1.4.6 Kauralexin biosynthesis genes

Maize *ent*-copalyl diphosphate synthase, termed *Anther Ear 2 (An2)* (GRMZM2G044481) catalyses the first reaction of the kauralexin pathway (Figure 1a). Harris et al. (2005) cloned *ZmAn2* in maize and confirmed it encodes a copalyl diphosphate synthase (CPS)-like protein with approximately 60% amino acid sequence similarity to the maize *Anther Ear 1 (An1)* gene product involved in gibberellin (GA) biosynthesis. *An2* has been shown to be induced by various fungal pathogens (Harris et al., 2005; Schmelz et al., 2011), including *F. verticillioides* (Lanubile et al., 2014; Vaughan et al., 2014) and *C. zeina* (Christie et al., 2017). To study the relationship between *An2* and kauralexins, Schmelz et al. (2011) examined transcript levels following *R. microsporus* inoculation. A highly significant increase in *An2* levels preceded significant kauralexin accumulation by approximately 20 hours. These findings implicate *An2*

as a possible regulator of induced kauralexin synthesis. Although rice does not contain an ent-copalyl diphosphate synthase, the *ZmAn2* gene is an orthologue of rice genes that supply precursors to diterpenoid phytoalexins (Harris et al., 2005). It is likely that *An2* performs the same function in maize. Thus, kauralexins are hypothesized to be the predominant downstream products of *ZmAn2* (Figure 1). A gene expression atlas study had shown that the three putative kauralexin genes, *CPS, KS2* and *KO*, accumulate in the first leaf of germinating maize seedlings (Sekhon et al., 2011). This validates the observations of Schmelz et al. (2011) that kauralexins are ubiquitous in maize seedlings and may be developmentally regulated.

An2 is also implicated in playing a role in drought tolerance. Knocking down expression of *An2* has been shown to make the roots of maize plants more susceptible to drought effects (Vaughan et al., 2015). This method of knocking down expression of a candidate gene involved inserting a transposon within the coding sequence. The *Ac*/*Ds* family of transposable genetic elements was used to knock-down *An2* expression in the study. The *Dissociation* (*Ds*) element of the *Ac/Ds* family of maize transposable elements had an insertion in the fourth exon of the *An2* line studied (Vollbrecht et al., 2010). Removal of the *Activator* (*Ac*) element led to stabilisation of *Ds*. As *Ds* is a large element it should prevent the gene from being transcribed.

There is still much more to learn about the genes involved in the maize kauralexin biosynthesis pathway. Two putative kauralexin biosynthetic genes downstream of *An2*, *ent-kaurene synthase (KS2)* (AC214360.3_FG001) and the *P450 ent-kaurene oxidase (KO*) (GRMZM2G161472), have recently been shown to be co-regulated with *An2* in maize by Christie et al. (2017). The genes were also shown to be significantly up-regulated in response to *C. zeina*-inoculation in the inbred maize line B73. *KS2* and *KO* are paralogues of *kaurene synthase-like* and *kaurene oxidase* (Figure 1a) whose position in the kauralexin biosynthesis pathway is approximated based on similar rice and diterpenoid pathways. *ZmKS2* and *ZmKO* share homology with their rice counterparts which are also implicated in potentially playing a role in the phytoalexin biosynthesis. *Ent-kaurene synthase-like* genes that may be involved in kauralexin biosynthesis have been identified by Fu et al. (2016).

1.5. *Fusarium verticillioides*

The genus *Fusarium* contains various plant-pathogenic fungi that attack a vast number of crop plants, including maize, worldwide. *F. verticillioides* Nirenberg (formerly/synonym: *Fusarium*

monilioforme) is reported to be the most common *Fusarium* spp. in maize in South Africa (Ncube et al., 2011), although it must be noted that distribution of *Fusarium* spp. varies according to year and geographic area (Boutigny et al., 2012). *F. vertillioides* is a hemibiotroph that initially grows within the plant as an endophyte (Bacon & Hinton, 1996) and can be found in plant residues in almost every maize field at harvest (Oren et al., 2003). *F. verticillioides* causes Fusarium ear rot, which is characterised by a white or light pink mould that reduces yield quality and can eventually lead to stalk rot. *F. verticillioides* has been shown to move from the roots to the stalk and eventually to the cob and kernels through GFP-tagging by Oren et al. (2003). No more than trace amounts of fungus were identified in above-ground tissues in the study - indicating it is more ubiquitous in the roots.

Fusarium spp. release toxic secondary metabolites known as mycotoxins in maize kernels. Mycotoxins not only harm the plant itself, but can also affect human and animal health. Fumonisins are the predominant *Fusarium* mycotoxin in South Africa and are primarily produced by *F. verticillioides* (Ncube et al., 2011). Fumonisin B1 is the most abundant of all the fumonisins (Shephard et al., 2007). Fumonisins have been shown to be carcinogenic in mice and rats (Gelderblom et al., 1991). They have also been highly associated with human oesophageal cancer in South Africa (Rheeder et al., 1992; Shephard et al., 2007) and in China (Ueno et al., 1997). Mycotoxins persist through processing and have been identified in processed foods (Bary, 2012).

Due to these potentially hazardous toxins, many countries have implemented legislation that regulates the maximum amount of mycotoxins levels considered acceptable in maize (European Commission, 2007). However, there is currently no enforced legislation in South Africa (Boutigny et al., 2012; Ncube et al., 2011), making mycotoxins a real threat to food safety, and further understanding of the disease is crucial. Fumonisins appear to be abundant in maize in South Africa with 62% of the maize samples shown to be contaminated with fumonisins in a previous study by Boutigny et al. (2012). Levels of fumonisins have shown values ranging from between 0 $\mu g.g^{-1}$ to 21.8 $\mu g.g^{-1}$. (Ncube et al., 2011). As a comparison, the Joint Food and Agricultural Organisation of the United Nations (FAO)/World Health Organisation (WHO) Expert Committee on Food Additives set a limit of 2 µg/g max fumonisin level.

Warm and dry conditions are ideal for *F. verticillioides* growth (Boutigny et al., 2012; Miller, 2014). Fumonisin levels are also highly correlated with warm, dry conditions with drought

stress believed to lead to higher levels of fumonisins (Candolara et al., 2008; Miller, 2014). Elevated [CO_2] also increases *F. verticillioides* growth, but not fumonisin production (Vaughan et al., 2014). Due to further predicted droughts and climate change in sub-Saharan Africa, one can predict *F. verticillioides* will only become more abundant.

One can work to prevent fungal growth in the field and postharvest storage, but this is costly and does not eliminate the problem (Bary, 2012). Tillage practices have been shown to have no effect on Fusarium ear rot incidence (Flett et al., 1998). Novel strategies are required for *F. verticillioides* control and fumonisin reduction. The ability of chemical elicitors that induce resistance against a broad range of pathogens was examined in a previous study by Small et al. (2012). BABA, BTH, hairpin protein, 2,6-dichloroisonicotinic acid (INA), methyl jasmonate (MeJA) and a fungicide (containing difenoconazole and azoxystrobin) were evaluated in field trials. However, none of them consistently reduced Fusarium ear rot and fumonisin contamination in artificially inoculated maize. Alternate strategies are therefore required to improve defence resistance.

F. verticillioides-inoculation has been shown to lead to up-regulation of phytoalexins and *An2* (Mellon & West, 1979; Vaughan et al., 2014, 2015, 2016). A study by Lanubile et al. (2014) compared *F. verticillioides*-resistant to susceptible maize genotypes and found *An2* had greater induction in the resistant lines. Phytoalexins have also shown to have direct antifungal activity against *F. verticillioides* with Kauralexin B3 as well as a mixture of zealexins both inhibiting *F. verticillioides* growth in a nutrient broth (Vaughan et al., 2014). Phytoalexins, and the kauralexin biosynthesis pathway in particular, are therefore a promising avenue of research. If phytoalexin genes show a functional role in *F. verticillioides* resistance, breeding phytoalexin alleles associated with resistance into maize lines could be a potential means of increasing resistance.

1.6. *Cercospora zeina*

The fungal pathogen, *C. zeina* is the causal organism of Grey Leaf Spot (GLS) disease in Sub-Saharan Africa (Meisel et al., 2009). GLS disease is one the most destructive maize foliar diseases worldwide. It has previously destroyed 60% of maize in an outbreak in Sub-Saharan Africa (Ward et al., 1999). GLS leads to tan or grey rectangular lesions on leaves and/or blighting of entire leaves. The lesions first appear as small tan spots with chlorotic borders until

the dense sporulation in the lesions assume a greyish cast, from which GLS gets its name (Latterell & Rossi, 1983; Ward et al., 1999). Lesions develop slowly compared to those caused by most foliar pathogens. It takes two to three weeks for the lesions to fully expand (Latterell & Rossi, 1983). Lesion expansion ultimately results in the coalescing of lesions and the blighting of entire leaves. Lesion development and blighting of leaves leads to much of the photosynthetic tissue becoming non-functional. Thus, limiting the production and translocation of photosynthate to developing kernels, which results in yield loss (Ward et al., 1999). Stalk deterioration can occur when lesions cover most of the leaf surface, leading to extreme water loss. The stalks also become weak which can lead to lodging (Latterell & Rossi, 1983). Environmental conditions such as constant temperature and prolonged high relative humidity are favoured by the fungus and greatly influences the risk of yield loss.

GLS can be caused by two biologically similar species, *C. zeina* and *Cercospora zeae-maydis*. These fungal pathogens are geographically separated, with *C. zeae-maydis* and *C. zeina* being the causal organism of GLS in North America (Ward et al., 1999) and Sub-Saharan Africa (Meisel et al., 2009), respectively. It is postulated that *C. zeina* entered South Africa through imported maize (Ward et al., 1999).

C. zeina / *C. zeae maydis* was considered a minor pathogen throughout most of its history. However, it has greatly increased in severity in the last 30 years, with factors such as reduced tillage and retention of reside cover (Ward et al., 1997) – where old fungal spores on dead plant material that has not been ploughed into the soil are free to infect new plants – and increased monoculture thought to heavily contribute to its greater abundance (Latterell & Rossi, 1983; Ward et al., 1999). It is anticipated GLS will become more widespread and destructive as these practices increase. Genetic resistance through the development of GLS-resistant hybrids is considered the most sustainable and cost-effective strategy for managing GLS (Ward et al., 1999). The kauralexin biosynthesis pathway may be a promising avenue of research as kauralexins - and the kauralexin genes *An2*, *KS2* and *KO* - have recently been shown to be highly up-regulated in *C. zeina*-inoculated maize (Christie et al., 2017).

1.7. Aims and Objectives

The main aim of this study was to characterise the functional role of *An2* in maize disease resistance in response to fungal pathogen attack by *F. verticillioides* and *C. zeina* by using

Ac/Ds transposon-insertion mutant lines purported to knock-out expression. A further aim was to clone *An2* into *Arabidopsis thaliana* to examine if kauralexins could be produced to confer increased fungal pathogen resistance.

Our initial hypothesis was that a reduction in *An2* expression in transposon-mutant lines would lead to reduced kauralexin accumulation and increased susceptibility to both *F. verticillioides* and *C. zeina*. With regards to cloning and overexpressing *An2*, we hypothesized that if lines could be obtained that produced kauralexins, then these lines would be more resistant.

The research questions were:

1. Do *Ds*-insertions significantly decrease kauralexin accumulation?
2. Do *Ds*-insertions knock out, or knock-down, *An2* expression in the mutant lines?
3. Does decreased *An2* expression have an effect on accumulation of other metabolites such as zealexins?
4. Do mutant lines inoculated with C. *zeina* or *F. verticillioides* have greater phenotypical disease symptoms compared to inoculated wild type lines?
5. Are mutant plants more susceptible to *F. verticillioide*s and/or *C. zeina* and contain greater fungal load than wild type line?
6. Does cloning *ZmAn2* into *A. thaliana* lead to kauralexin production?

The objectives were:

1. Identify plants with a *Ds* transposon in *An2*
2. Examine and compare *An2* gene expression and kauralexin accumulation in the transposon-mutant and wild type maize lines
3. Inoculate transposon-mutant lines with *F. verticillioides* and examine phytoalexin accumulation, *An2* gene expression, fungal quantification and phenotypic disease symptoms
4. Inoculate transposon-mutant lines with *C. zeina* and examine phytoalexin accumulation, *An2* gene expression, fungal quantification and phenotypic disease symptoms
5. Clone *ZmAn2* in order to express it in *Arabidopsis thaliana*. Ultimately transgenic *A. thaliana* lines would be evaluated for accumulation of *An2*-downstream products, including kauralexins

Chapter 2: Materials and Methods

2.1 Evaluation of *Ds*-insertion mutant lines

2.1.1. *Ac/Ds* transposable element system

The *Ac/Ds* transposable elements were manipulated to produce a stable *Ds* transposon located within the fourth exon of *An2* (B.W06.0419) which was maintained in the W22 maize inbred line (Ahern et al., 2009; Vollbrecht et al., 2010). Twelve seeds were received from the *Ac/Ds* Tagging Facility at the Boyce Thompson Institute for Plant Research with a potential *Ds* insertion in one or both alleles in the fourth exon of *An2* (http://acdstagging.org/). The genotype of each seed was unknown at the time of receiving and planting.

2.1.2. Genomic DNA extraction

Plant and fungus gDNA were both extracted following the protocol described by Meisel et al. (2009). For plants, 50 – 100mg of plant tissue was used. For fungus, mycelia were scraped off subculture plates and ground to extract fungal gDNA. The DNA quantity and quality was evaluated using the NanoDrop ND-1000 Spectrophotometer (Inqaba Biotech, Pretoria, South Africa).

2.1.3. Plant genotype identification via polymerase chain reaction (PCR)

Two PCRs were used to identify the genotype. In order to detect if the *Ds* transposon was present, an *An2*-specific 5' flanking primer, F312, and a *Ds*-specific primer, JGP3 were used in one PCR (Table 2). A positive product in this PCR indicated the sample was a mutant, either homozygous or heterozygous. In order to determine if *Ds* was present in one or both alleles of diploid maize, another PCR was performed using F312 in combination with an *An2*-specific flanking primer designed on the 3' end (Table 2). The presence of the large *Ds* transposons would prevent products from forming in homozygous mutants. The KAPA Taq ReadyMix PCR Kit (Kapa Biosystems, Boston, USA) was used, following manufacturer's protocol, with 1µl of 50ng of DNA in a 20µl reaction. PCR products were run on an agarose electrophoresis gel to detect their presence or absence. The sequences of all primers used are listed in Table 2.

Table 2: Primers used throughout the study

Gene/ Vector	Purpose	Primers	Source	Accession No.	Sequence
An2	Gene expression	An2 F An2 R	Schmelz et al. (2011)	GRMZM2G044481	F: TGTTCTTGTGAAGGCAGTTC R: TCATTCGAGCTAAAAGCAGA
	Ds-specific Genotyping	F312 JGP3	Vollbrecht et al. (2010)		5' GATCGCCTGGAGCGTCTCGG 5' ACCCGACCGGATCGTATCGG
	An2-specific Genotyping	F312 AcDs_R	Vollbrecht et al. (2010); Self (R)		F: GATCGCCTGGAGCGTCTCGG R: GCTGCATCTGCCTTCTCCCTGAC
	Cloning	CPS2_F CPS2_R	Self		F: ATGGTTCTTTCATCGTCTTGC R: TTATTTTGCGGCGGAAACAG
KS2	Gene expression	KS F KS R	Self; Christie et al. (2017)	AC214360.3_FG001	F: ATGACGCCGTTGAGGTACG R: CTAGTTTTGGTTTGACCGGACG
KO	Gene expression	KO F KO R	Self; Christie et al. (2017)	GRMZM2G161472	F: ATGCAGTCCTTGCTTGCAGGA R: AGACGACCGGATCTGCTTTCATT
TPS11	Gene Expression	TPS11 F TPS11 R	Huffaker et al 2011	GRMZM2G127087	F: GAAATGCGACAAAGGGCTG R: TCTTGAAGGCATCTCGTAGTA
LUG	Gene expression	LUG F LUG R	(Manoli et al., 2012)	GRMZM2G425377	F: GATCGCCTGGAGCGTCTCGG R: GTTAGTTCTTGAGCCCACGC
MEP	Gene expression	MEP F MEP R	(Manoli et al., 2012)	GRMZM2G018103	F: TGTACTCGGCAATGCTCTTG R: TTTGATGCTCCAGGCTTACC
UBCP	Gene expression	UBCP F UBCP R	(Manoli et al., 2012)	GRMZM2G102471	F: CAGGTGGGGTATTCTTGGTG R: ATGTTCGGGTGGAAAACCTT
EF1α	Fungal quant.	Fver356 F Fver412 R	Nicolaisen et al. (2009)	Q1AAA9	F: CGTTTCTGCCCTCTCCCA R: TGCTTGACACGTGACGATGA
CPR1	Fungal quant.	CPR1_2F CPR1_2 R	Korsman et al. (2012)	AF448828	F: TCCACTCTCGCTCAATTCG-3 R: TCTCTCTTGGACGAAACC
pENTR-1A ™	Sequencing	pENTR F pENTR R	Dr Rob Ingle (pers. comm.)	N/A	F: GCCTTTTTGCGTTTCTACAA R: CAGAGATTTTGAGACACGGG
TOPO TA	Sequencing	GW1 GW2	pCR8/GW/TOPO TA Cloning Kit (Invitrogen)	N/A	F: GTTGCAACAAATTGATGAGCAATGC R: GTTGCAACAAATTGATGAGCAATTA

2.1.4. Agarose gel electrophoresis

Gel electrophoresis was performed using 1% (w/v) agarose gels containing 0.02µg.ml^{-1} ethidium bromide (EtBR) in 0.5xTBE (40mM Tris-Cl pH 8.3, 45mM boric acid, 1mM ethylenediaminetetraacetic acid [EDTA]) buffer. Either 1 kb DNA ladder, or 100 bp DNA ladder (New England Biolabs, Ipswich, USA) was used in all instances as a marker.

2.2 Seedling analysis

2.2.1. Plant material and growth conditions

Experiments were conducted using the inbred *Z. mays* W22. The W22 cultivar was used for all maize experiments as that is the line the transposon-mutants were maintained in. One seed was planted per 12.5 x 12.5 cm pot with soil mixture containing peat, vermiculite. Plants were grown in growth rooms at the Molecular and Cell Biology Department at UCT. Conditions

were controlled with a constant temperature of 25°C, light intensity of 150 µmol.m^{-2}.s^{-1}, 55% relative humidity and a 16/8hr light-dark cycle.

After 14 days the first leaf of each plant was harvested at the V3 stage of vegetation - at which the collar of the third leaf was visible (Dash et al., 2012) - and flash-frozen in liquid nitrogen to be stored at -80°C until further use.

2.2.2. Cross-pollination

Cross pollination was performed in order to bulk up the available seed. In order to facilitate this, staggered planting of the seeds was carried out so as to obtain pollen at the time when the maize silks emerged. Two batches of four seeds each were planted one week apart. The other four seeds were kept as back-up. The pollen produced by the anthers on the tassels of one plant was transferred to the stigmas (silk) found on another maize ear. Transference was performed using a paper bag to catch pollen from anthers which was then spread over the silk of the other maize plant. Maize cobs emerged from the silk and the seeds were only removed from the cob when it was dry to improve seed viability. Seeds obtained from cross-pollination were designated as F_1 segregating seeds.

2.2.3. RNA extraction and cDNA synthesis

The PureLink® Plant RNA reagent (Thermo Fisher Scientific, Waltham, USA) was used to carry out total RNA extractions, following the manufacturer's protocol for small-scale isolation, using 0.1g of plant tissue. The quality and quantity of RNA was assessed with a NanoDrop ND-1000 Spectrophotometer (Inqaba Biotech, Pretoria, South Africa). PureLink® Plant RNA reagent on maize tissue had previously been evaluated through BioAnalyzer analysis at the Centre for Proteomic and Genomic Research (CPGR, Cape Town) and received RNA Integrity Numbers (RIN) values averaging 7.9 (Wighard & Murray, 2014) which gave confidence in the integrity and quality of RNA obtained using this reagent.

cDNA was synthesized using 1µg of total RNA with the Maxima First Strand cDNA Synthesis Kit for RT-qPCR with dsDNase (Thermo Scientific, Waltham, USA), following manufacturer's protocol.

2.2.4. Gene expression transcription profiling

Real-Time PCR (qPCR) was carried using the KAPA SYBR® FAST qPCR Kit Master Mix (2X) Universal (Kapa Biosystems, Boston, USA). The *An2* qPCR primer sequence was obtained from Schmeltz et al. (2011). Primers that targeted the region where the microarray probes bound were designed for the *KS2* and *KO* genes (Wighard & Murray, 2014). Primer 3 Plus (http://primer3plus.com/) and OligoAnalayzer 3.1 (Integrated DNA Technologies, Coralville, USA*)* were used to help design primers with a similar Tm, GC content and length as well as a low chance of hairpin, homodimer and heterodimer secondary structure formation. qPCR was performed on a Rotor-Gene 6000 (Corbett, Sydney, Australia). All 3 biological replicates were analysed in triplicate. An aliquot of each sample was pooled and diluted 1:5; this was used as a starting point. Subsequent serial dilutions from this were made to obtain a dilution series of 1:2, 1:4, 1:8, 1:16, 1:32, 1:64 and 1:128 that served as the standards to calculate the concentration of each sample. Threshold cycle (Ct) values, a measure of calculating concentration, for each gene were normalised to three reference genes. Relative quantification was performed using three candidate reference genes, *leunig (LUG)*, *membrane protein (MEP)* and *ubiquitin carrier protein* (*UBCP*) which have previously been shown to be extremely stable reference genes of great use for qPCR in maize by Manoli et al. (2012). Specificity of qPCR primers was tested using a dissociation curve (melt) analysis. More details about the primers used can be seen in Table 2.

2.3. F. verticillioides inoculations

2.3.1. Plant material and growth conditions

Murashige and Skoog (MS) media (Murashige & Skoog, 1962) was made up using Phytagel™ (Sigma-Aldrich, St. Louis, USA) (2.2g per 1L). Fifty ml of MS media was added to sterile glass jars that measured 6 x 9.5 cm. *F. verticillioides*- or mock-inoculated seeds were placed in the media using sterile forceps with 50% of the seed inserted in media and oriented so that the radicle (point where root emerges) faced directly upwards. The jars were enclosed with lids and incubated in a controlled plant growth chamber (Percival Scientific, Perry, USA), with light intensity of 100 $\mu mol.m^{-2}.s^{-1}$, constant temperature of 28°C and a 16/8hr light-dark cycle. Relative humidity was set at 70% but as plants were enclosed in jars, conditions were closer to 100% relative humidity.

2.3.2. Fungal subculture and seed-inoculation

Fungal cultures from *F. verticillioides* strain MRC826 (Marasas et al., 2004) were streaked onto Potato Dextrose Agar (PDA) medium plates in a Class II Biosafety Cabinet (ESCO Life Sciences, Singapore). Plates were sealed with parafilm and incubated at 30°C. After approximately seven days, the *F. verticillioides* cultures exhibited a violet colour indicating sporulation was occurring. The conidiospores were then scraped off the mycelium and resuspended in a 0.2% Tween 20 solution with a sterile blade. Using a haemocytometer, the spore count was estimated and diluted to 1 x 10^3 conidiospores.ml^{-1}.

Seeds were surface sterilized by the following process: covered in absolute ethanol for one minute, shaken, ethanol replaced with 50% commercial bleach, left for 15 minutes, shaken, bleach replaced with sterile water, washed with water five times, left to stand for five minutes after the last wash, and all water removed. The seed inoculation method from Oren et al. (2003) was followed, with seeds placed in the 1 x 10^3 conidiospores.ml^{-1} solution. Control mock-inoculated seeds were suspended in 0.2% Tween 20. Afterward, the seeds were dried on sterile filter paper in the Class II Biosafety Cabinet overnight. The dried seeds were then placed into the glass jars containing MS media with sterile forceps. After 14 days, the aboveground and root tissue were harvested separately and flash-frozen in liquid nitrogen.

2.3.3. Evaluation of maize susceptibility to fungal inoculation

A scoring system was created wherein the *F. verticillioides*-inoculated plants were evaluated in comparison to the control mock-inoculated samples. This scoring system took into account shoot truncation, leaf one truncation, leaf senescence (yellowing due to cell death), root truncation, root disfiguration (corkscrew appearance) and extent of red colour in roots. Values ranging from 0 – 3 were given for inoculated samples. A value of either 1 or 0 was given for presence or absence of shoot truncation, root truncation, leaf one truncation and leaf senescence. Root disfiguration (indicated by a root 'corkscrew' appearance) and diameter of roots that were red were quantified. Values were given as follows: **0**: 0 cm; **1**: 0 – 1 cm; **2**: 1 – 2 cm; **3**: 2 – 3 cm. The mean values for each genotype was then calculated.

2.4. *C. zeina* inoculation

2.4.1. Plant material and growth conditions

Seeds were germinated in a soil mixture containing 1:1 peat:vermiculite in 12.5 x 12.5 cm pots. The plants were kept in a plant growth chamber (Conviron, Winnipeg, Canada), with light intensity of 150 µmol.m^{-2}.s^{-1}, humidity of 70%, constant temperature of 28°C and a 16/8hr light-dark cycle.

2.4.2. Fungal subculture and inoculation of maize leaves

C. zeina isolate CMW 25467, from Zambia, was used (Meisel et al., 2009). It was cultured on a plate containing V8 medium (800 ml of distilled water, 200 ml of V8 tomato juice, 15 g of agar, 2 g of CaCO3) as described in Meisel et al. (2009). Culture plates were stored in the dark at 22 +/− 4°C. *C. zeina* was sub-cultured every six days - when the culture appeared dense and dark grey - onto fresh V8 media to propagate the spores. When spores were dense enough, 300µl of sterile water was added to each plate and spores dislodged into the water solution using a sterile spreader. The spore count was estimated using a haemocytometer. A spore count of 5 x 10^5 conidiospores.ml^{-1} was used for inoculation on W22 plants, and a count of 1 x 10^5 spores conidiospores.ml^{-1} was used to inoculate the F_1 segregating plants. From the conidiospore solution, 50 µl was added to the forming whorl of each plant. Sterile water alone was added to whorls of control mock-inoculated plants. After inoculation, lights were turned off overnight and humidity was increased to 90%. After 24 hours, normal light conditions resumed and humidity was decreased to 70% again. This overnight darkness had been shown to increase inoculation success (Dr Bridget Crampton, pers. comm.). A 12 cm section of the leaf that covered the point of inoculation was harvested 10 days post inoculation (dpi) and flash-frozen.

2.5. Evaluation of knock-down inoculated lines

2.5.1. Fungal Quantification in inoculated maize samples using real-time PCR

The ratio of fungal DNA to plant DNA was determined through qPCR on the Rotor-Gene 6000 (Corbett, Sydney, Australia). Primers specific to each fungal pathogen were used to quantify fungal DNA in samples and were divided by the amount of plant DNA quantified using reference gene primers. For *F. verticillioides*, *elongation factor 1 α (EF1α)* (Nicolaisen et al.,

2009) (Table 2) was used for quantifying fungal DNA, with *MEP* used as a proxy for plant DNA. For *C. zeina, cytochrome P450 reductase 1 gene (cpr*1) (Korsman et al., 2012) (Table 2) quantified *C. zeina* fungal DNA and *LUG* was used to determine the amount of plant DNA. Pure fungal DNA was diluted to 5, 1, 0.5, 0.2, 0.4, 0.002 and 0.001ng/µl standards for both fungi. The standards for plant DNA were obtained by using DNA of W22 and making serial dilutions ranging from 100ng/µl to 3.125ng/µl. The protocol for fungal quantification described by Korsman et al. (2012) was followed. Real-time PCR reactions were performed in triplicate for each standard curve sample. Standard curves were analysed and the Ct values of the unknown samples was determined by comparing to the known standards. The fungal DNA was divided by maize genomic DNA to normalise gene quantification. The subsequent value was multiplied to get ng fungal DNA/µg maize DNA.

2.5.2. Quantification of maize metabolites

Ground maize leaf tissue (0.2g) was delivered frozen to the gas chromatography–mass spectrometry (GC-MS) facility at the United States Department of Agriculture (USDA) where metabolite identification took place by Dr Shawn Christensen. The protocol described in Schmelz et al. (2011) was followed to quantify kauralexins, zealexins, phytohormones and free fatty acids. ^{13}C-linolenic acid was used as the internal standard.

2.5.3. Statistical analysis

The qPCR results were analysed using qBase+ software (Biogazelle, Gent, Belgium) which uses an algorithm to normalise the genes of interest to the chosen reference genes. Biogazelle calculated M and CV values for the three reference genes used. M values are measures of average expression stability values and CV (coefficient of variation) measures variation between samples. M values below 1 and CV values below 0.3 are reliable indicators that reference gene stability can be trusted (Vandesompele et al., 2002). These values were used as limits for the genes in this study. All three genes were analysed and used if the combined M and CV values stayed below the limit. Where one gene caused the M and CV values to fall outside the limit, the other two refernce genes were used. The chosen reference genes for each RT-qPCR experiment are indicated under the figure legend.

The results were also analysed in GraphPad Prism 6 (GraphPad Software, San Diego, USA). A student's t-test was used when analysing two samples. Analysis of variance (ANOVA) was

used to determine if there were differences between the multiple group means of the samples analysed. A p-value < 0.05 was considered significant for both tests. If an ANOVA test yielded a significant result, a post hoc test was then performed to identify which specific groups differed. Tukey's HSD post hoc test was performed to account for multiple comparisons.

To determine Pearson's correlation coefficient (r), the 'CORREL' function on Microsoft Excel was utilised with kauralexin accumulation, *An2* gene expression and fungal quantification set as arrays.

2.6. Cloning An2

2.6.1. Entry vectors for cloning

Two different entry vectors were used in order to attempt *An2* cloning towards *A. thaliana* overexpression. The Gateway® vectors, pENTR-1A and pCR™8 TOPO® TA (Invitrogen, Thermo Scientific, Waltham, USA), were used. Maps of the vectors are shown in Figure 3.

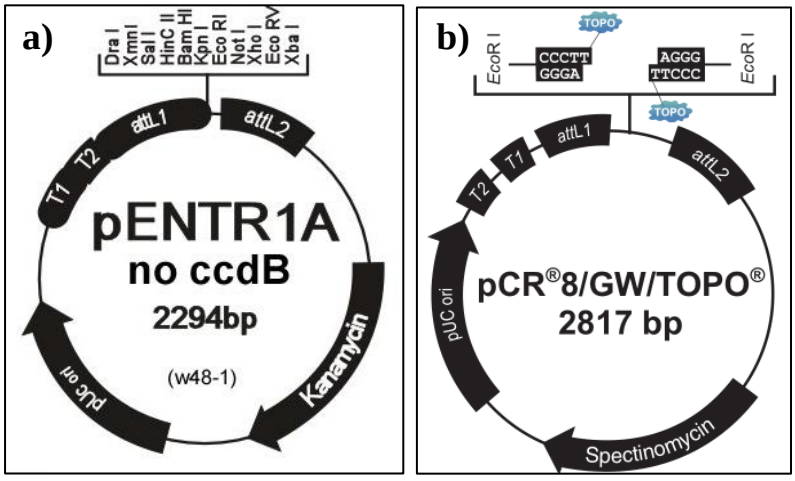

Figure 3: Gateway vectors used for cloning of *An2*.
a) Vector map of Gateway® pENTR-1A vector, without the *ccdB* gene (https://www.addgene.org).
b) Vector map of Gateway® pCR™8 TOPO® TA (Instruction Manual, Invitrogen, 2012)

2.6.2. Amplifying and purifying *An2* cDNA

Primers were designed that spanned the entire end cDNA sequence for *An2* using the available B73 sequence (http://ensembl.gramene.org/) with restriction sites inserted at both ends, designed to fit in-frame into the Gateway® pENTR-1A vector (Thermo Fisher Scientific, Waltham, USA) (Figure 3a). Phusion® High-Fidelity DNA Polymerase (New England

Biolabs, Ipswich, USA) was used to amplify the *An2* cDNA, following the manufacturer's protocol. The PCR products were gel electrophoresed on a 1% (w/v) agarose TBE gel, gel extracted and purified using Zymoclean™ Gel DNA Recovery Kit (Zymo Research, Irvine, USA) according to the manufacturer's instructions. For pENTR-1A cloning, restriction enzymes (New England Biolabs, Ipswich, USA) were used to digest the vector and insert per the manufacturer's protocol. The TOPO vector did not require restriction enzyme digestion.

2.6.3. Ligation and Transformation

A ligation of *An2* insert and vector was performed with T4 DNA Ligase (New England Biolabs, Ipswich, USA), followed by a heat-shock transformation (Sambrook et al., 1989) using chemically competent DH5α *Escherichia coli* cells. *An2*-pENTR-1A transformants were applied to Luria Bertani Agar (LBA) supplemented with 50 $\mu g.ml^{-1}$kanimycin. *An2*-TOPO transformants were applied to LBA supplemented with 50 $\mu g.ml^{-1}$ spectinomycin. The plates were incubated at 37ºC for 18 hours. Single colonies from the transformations were tested for the presence of the correct insert using colony PCR and positive colonies were subjected to plasmid DNA extraction using the GeneJET Plasmid Miniprep Kit (Thermo Scientific, Waltham, USA).

2.6.4. Sequencing

Plasmid DNA was Sanger sequenced using the pENTR-1A and cDNA primers at the Central Analytical Facility (CAF) at Stellenbosch University. The Clustal X algorithm within BioEdit Sequence Alignment Editor (Hall, 1999) was used to align and compare the sequences. The ends of the sequences, with mismatches and background noise, were removed.

Chapter 3: Results and Discussion

The kauralexin biosynthesis gene, *ent-copalyl diphosphate synthase (An2)* as well as the two putative kauralexin genes, *ent-kaurene synthase (KS2)* and the *P450 ent-kaurene oxidase (KO)*, have been shown to be co-expressed across a Recombinant Inbred Line (RIL) population. All three genes have shown significant up-regulation in response to the fungal pathogen, *C. zeina* and this expression was strongly correlated to GLS lesion development (Christie et al., 2017). *An2* has also been shown to be up-regulated in response to the fungal pathogens *F. graminearum* (Harris et al., 2005; Schmelz et al., 2011) and *F. verticillioides* (Vaughan et al., 2015).

In this study a knock-down mutant of *An2* was isolated in order to determine if *An2* plays a functional role in disease resistance to fungal pathogens. *Ds* transposon-mutants inserted into the *An2* fourth exon were obtained with the goal of preventing *An2* gene expression, kauralexin accumulation and further characterising the responses of these mutants to the fungal pathogens *F. verticillioides* and *C. zeina* (Ahern et al., 2009; Vollbrecht et al., 2010). Kauralexin accumulation, gene expression, fungal quantification and fungal phenotypic symptoms were all determined. An attempt was then made to clone *An2* into *Arabidopsis thaliana* in order to determine if kauralexins could be produced in a dicotyledonous plant.

Initially, *KS2* the putative kauralexin biosynthetic gene downstream of *An2* (http://maizecyc.maizegdb.org) was also going to be examined through transposon-insertion analysis. A transposon-mutant line was obtained for *KS2*, however, germination frequency was poor for all seeds and no positive transposon mutants were identified in the few plants that did grow. A transposon mutant for *KO* also was not found. The *An2* mutant thus became the main focus of this study.

3.1. Healthy seedling analysis

3.1.1. Genotyping reveals heterozygous mutant and wild type plants

A line of transposon-insertion mutant seeds (AcDs-00047) maintained in a uniform W22 inbred line was received from the Boyce Thompson Institute for Plant Research. The seeds were expected to potentially contain a *Ds*-transposon insertion in the fourth exon of *An2*

(http://acdstagging.org). Twelve seeds were obtained and the genotype of each seed was not known. For the purposes of this study, these seeds were designated as F_0.

Eight F_0 seeds were grown and analysed. The first leaf was harvested from each plant after 14 days at the V3 stage of vegetation - the developmental plant stage when the third leaf collar is visible - to be used for further DNA and RNA extractions. The DNA obtained was analysed using two separate PCR reactions to determine genotype. The first PCR, containing a *Ds* transposon-specific primer and a flanking 5' *An2*-specific primer (Table 1) was used to determine if the samples contained the *Ds*-insertion. A positive PCR product of 412 bp (Figure 4a) verified them as mutants. The second PCR contained the flanking 5' *An2*-specific primer used for the previous PCR, as well as a flanking 3' *An2* primer designed to be downstream of the *Ds*-insertion. This second PCR served to determine if any mutants were heterozygous or homozygous as the expected 1900 bp PCR product (Figure 4b) would not form if the large 2kb *Ds*-insertion was present in both alleles. The positon of the genotyping primers in relation to the exons of *An2* is illustrated in red in Figure 4. The primers that were used for RT-qPCR at a later stage are indicated in blue towards the 3' end of *An2* (Figure 4c). Note that the figure is not drawn to scale.

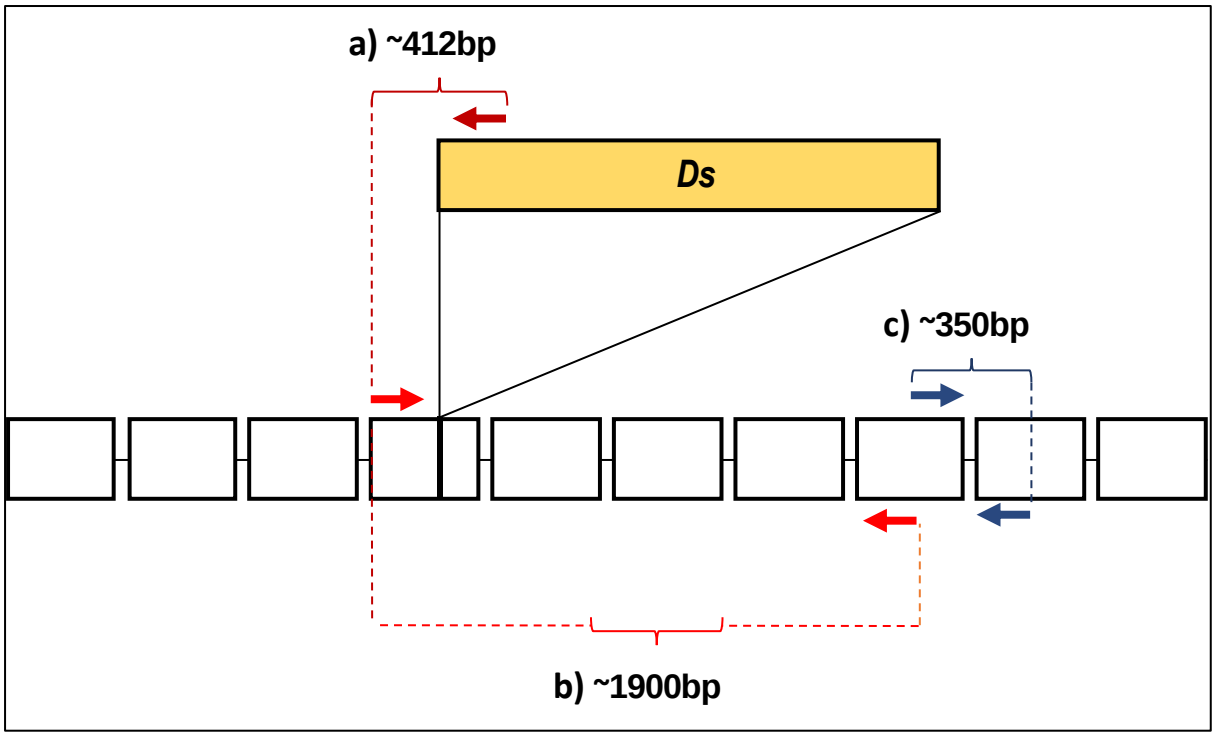

Figure 4: Position of primers used for analysis in *An2*
a) *Ds*-specific and flanking primers test for presence of the *Ds* transposon
b) *An2*-specific primers flank the site of possible transposition. A product won't be formed in homozygous mutants due to the large size of *Ds*
c) RT-qPCR primers used for gene expression are located after the point of *Ds*-insertion

As a diploid plant, maize has two alleles. Therefore, one allele could contain *Ds* and one could not, making it heterozygous (*AN2:an2*). *AN2:an2* would get positive products in both PCRs, a homozygote (*an2:an2*) would only get a product in the *Ds*-specific PCR and a wild type W22 (*AN2:AN2*) would only get a product in the *An2*-specific PCR.

Of the eight plants analysed, four had PCR products of the expected 412bp size in the *Ds*-specific PCR (Figure 5), meaning half the seeds analysed were transposon-mutants.

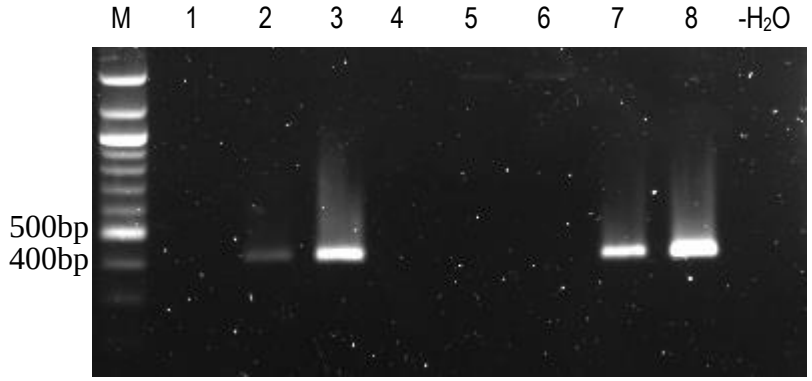

Figure 5: Electrophoresis gel of PCR products obtained after using *Ds*-specific primers on eight seedling samples. Samples 2, 3, 7 and 8 produced products of the expected ~412bp size, indicating they were mutants with *Ds*-inserts *in An2*. NEB 100bp ladder used as the marker.

Analysis using the second PCR with *An2*-specific primers produced a product of the expected size in all eight samples (Figure 6). This indicated the mutants were *AN2:an2* and the other four plants were wild type W22 (*AN2:AN2*).

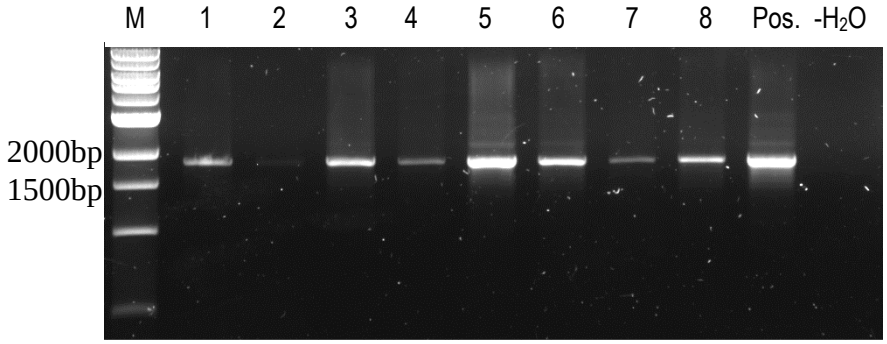

Figure 6: Electrophoresis gel of PCR products obtained after using *An2*-specific primers on the eight seedling samples. All the samples produced PCR products of ~1900bp, meaning the previously identified mutants, 2, 3,7 and 8 are *AN2*:*an2* while the rest of the samples are W22. Although faint, the product in sample 2 was visible during gel imaging. W22 DNA was used as the positive control. NEB 1kb marker ladder was used.

Two positive products from each PCR reaction (i.e. the ~412 and ~1900bp products) were sequenced with the resulting sequences trimmed and analysed through NCBI nucleotide

BLAST (https://blast.ncbi.nlm.nih.gov/Blast.cgi) (Table 3). The sequence results confirmed the primers were binding to the expected regions – *Ds* using *Ds*-specific primer and *An2* using *An2*-specific primers. Sequence identity ranged from 82 – 100% and Expect (E) values were all less than 1^{-10} which strongly confirms that the BLAST search had correctly identified the query sequence. Through analysis of the sequence results, the fourth exon was confirmed to be the point of insertion (data not shown). This site of *Ds*-insertion was expected based on previous work on *an2* mutants (Vaughan et al., 2015).

Table 3: Top three BLAST hits for each of the four genotyping primers sequenced on W22 and *AN2:an2* DNA. The description, nucleotide sequence identity match and E value are all indicated.

Sample	**Description**	**Sequence Identity**	**E value**
An2*-forward primer on *AN2:an2	Maize mutant sh-m5933 transposable element ***Dissociation* (*DS*)** in the endosperm *sucrose synthetase* gene	100%	2^{-76}
	Zea mays cultivar W22 transposon ***Dissociation***, complete sequence	100%	3^{-75}
	Zea mays ***Ds*6-like insertion** element, complete sequence	100%	3^{-75}
Ds*-reverse primer on *AN2:an2	Maize mutant sh-m5933 transposable element ***Dissociation* (*DS*)** in the endosperm *sucrose synthetase* gene	100%	4^{-39}
	Zea mays transposable element sesqui-***Ds***, complete sequence	100%	4^{-39}
	Zea mays cultivar W22 transposon **Dissociation**, complete sequence	100%	6^{-38}
***An2*-forward on W22**	*Zea mays ent-copalyl diphosphate synthase* (***An2***) gene, complete cds	99%	2^{-66}
	Zea mays kaurene synthase 2 **(*an2*)**, mRNA	100%	3^{-55}
	Zea mays ent-copalyl diphosphate synthase (***An2***) mRNA, complete cds	100%	3^{-55}
***An2* reverse on W22**	*Zea mays ent-copalyl diphosphate synthase* (***An2***) gene, complete cds	86%	2^{-80}
	Zea mays kaurene synthase 2 (***an2***), mRNA	82%	3^{-34}
	Zea mays full-length cDNA clone ZM_BFc0088O06 mRNA, complete cds	82%	3^{-34}

As it can be seen, the identity didn't match entirely using the reverse *An2* primer (86 – 82% on Table 3), however, the B73 reference genome was used in primer design and there are an expected number of polymorphisms between B73 and the W22 genome (Dooner & He, 2008). Repeating this analysis with the W22 reference genome, when it is freely available, would help confirm this.

3.1.2. *AN2:an2* mutants do not display reduced gene expression in seedlings

The RNA from the first leaf of each plant was extracted for gene expression analysis at the V3 stage (after 14 days). This specific tissue and stage of vegetation was chosen as *An2* has been shown to be up-regulated in the first leaf of plants at the V3 stage in B73 maize seedlings by Sekhon et al. (2011). B73 maize RNA was thus used as a positive control.

Gene expression of the eight samples was analysed through RT-qPCR using *An2* primers (Schmelz et al., 2011). These primers have previously been used to detect *An2* transcript levels in W22 plants by Vaughan et al. (2015). *An2* expression was minimal in all samples and there was no reduction in *AN2:an2* compared to wild type W22 as shown in Figure 7. Mean expression was actually slightly higher in *AN2:an2*; however, variability was high across all samples with no significant differences being found (one-way ANOVA, $p > 0.05$).

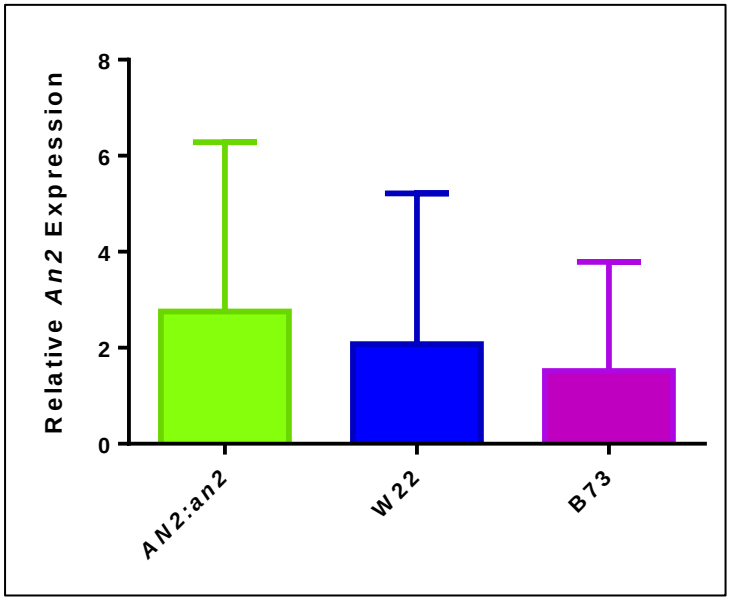

Figure 7: RT-qPCR showing *An2* expression levels for *AN2*:*an2*, W22 and B73 in the first leaf at the V3 stage (mean + s.d.; n = 4). Gene expression was normalised to *LUG, MEP* and *UBCP*. Reactions carried out in triplicate. There was no significant difference between the three groups (one-way ANOVA, $p = 0.85$).

An2 expression was neither knocked out nor reduced in *AN2:an2*, however, levels were low across all samples. The positive control B73 also did not produce significant *An2* up-regulation. These minimal expression levels are similar to previous work done in our lab (Wighard & Murray, 2014) under the same growth conditions which also showed low *An2* up-regulation in the first leaf of B73 seedlings at the V3 stage. The disparity between these results and published data (Sekhon et al., 2011) is likely due to differences in growth conditions.

A hypothesis for the expression found in *AN2:an2* is that a *Ds*-insertion in only one allele is unable to prevent transcription. In order to determine if *Ds* knocks out or reduces *An2* gene expression, both alleles need to have *Ds* inserted.

3.1.3. *an2:an2* Mutants do not display reduced *An2* expression in seedlings

In order to obtain homozygous (*an2*:*an2*) mutants as well as a far greater number of samples, *AN2*:*an2* plants were grown and cross-pollinated against one another. In order to facilitate this, half the seeds were initially grown one week apart as W22 maize cannot self-pollinate due to male tassels appearing approximately a week before the female silk. The pollen is produced by the anthers on the tassels and needs to come into contact with the silk found on another maize cob to pollinate. The maize was successfully grown and cross-pollinated to one another, with viable maize seed obtained approximately four months after planting of the initial seeds as shown in Figure 8. These seeds were designated as the F_1 generation

Figure 8: One of the three maize cobs obtained after cross-pollination of two *AN2:an2* plants. Note that the seed phenotype has no indication on its genotype.

Yellow, purple and spotted seeds with both colours were obtained. Spotted seeds were left out of further analysis as spotting can be an indication of somatic excision of *Ds* due to a mobile *Ac* element (Vollbrecht et al., 2010). This means the *Ds* transposon may not be stable and could

be moved from *An2* to elsewhere in the genome. On the other hand, the yellow and purple seeds will not have mobile *Ac* elements and were therefore used for subsequent analysis.

In total three maize cobs were obtained. One cob had seeds with markings which could have been an indication of a pathogen, or alternatively heat damage, but no seeds from this cob were used so as to be cautious.

From the other two cobs, the germination frequency was tested with 18 seeds being planted from each cob. One had 100% germination frequency with all plants growing at the same rate, while the other had a germination frequency of 60%. The cob with 100% germination frequency was chosen for all further experiments. The 18 seeds from this cob were grown and leaf one harvested after 14 days, as was done previously for the initial eight F_0 seeds. DNA was extracted with *an2:an2* samples being obtained as illustrated in Figure 9, where the genotype of six of the samples is illustrated. All six obtained a *Ds*-specific product (Figure 9a) and four obtained *An2*-specific products (Figure 9b). This indicates that out of those six samples, four were *AN2:an2* and two were *an2:an2*.

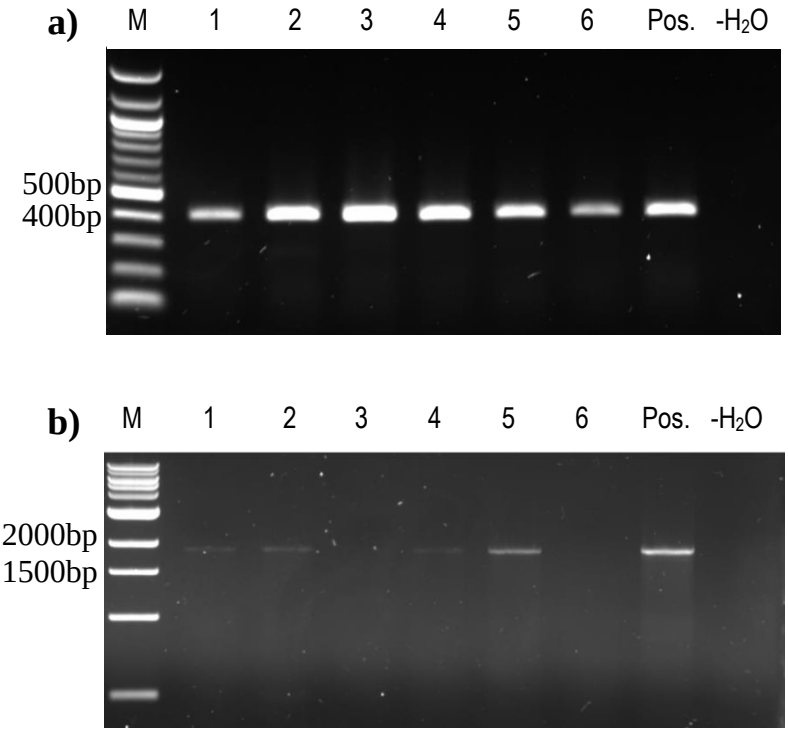

Figure 9: Six seeds of the segregating line were genotyped using two PCRs.
a) All six of these samples produced a product of the correct size (~412bp) using a *Ds*-specific and flanking *An2* primer, confirming they all had a *Ds* insertion in *An2*.
b) Samples 1, 2, 4 and 5 all produced products of the expected size (~1900bp) using the *An2*-specific primers, indicating they were *AN2:an2*. Samples 3 and 6 did not produce a product, indicating the *Ds* insert was present in both alleles, making them *an2:an2*.

The rest of the samples were genotyped (data not shown) and W22, *AN2:an2* and *an2:an2* were shown to be present in 5:8:5 ratios, respectively. This is not far from the expected 1:2:1 Mendelian ratios when two diploid heterozygotes are crossed. The predicted dispersal using Mendelian genetics for 18 samples is 4½:9:4½ which is not even possible.

With the presence of *an2:an2* and a larger sample size, gene expression analysis was again carried out to determine if two mutant alleles are required for knock out of *An2*. The RNA from the first leaf of a 14-day old plant was used for RT-qPCR analysis with *An2* primers (Figure 10). Expression was again very low for all samples and W22 samples were slightly lower than the *an2* mutants, however, there was no significant difference between any of the sample groups (one-way ANOVA, $p > 0.05$).

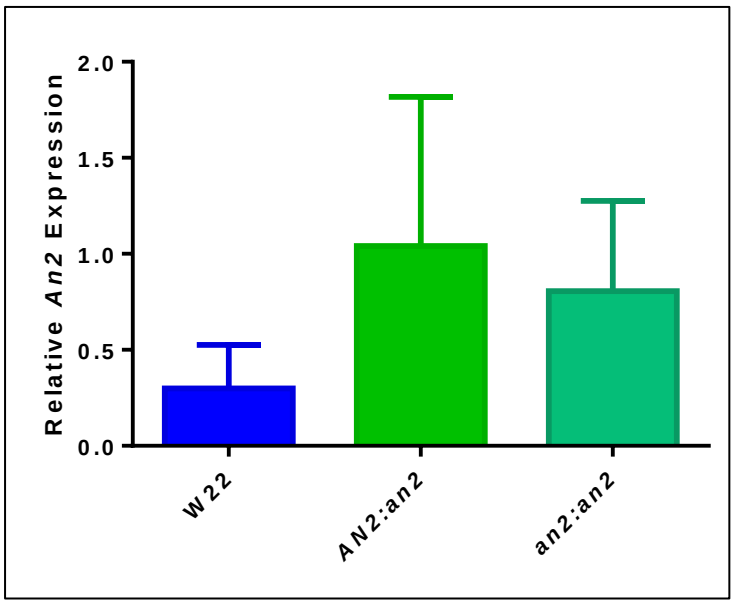

Figure 10: RT-qPCR for *An2* expression (mean + s.d.; n = 5 - 8) on seedling maize foliar tissue. Reactions carried out in triplicate and normalised to the reference genes, *LUG* and *MEP*. There was no significant difference between the sample groups analysed (one-way ANOVA, $p = 0.26$).

An2 appeared to be expressed in *an2:an2* which was unexpected. Expression did not even appear reduced as *an2:an2* mean expression was actually higher than W22, however, this difference was not significant. As *Ds*-insertion in the *An2* exon is expected to prevent *An2* transcription, one might think *Ds* was not present, however, its presence had been confirmed via genotyping and subsequent sequencing (Table 3). These results indicate that *An2* transcript is still being transcribed despite the presence of *Ds.* It may be noticed that overall expression appeared less in this experiment than in Figure 7, however, as expression is relative, y axes cannot be directly compared across different experiments.

3.1.4. Discussion of *an2* mutant seedling analysis

The *Ds* transposon was successfully identified as an insertion in the fourth exon of *An2* (Table 3) and lines were obtained with wild type W22, *AN2:an2* and *an2:an2*. Segregation of the three genotypes was close to the expected 1:2:1 ratio. *An2* levels in W22 appear similar to B73 in the first leaf of 14-day seedlings, based on this study (Figure 7). Overall, *An2* expression was low for all plants analysed. This is despite a gene expression atlas analysis of B73 maize tissue suggesting *An2* is highly up-regulated in leaf one at the V3 stage of vegetation (Sekhon et al., 2011). Kauralexins have also been shown to accumulate in the scutella of healthy seedlings after 14 days in a range of diverse inbred lines - including B73 - by Schmelz et al. (2011). This seems to indicate *An2* and kauralexins are up-regulated in healthy seedlings and may be developmentally regulated. Perhaps the phytoalexins initially act as phytoanticipins, as has been known to happen (Meyer et al., 2016), or accumulation is due to soil microbes. However, previous work in the lab (Wighard & Murray, 2014) analysed leaf one at the V3 stage in B73 tissue and found low *An2* expression, tying in with these most recent results. This disparity compared to published results could be for a number of reasons, including different environmental conditions. Difference in soil composition, light intensity and duration, temperature and humidity all affect plant growth and hormonal responses within the plant. As *An2* encodes a phytoalexin biosynthetic gene which is expressed in response to signals, differences in the environment means the window when *An2* was expressed could have been missed, or alternatively it was simply not expressed much at all in seedlings under these conditions.

The insertion of *Ds* in one or both alleles of *An2* did not knock-out expression as expected as shown by RT-qPCR analyses (Figures 7 and 10). There was not even a decrease in expression compared to wild type W22. This was surprising as it was thought the presence of the large *Ds*, which is approximately 2kb in length, would prevent *An2* from being transcribed. What is more, the RT-qPCR primers were located near the end of the *An2* gene, after the point of *Ds*-insertion (Figure 4c), meaning if *Ds* prevented *An2* expression it should be reflected in the RT-qPCR results. Although this was unexpected it has previously been observed that *Ds*-insertions from the *Ac/Ds* tagging system do not always prevent transcription, with similar amounts of mRNA for some *Ds*-insertion alleles compared to their respective wild type (Dr Erica Unger-Wallace, pers. comm.).

It is possible that the gene was still transcribed despite the presence of *Ds*. In order to determine if this is the case one could sequence the mutant transcript to see if it is stable with *Ds*, however, a long range PCR product is needed to cover the full *An2* gene plus *Ds*. Designing RT-qPCR primers upstream of the *Ds*-insertion and analysing gene expression may shed more light on what is taking place. There is also a chance that the *Ds* presence has somehow affected splicing, although *An2* only has one known transcript (http://plants.ensembl.org).

Overall, the results showed *Ds* insertions did not stop *An2* expression. There was not even a reduction in expression compared to W22. It is possible that the *An2* transcript was still being transcribed despite the presence of *Ds.* If that was the case, there would be greater chances of secondary structure formation and potentially a transcript that is more unstable than in W22. However, as expression levels were low for all samples analysed, it was believed that inducing *An2* expression through a fungal pathogen might lead to noticeable differences between *an2* mutant and W22 lines.

3.2. *Fusarium verticillioides* inoculation

3.2.1. *An2* is up-regulated in response to *F. verticillioides* in W22 root tissue

F. verticillioides has been shown to lead to phytoalexin production in maize in B73 (Mellon & West, 1979), Golden Queen (Vaughan et al., 2014, 2016) and W22 (Vaughan et al., 2015). One would therefore expect *An2* to be expressed in W22 lines after *F. verticillioides* inoculation.

In order to confirm if *F. verticillioides* would induce *An2* up-regulation in W22 - the line in which *an2* mutants are maintained, wild type W22 samples were inoculated. The W22 seeds used came from a separate batch to the segregating line. Four seeds were inoculated with *F. verticillioides* (Oren et al., 2003), with four others mock-inoculated to use as controls. All plants were grown in clear MS media in glass jars in a plant growth chamber. Symptoms of *F. verticillioides* fungus were clear in the inoculated samples, while the controls showing no signs of infection (Figure 11). Two of the inoculated seeds did not germinate fully and appeared unable to overcome *F. verticillioides* fungal growth (Figure 11a), while the other two inoculated seeds had noticeably less shoot and root growth compared to the controls (11b).

Figure 11: Pictures of 14-day old W22 seedlings in jars show *F. verticillioides*-inoculated and mock-inoculated control samples.
a) Light grey mould symptomatic of *F. verticillioides* covered all four seeds, preventing two from germinating fully. There was very little growth of roots, stem and leaves.
b) Controls had noticeably greater root, stem and leaf tissue, no fungal mould, and clear media.

The tissue was harvested 14 dpi. This time point was chosen for a number of reasons: It was used in the previous healthy seedling analyses; *F. verticillioides* has previously been detected at 14 dpi in maize seedlings (Becker et al., 2014); fungal disease symptoms were clearly apparent at this time (Figure 11) and tissue quantity was sufficient to be divided up for further DNA, RNA and phytoalexin extractions.

W22 roots have been shown to lead to high up-regulation of *An2* in response to *F. verticillioides* (Vaughan et al., 2015), so this tissue was analysed separately to the aboveground stem and leaf material – known henceforth as shoots. Root and shoot tissue was harvested separately after 14 days. Unfortunately, only two *F. verticillioides*-inoculated samples could be used for gene expression analysis as no useable tissue was obtained from the seed that did not germinate.

An2 expression was shown to be up-regulated in response to *F. verticillioides* in wild type W22 in roots and shoots, but to a much greater extent in roots (Figure 12). A student's t-test did not show significance ($p > 0.05$) between the control (W22_Cont) and inoculated (W22_Fv) in root samples, nor was there significance in the shoots. It is interesting to note that there was a small amount of *An2* expression in W22_Cont roots (mean of 2.6 to 0.3 expressed in shoots).

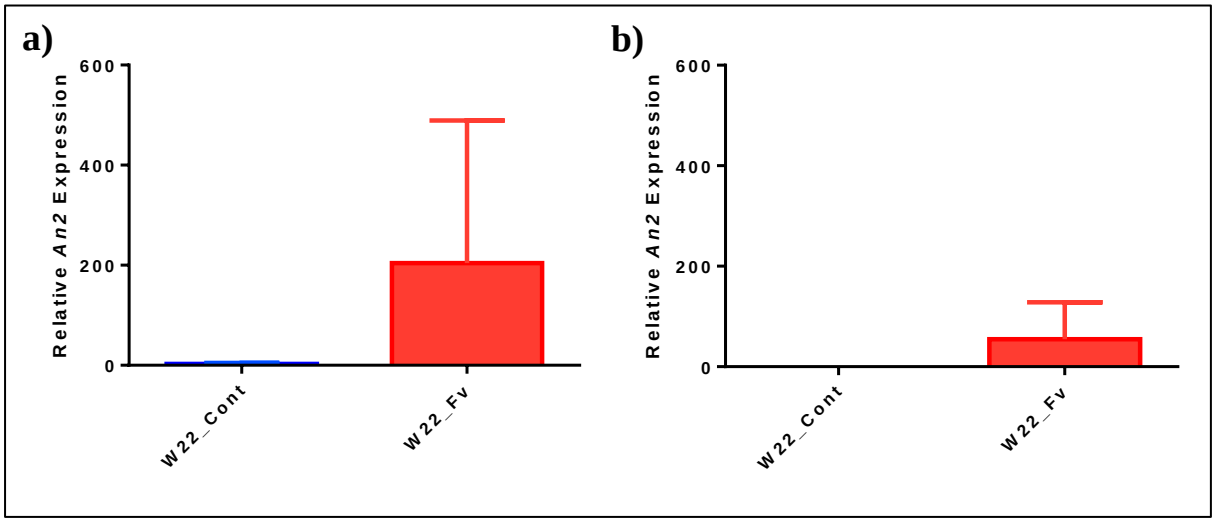

Figure 12: RT-qPCR showing *An2* expression in a) root and b) shoot tissue of 14-day old seedlings (mean + s.d.; n = 2 - 4). Reactions were carried out in triplicate and normalised to the reference genes *LUG* and *MEP*. A student's t-test showed no significance between W22_Cont and W22_Fv in a) roots ($p = 0.18$) and b) shoots ($p = 0.16$). Mean W22_Fv expression was much higher in the roots.

The high variability between samples can be seen by the large standard deviation error bars. The non-significance can be put down to a few factors including natural biological variation between samples and the small sample size of W22_Fv (n = 2). The experiment should be carried out with a larger number of W22_Fv samples in order to determine if there is a statistically significant difference.

Overall expression was far greater than previously seen in healthy leaf tissue (Figures 7 & 10). The experiments showed that *An2* expression was highest in the roots in both W22_Cont and W22_Fv making this the tissue to focus most of the attention on. With higher *An2* expression, any potential reduction in *an2* mutants would be noticeable and these differences could then be analysed. The 14-day time point was also shown to be suitable as a harvest time point for further *F. verticillioides* studies.

3.2.2. *an2* Mutant lines screened in response to *F. verticillioides*-inoculation

As the genotypes of the F_1 segregating line of seed could not be determined prior to seed inoculation, 18 seeds were randomly chosen for *F. verticillioides*-inoculation in the expectation of obtaining at least three wild type W22 and three *an2:an2* inoculated samples. Three W22 seeds – from the line used in the preliminary W22 inoculation (Figure 11) – were mock-inoculated and used as controls. Root and shoot tissue was harvested separately after 14 days as done previously. As the experiment was blinded, a careful account was taken of each individual sample, with all symptoms recorded and a number of pictures taken before harvesting. All seeds germinated fully, with the exception of one sample which was overcome by *F. verticillioides* before root and stem tissue could fully extend.

The harvested tissue was ground up and used for all further analyses including DNA extraction and genotyping. Each sample was genotyped using the two PCRs as described previously (Figure 4). The genotyping was repeated on both root and shoot samples to confirm results. Three W22, twelve *AN2*:*an2* and three *an2*:*an2* samples were identified (Table 4).

Table 4: Genotyping results of 18 samples from the segregating line used for *F. verticillioides*-inoculation.

Sample	*Ds*	*An2*	Genotype	Sample	*Ds*	*An2*	Genotype
1	✓	×	***an2:an2***	**10**	✓	✓	*AN2*:*an2*
2	✓	✓	*AN2*:*an2*	**11**	✓	✓	*AN2*:*an2*
3	×	✓	**W22**	**12**	✓	✓	*AN2*:*an2*
4	✓	✓	*AN2*:*an2*	**13**	×	✓	**W22**
5	✓	✓	*AN2*:*an2*	**14**	✓	✓	*AN2*:*an2*
6	×	✓	**W22**	**15**	✓	×	***an2:an2***
7	✓	✓	*AN2*:*an2*	**16**	✓	✓	*AN2*:*an2*
8	✓	×	***an2:an2***	**17**	✓	✓	*AN2*:*an2*
9	✓	✓	*AN2*:*an2*	**18**	✓	✓	*AN2*:*an2*

Presence or absence of a PCR product using *Ds*-specific primers and *An2*-specific primers is indicated by a tick or a cross, respectively.

DNA was extracted from the seed that was overcome with the fungal growth (Sample 1) to test the hypothesis that it could be *an2:an2* and therefore more susceptible to *F. verticillioides.* The *an2:an2* genotype was confirmed as shown in Table 1. The hypothesis that the *an2*:*an2* mutant did not germinate fully as it was more susceptible to *F. verticillioides* inoculation could not be rejected. However, it could also be by chance that the sample didn't germinate, as happened in

two of the inoculated W22 samples in the preliminary study (Figure 11). It should be noted that a different batch of W22 seeds – with a lower recorded germination frequency - were used for the preliminary study. Seeds from the F_1 segregating line germinated 35 out of 36 times with this one notable exception. Definite conclusions cannot be drawn from one sample, but it is interesting to take note of. If kauralexins act against *F. verticillioides* in the seed, then their expected loss in *an2:an2* could potentially lead to increased susceptibility to pathogens such as *F. verticillioides*. Very little has been studied on the role of phytoalexins in disease resistance in monocot seeds. Stilbene phytoalexins have, however, been demonstrated to accumulate in the seeds of the angiosperm, peanuts (*Arachis hypogaea*), in response to the fungal pathogens *A. flavus* (Sobolev, 2008) and *Rhizopus oligosporus* (Wu et al., 2011). Decreased phytoalexin accumulation in peanuts has also been associated with increased *A. flavus* susceptibility (Dorner et al., 1989; Wotton & Strange, 1987). Kauralexins could play a similar role in response to *F. verticillioides*. Further work examining the role of diterpenoid phytoalexins in maize seeds is necessary to confirm or deny this.

Unfortunately, the seed tissue obtained from the *an2:an2* sample that did not germinate could not be compared to the other samples' root and shoot tissue in further analyses. This meant only two *an2:an2* samples could be analysed further. In order to try compensate for the low number of mutants, three randomly chosen *AN2*:*an2* samples were included for subsequent analyses. The three control and inoculated W22 samples were also used.

3.2.3. *an2* Mutants have reduced kauralexin accumulation

Kauralexin accumulation was profiled through GC-MS on the root tissue of the selected samples. Production of each individual kauralexin compound per fresh weight (FW) of the sample was determined relative to the internal control ^{13}C-linolenic acid and summed to get the total µg kauralexins.g^{-1} FW (Figure 13a). One-way ANOVA was performed on the samples and significant differences were found ($p < 0.05$). Kauralexins accumulated to significantly higher levels in W22_Fv compared to W22_Cont. This confirms that *F. verticillioides* induces kauralexin production in W22 root tissue, validating work by Vaughan et al. (2015). Kauralexins appeared to be downregulated in inoculated *AN2:an2* (*AN2:an2*_Fv) and particularly in *an2:an2* (*an2:an2*_Fv) compared to W22_Fv, however, these results were not considered statistically significant. This is likely due to the small sample number (n=2) of *an2:an2*. As *AN2:an2*_Fv also showed reduced kauralexin accumulation and was not significantly different to *an2:an2*_Fv, the two mutant lines were combined for analysis

(*an2*_Fv), thus increasing the sample size and giving greater statistical power. With the mutants combined, a significant difference was found between W22_Fv and *an2*_Fv (Figure 13b).

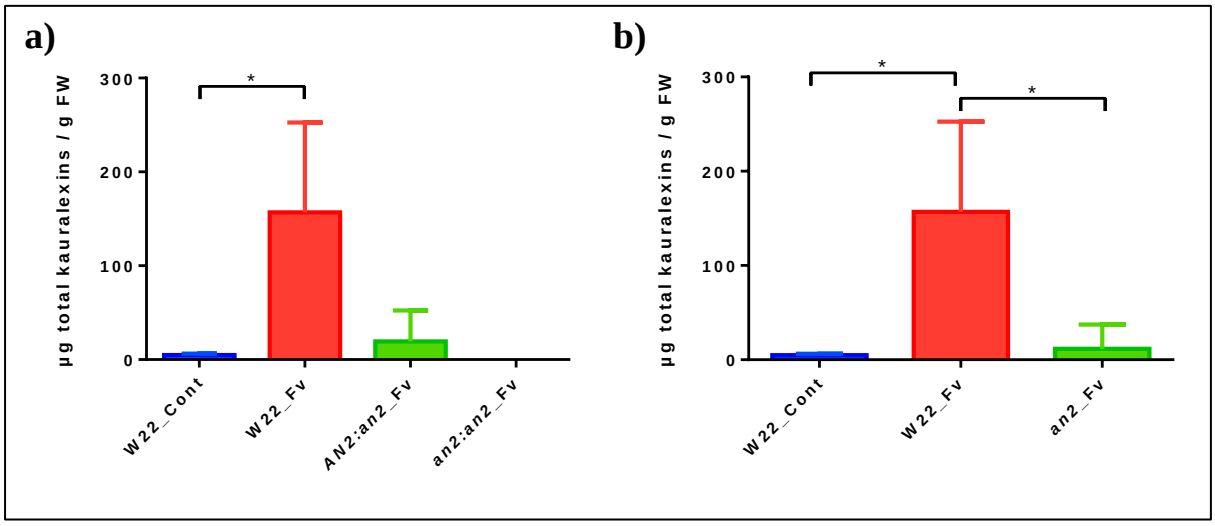

Figure 13: Total kauralexin accumulation examined in selected lines through GC-MS.
a) *AN2:an2*_Fv and *an2:an2*_Fv were examined separately along with W22_Cont and W22_Fv (mean + s.d.; n = 2 – 3). W22_Fv had the greatest kauralexin accumulation. One-way ANOVA showed significance between samples ($p = 0.03$), however only W22_Cont and W22_Fv were considered significantly different. **b)** *AN2:an2*_Fv and *an2:an2*_Fv were analysed together as *an2*_Fv. W22_Fv and *an2*_Fv were shown to be significantly different from one another (one-way ANOVA, $p = 0.01$). Tukey's HSD post hoc test was performed. Asterisks indicate significant differences (* $p < 0.05$).

As *AN2:an2*_Fv had less kauralexin accumulation compared to W22_Fv and was not significantly different to *an2*_Fv, it is probable that the presence of *Ds* in one allele has an effect on *An2* transcription following inoculation by *F. verticillioides*. Due to the small sample number of *an2:an2*, the *an2* mutants were combined for all further analysis hereon.

Individual accumulation of all six kauralexins is shown in Figure 14. Kauralexin A accumulation was greatest for Kauralexin A1, and lowest for A2. This trend was the same for the kauralexin Bs: B1 had the most, followed by B3 and B2, respectively. Kauralexin accumulation was significantly less in *an2*_Fv compared to W22_Fv for all the kauralexins analysed (one-way ANOVA, $p < 0.5$).

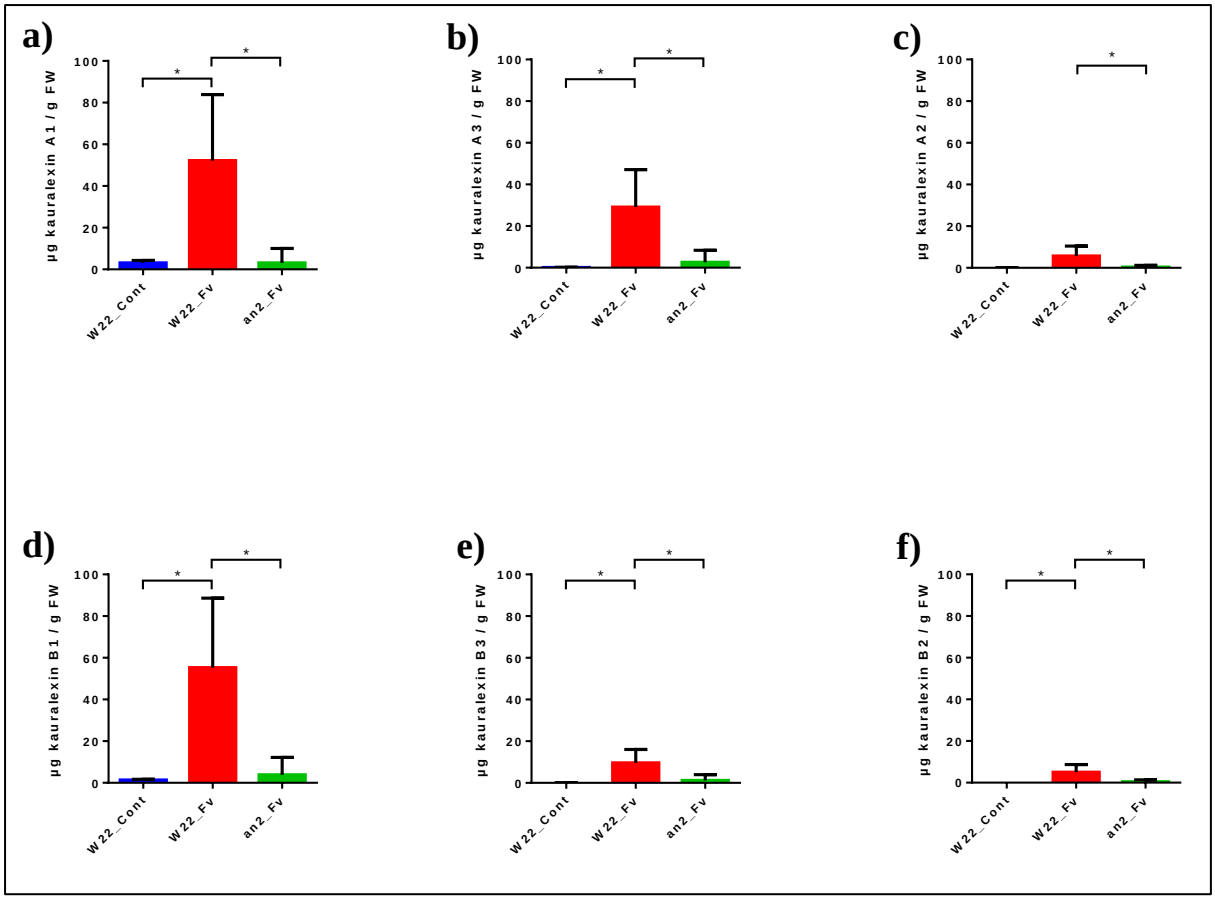

Figure 14: GC-MS profiling of root tissue indicate kauralexins have significantly less accumulation in *an2*_Fv compared to W22_Fv. The data was normalised to the internal control ^{13}C-linolenic acid. For the kauralexin As, accumulation was greatest for **a)** A1, then **b)** A3, then **c)** A2 having the lowest. Kauralexin B, accumulation was greatest for **d)** B1, then **e)** B3 and finally **f)** B2. One-way ANOVA was performed with significant differences found for all kauralexins ($p < 0.05$). W22_Fv was significantly up-regulated compared to W22_Cont in all samples, but kauralexin A2. Tukey's HSD post hoc test was performed. Asterisks indicate significant differences (* $p < 0.05$).

The trend of decreasing kauralexin accumulation beginning with A1 and B1 and ending in A2 and B2 reflects their order of oxidation, despite their nomenclature (they were discovered before A3 and B3 which are intermediate). Thus, kauralexin accumulation follows the expected trend giving greater confidence to the validity of the metabolite results as well as the understanding of the kauralexin biosynthesis pathway. The level of kauralexin As and Bs produced were similar, which is expected as they both lie downstream of *An2* (Figure 1).

Overall, the results strongly indicate that a *Ds*-insertion in *An2* reduces all kauralexin production, even when *Ds* is only inserted in one allele. This suggests *Ds* prevents *An2* from being fully or stably transcribed. If this is the case, one would expect *An2* gene expression to also be reduced in *an2*_Fv.

3.2.4. *an2* Mutants display reduced *An2* expression

An2 gene expression was analysed in root tissue in the selected samples, with significant differences found between groups (one-way ANOVA, $p < 0.01$) (Figure 15). *An2* expression in W22_Fv was shown to be significantly up-regulated in response to *F. verticillioides* compared to W22_Cont. Notably, there was significantly less *An2* expressed in *an2*_Fv compared to W22_Fv. There was still significantly greater expression in *an2*_Fv compared to W22_Cont ($p < 0.05$) (not shown in figure). This indicates *Ds*-insertions reduced or knocked down *An2* expression in response to *F. verticillioides*, although a moderate amount was still able to be transcribed.

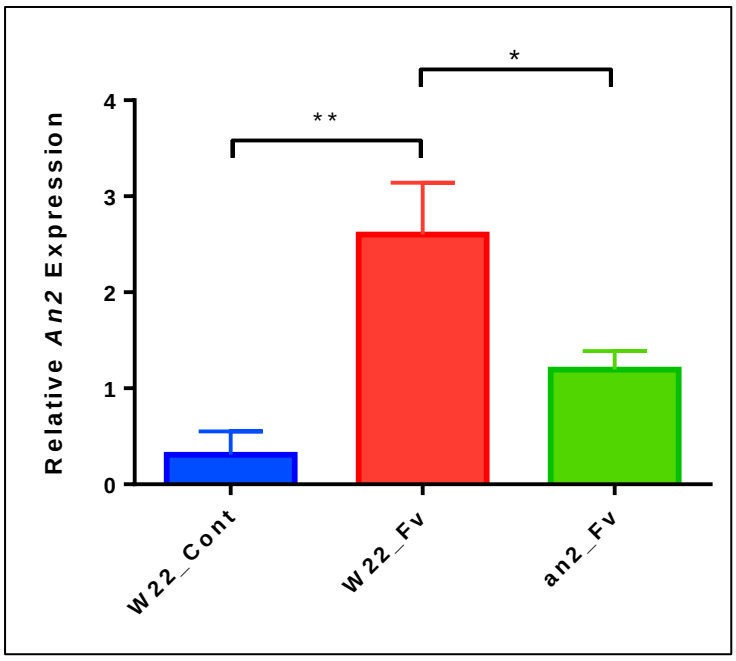

Figure 15: RT-qPCR showing *An2* expression (mean ± s.d.; n = 3 - 5) in W22_Cont, W22_Fv and *an2*_Fv. Reactions were carried out in triplicate and normalised to *LUG*, *MEP* and *UBCP*. There was a significant difference between all three groups (one-way ANOVA, $p = 0.004$) with W22_Cont expressing the least and W22_Fv expressing the most. Tukey's HSD post hoc test was performed. Asterisks indicate significant differences (* $p < 0.05$, ** $p < 0.01$).

These results show that *Ds*-insertions in *An2* did decrease expression, even though the gene could still be transcribed. As seen in previous experiments, *An2* was not knocked out entirely in *an2* mutants (Figure 10). The decreased expression could be due to increased secondary structures as previously hypothesized. Gene expression was correlated with kauralexin accumulation (Figure 13b) across all three sample groups, with a Pearson correlation coefficient value (r) of 0.94. *An2* expression therefore correlates very well with kauralexin accumulation, further indicating that *An2* expression leads to kauralexin production. The

positive correlation coefficient ties in with previous work showing a correlation coefficient of 0.93 between *An2* expression and kauralexin accumulation in a *C. zeina*-inoculated B73 line (Ntuli & Murray, 2016). This correlation indicates that transcription of the *An2* coding sequence leads to kauralexin accumulation, a theory which is supported by Schmelz et al. (2011).

KS2 and *KO*, the putative kauralexin biosynthetic genes that are co-expressed with *An2* (Christie et al., 2017) were also examined as shown in Figure 16. No significant differences were found in *KS2* expression (one-way ANOVA, $p < 0.5$), while *KO* was significantly up-regulated in W22_Fv compared to W22_Cont (student's t test, $p < 0.01$). There was no difference in *KS2* and *KO* expression between W22_Fv and an2_Fv.

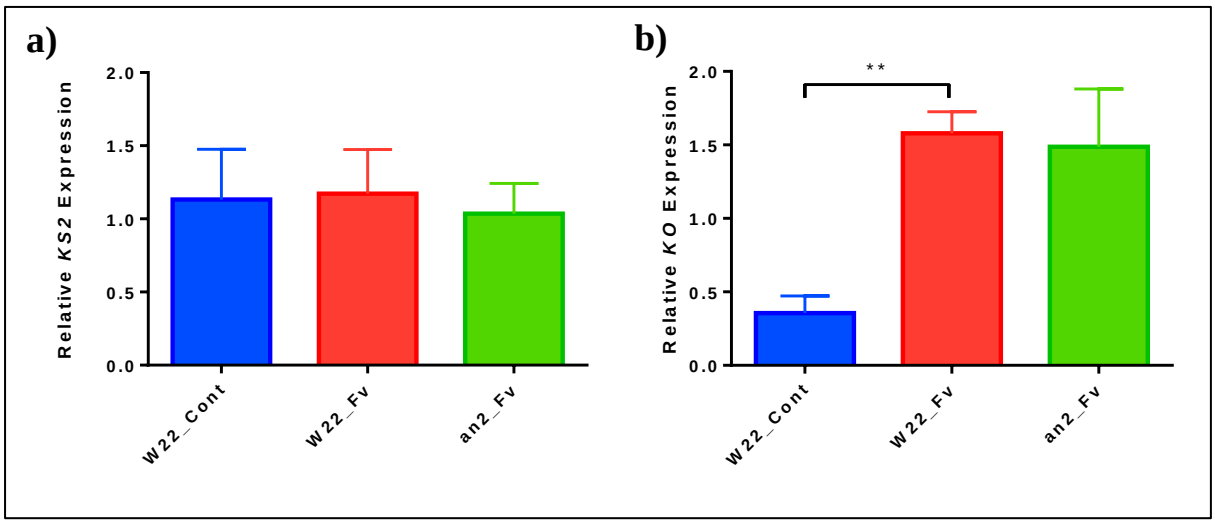

Figure 16: RT-qPCR showing *KS2* and *KO* gene expression (mean + s.d.; n = 3 - 5) in the roots of W22_Cont, W22_Fv and *an2*_Fv, normalised to *LUG*, *MEP* and *UBCP*.
a) *KS2* shows basal levels of expression in W22_Cont. There levels don't vary in W22_Fv and an2_Fv (one-way ANOVA, $p = 0.9$).
b) *KO* shows differential expression levels between samples with significant up-regulation in W22_Fv compared to W22_Cont (student's t test, $p = 0.002$), but no significant difference between W22_Fv and an2_Fv.

KS2 was not up-regulated in response to *F. verticillioides* inoculation (Figure 16a), indicating *F. verticillioides* may not have a regulatory effect on *KS2* expression in W22 roots. *KS2* may have already been induced and therefore *F. verticillioides*-inoculation had no impact. Stressors such as light (the roots were in clear media) or the stress of roots growing against the glass bottle could potentially have induced *KS2* expression, although no studies have been found to indicate light affects *KS2* expression. Another explanation for the pattern of *KS2* expression in W22_Cont roots is that it is developmentally regulated and is initially expressed constitutively

at low levels in W22 roots. Fu et al. (2016) identified a *kaurene synthase-like* gene that is constitutively expressed in B73 roots at low levels. However, in that study subsequent *F. graminearum*-inoculation increased transcript abundance which was not the case here. Further work analysing *KS2* in roots in various environmental conditions is necessary before drawing any conclusions about the role of *KS2*. *KO*, on the other hand, did show significant up-regulation in response to *F. verticillioides* (Figure 16b) and may play a role in disease resistance.

There was no clear difference in both genes' expression in *an2*_Fv compared to W22_Fv (Figure 15). These putative kauralexin biosynthetic genes have been shown to be co-regulated with *An2* (Christie et al., 2017), however, decreasing *An2* expression has no impact on expression of these downstream *KS2* and *KO* genes in the roots of *F. verticillioides*-inoculated W22 plants. Co-regulation of the three kauralexin genes could be due to transcriptional factors binding to common *cis*-regulatory elements in the genes, instead of by the upstream enzyme in the pathway. Another potential reason is that the small amount of kauralexin produced by *An2* is sufficient for *KS2* and *KO* to be expressed – if indeed they are reliant on upstream *An2* expression.

The zealexin biosynthesis gene, *terpene synthase 11* (*TPS11*) (GRMZM2G127087) is deemed to potentially induce zealexins accumulation (Huffaker et al., 2011). *Terpene synthase 6 (TPS6)* has also been linked with zealexin accumulation, however, we have previously only measured *TPS11* expression levels in African maize lines (unpublished). Therefore, we focused on *TPS11*. Gene expression analysis on *TPS11* led to significant differences being found (one-way ANOVA, $p < 0.05$), including up-regulation in W22_Fv and *an2*_Fv compared to W22_Cont (Figure 17).

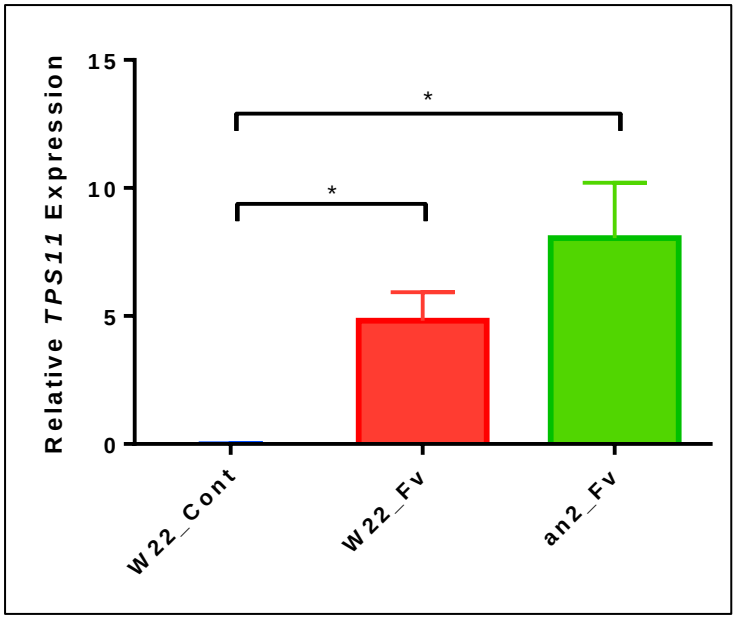

Figure 17: *TPS11* expression normalised to *LUG*, *MEP* and *UBCP* through RT-qPCR (mean + s.d.; n = 3 - 5). One-way ANOVA analysis showed significant differences between samples ($p = 0.04$) with significantly greater up-regulation in W22_Fv and *an2*_Fv compared to W22_Cont. Tukey's HSD post hoc test was performed. Asterisks indicate significant differences (* $p < 0.05$).

TPS11 showed significant up-regulation in response to *F. verticillioides*, which was not unexpected as *TPS11* has been shown to be up-regulated in response to the fungal pathogens *F. graminearum* and *A. flavus* in the hybrid maize Golden Queen (Huffaker et al., 2011). *TPS11* expression was slightly higher in *An2*_Fv than W22_Fv although the difference was not significant. *TPS11* is independent of *An2* so no reduction was expected. Interestingly, induction of *TPS11* expression (Figure 17) was much higher in comparison to the kauralexin genes (Figures 15 & 16).

Another experiment was conducted where nine F_1 segregating seeds were mock-inoculated and three W22 seeds *F. verticillioides*-inoculated. After 14 days the root tissue was harvested from the plants to examine *An2* expression in roots. There was no significant difference between mock-inoculated *an2* (*an2*_Cont) and W22_Cont. W22_Fv had markedly higher *An2* expression (Figure S1). Thus, confirming the significant difference in *An2* expression between *an2*_Fv and W22_Fv (Figure 15) was a result of *F. verticillioides* induction of gene expression, rather than as a result of *Ds*-insertion alone affecting *An2* expression in roots. No marked or significant differences in expression of *KS2*, *KO* and *TPS11* were found between *an2*_Cont and W22_Cont (data not shown).

3.2.5. *an2* Mutants show greater *F. verticillioides* disease symptoms than W22

After 14 days, *F. verticillioides* symptoms were apparent in the inoculated samples. Before harvesting, careful note was taken of the symptoms displayed by each sample and pictures were taken from the side and from below each jar. The phenotypes of two W22_Cont, two W22_Fv and two *an2*_Fv samples are shown in Figure 18. The W22_Cont samples had the most growth in above- and below-ground tissue (Figure 18a). The MS media the seeds germinated in was clear and the leaves appeared healthy with no visible senescence (yellowing due to cell death). The W22_Fv samples (Figure 18b) had noticeable symptoms of *F. verticillioides*-inoculation with senescence in leaves, light grey fungal mould around seeds, some red root discolouration and less tissue growth. The *an2*_Fv sample had more extreme *F. verticillioides* symptoms with even less growth in the leaves and roots and far more red discolouration in the roots (Figure 18c). Although not pictured, a root disfiguration was identified, and only seen, in *F. verticillioides*-inoculated samples. A 'corkscrew' appearance was apparent on a secondary root for many inoculated samples. Length of the 'corkscrew' varied, with some samples displaying this phenotype for up to 3cm long.

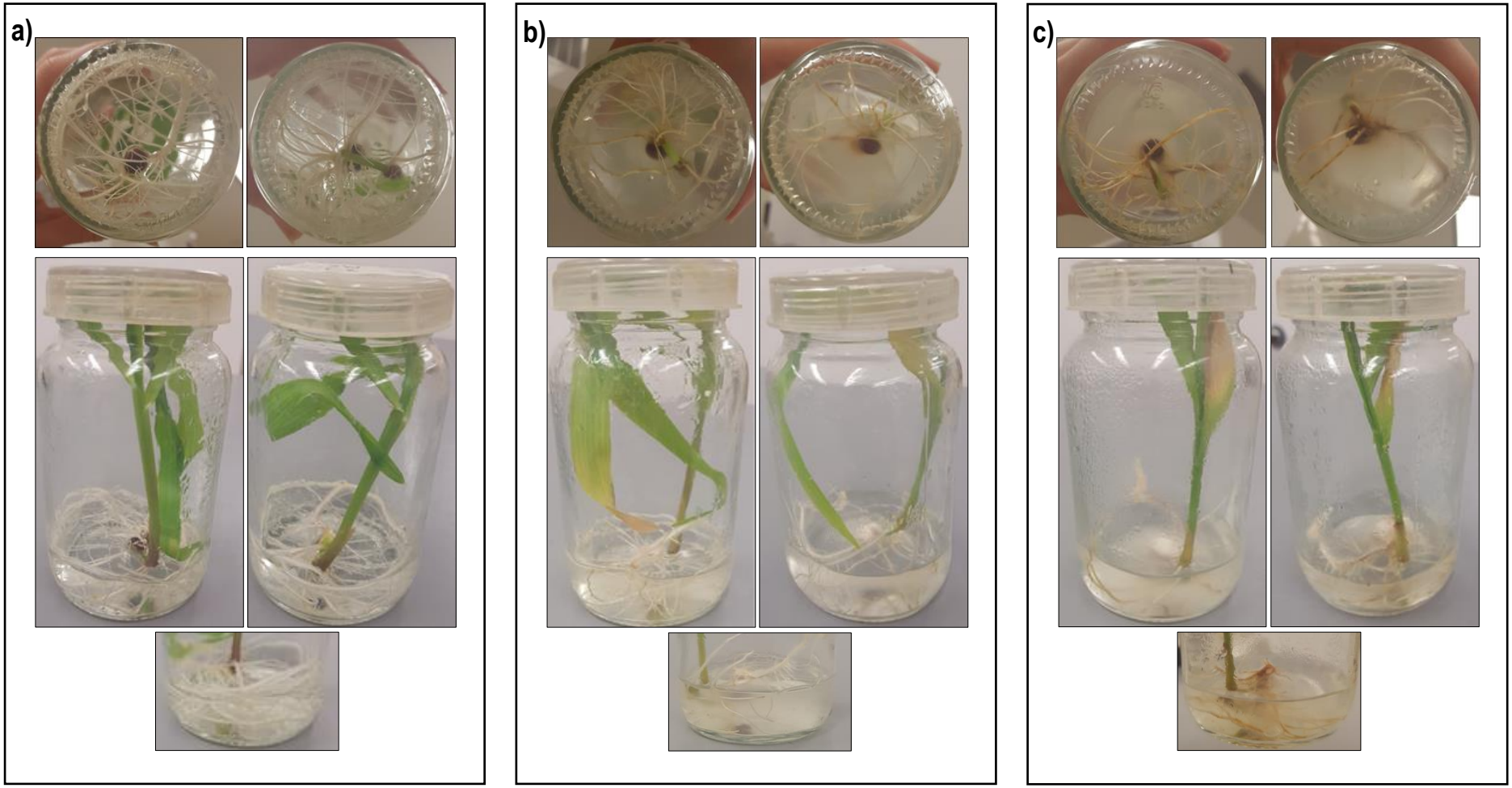

Figure 18: Pictures displaying phenotypes of W22_Cont, W22_Fv and *an2:an2*_Fv

a) Control W22 samples displayed healthy seedling growth in roots and shoots, with no senescence on leaves and clear MS media.

b) W22_Fv had truncated shoot and root growth compared to a, as well as leaf senescence and light grey fungal growth present in MS media.

c) *an2:an2*_Fv mutants had noticeably truncated root and shoot growth and greater senescence compared to b. Root redness and fungal growth was also more extreme.

The phenotypic differences between inoculated *an2*:*an2* and W22 are apparent (Figure 18). As can be seen, phenotypic fungal symptoms were far more extreme in the mutant plants. A scoring system was devised that took into account a number of factors, including truncation of root tissue, root disfiguration (indicated by 'corkscrew' root phenotype), red root discolouration, truncation of shoots, specific truncation of leaf one, and leaf senescence. Scores were given for each category by a comparison to the mock-inoculated control W22 samples. Values of 0 or 1 were given for absence or presence of shoot/root/leaf one truncation, or senescence. Values ranging from 0 to 3 were given for root redness or corkscrew root growth as those could be quantified through measurements. Further details of the scoring system and the individual values for each sample can be seen in Supplementary Table S1.

The scores were analysed and averaged, with the mean score values of W22_Cont, W22_Fv and *an2*_Fv shown in Figure 19. There were highly significant differences between the samples (one-way ANOVA, $p < 0{,}0001$), with W22_Fv showing significantly more *F. verticillioides* fungal symptoms than W22_Cont, and *an2*_Fv showing significantly greater difference than W22_Fv.

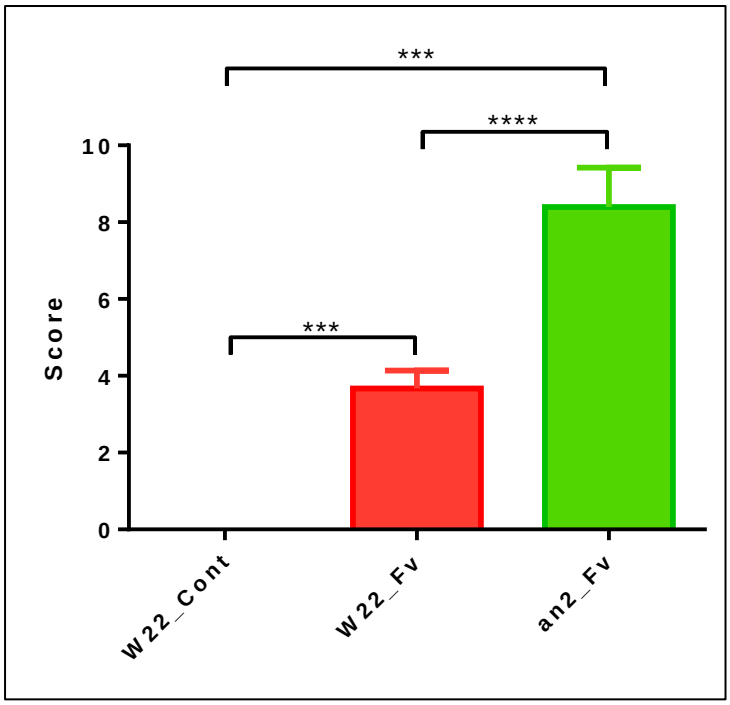

Figure 19: *F. verticillioides* phenotypic scores for the three sample groups. The scoring system took into account root, shoot and leaf one truncation as well as leaf senescence, root redness and root disfiguration. W22_Cont was set to 0, with any phenotypic differences compared to W22_Cont given values ranging from 1-3. One-way ANOVA showed significant differences ($p < 0{,}0001$), with an2_Fv having the highest score. Tukey's HSD post hoc test was performed. Asterisks indicate significant differences (*** $p < 0.001$, **** $p < 0.0001$).

W22_Cont did not display any symptoms of *F. verticillioides*-inoculation such as light grey mould, root redness, root disfiguration or leaf senescence. Their phenotypes looked far healthier, with greater root and shoot growth, than the inoculated samples Phenotypically *an2*_Fv appeared more susceptible to *F. verticillioides* than W22_Fv. The mutants displayed the same symptoms as W22_Fv but to a more extreme extent. Although the symptoms were noticeable, the scoring system had an element of subjectivity to it. To compensate for this, we used a range of values only when it could be quantified (diameter of corkscrew and root redness) and otherwise only gave values of 0 or 1 for the presence or absence of a distinct phenotype. Every phenotype was also compared to W22_Cont. However, it is hard to completely remove subjectivity so a fungal quantification of *F. verticillioides* was performed in order to validate the phenotypic results.

3.2.6. Inoculated *an2* mutants have greater fungal load compared to W22

The amount of *F. verticillioides* DNA relative to maize DNA was estimated with qPCR in order to obtain a quantified measure of fungal presence. Primers specifically designed for *F. verticillioides* (Nicolaisen et al., 2009) were used to quantify fungal DNA. This PCR product was sequenced in our lab and confirmed that the product was *EF1α* from *F. verticillioides* (Amy Veenstra, pers. comm.). Importantly, no fungus was detected in W22_Cont, confirming there was no *F. verticillioides* contamination and reinforcing its importance as a control. Overall, *an2*_Fv showed a large increase of fungus compared to W22_Fv in the root tissue (Figure 20). Greater fungus was expected in *an2* mutants if indeed they are important in disease resistance. However, the differences between all the sample groups was not considered significant using one-way ANOVA ($p > 0.05$).

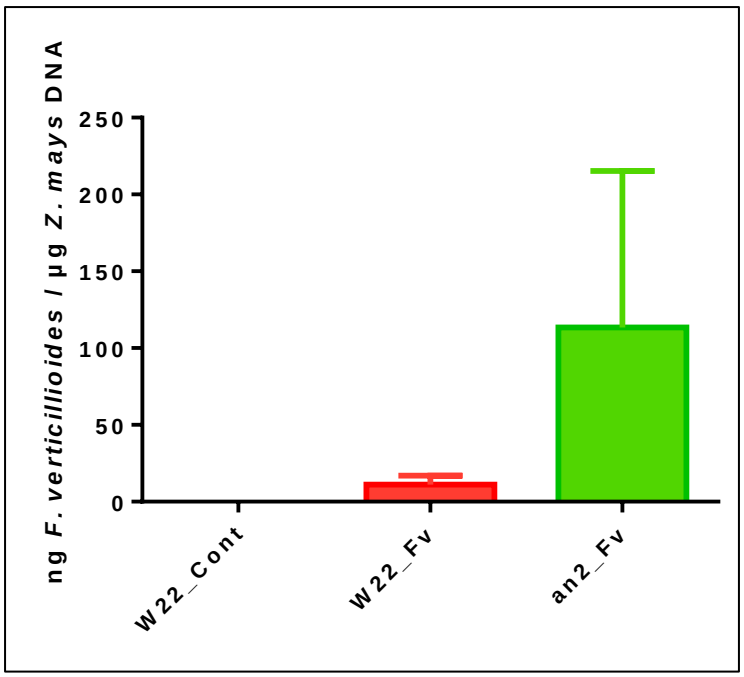

Figure 20: Fungal quantification in roots calculated through qPCR (mean + s.d.; n = 3 – 5). Fungal load determined based on the ratio of *EF1α* (encoding *F. verticillioides* DNA) to *LUG* (encoding plant DNA). There was an increase in fungal count in W22_Fv, with an even more marked increase in *an2*_Fv compared to W22_Fv. Differences between sample groups was not deemed significant (one-way ANOVA, p = 0.10).

W22 displayed mean *F. verticillioides* fungal load of 11.17 ng/µg. This in itself is a high fungal count, compared to previous *F. verticillioides*-inoculation assays in lab (unpublished) as well as amount of fungus quantified in other fungal pathogen inoculations (Korsman et al., 2012; Ntuli & Murray, 2016). Fungal load was even higher in *An2*_Fv with a mean of 113.5 ng/µg. However, none of this was considered statistically significant. A major reason as to why it was not considered significant is due to the high variation within the sample groups. Biological variation will always be expected between plants. Each plant system sends out its own defence signals (Dangl & Jones, 2001) and although the underlying mechanisms are the same, each system will have slight differences in its reactions. Even between wild type samples one expects variation in responses. There is also variability in how well the *F. verticillioides* fungus enters the seed. Thus, there is the variability of two biological systems – plant and pathogen – to take into account. These variations are controlled as well as possible, e.g. they are suspended in the same inoculum and kept under the same growth conditions, but variation will always occur. The small sample sizes (n = 3 - 5) also decrease the chances of acquiring a significant result. An example of how the statistics can be ambiguous is shown by the fact that neither W22_Fv nor *an2*_Fv were determined to have significantly more *F. verticillioides* fungus than

W22_Cont, despite the former being inoculated with it – and displaying high fungal load - and W22_Cont not.

Although the differences were not significant the results are still promising, especially when taken together with the fungal symptoms (Figure 18). The trend displayed by the phenotypic scoring system and fungal quantification was the same. There was a trend of increasing *F. verticillioides* from W22_Cont to W22_Fv to *an2*_Fv which is similar to the increased phenotypic symptoms displayed in Figure 19. Taken together, the increased *F. verticillioides* fungal DNA as well as the more severe fungal symptoms in *an2* mutants lend support to the initial hypothesis that *An2* knock-down mutants are more susceptible to *F. verticillioides*. However, due to the non-significant fungal quantification results the hypothesis cannot be proven. This experiment should be repeated with a larger sample size in order to be certain of whether or not *an2*_Fv accumulates more fungus.

The increased fungal load in *an2*_Fv compared to W22_Fv correlated negatively (r = -1.00) with both *An2* expression and kauralexin accumulation. This indicates that decreased kauralexin accumulation - due to reduced *An2* expression – made *an2* mutants more susceptible to *F. verticillioides*. This suggests the antifungal properties of kauralexins play a vital role in W22 maize resistance to *F. verticillioides*.

Fungal accumulation was also analysed in the shoots, and was determined to be much less (Figure S2). Very low amounts of fungus were present in the inoculated samples, with slightly more in *an2*_Fv, although not deemed significant. Although there was very little fungus present in this tissue, shoot growth was clearly affected as shown in Figure 18. This is most likely due to the aboveground tissue obtaining less nutrients from the roots. Greater fungal accumulation in the roots compared to shoots ties in with the work of Oren et al. (2003) who detected very little fungus in aboveground tissue.

3.2.7. *an2* Mutants have reduced zealexin accumulation

Through GC-MS profiling, a number of other metabolites were also measured, including zealexins. Zealexins A1, B1, A3 and A4 were detected, with high levels in A1 and B1 (means of 10.7 and 12.3 µg/g) and very low accumulation in A3 and A4 (means of 0.1 and 0.4 µg/g) in W22_Fv. Zealexin A1 has previously been shown to be highly accumulated in response to pathogen-induction by Huffaker et al. (2011), however, zealexin B1 did not show high accumulation in that study. The sum of the average accumulation of all four zealexins was

determined for the samples analysed, with significant differences found (one-way ANOVA, $p < 0.01$) (Figure 21). There was significantly greater total zealexin accumulation in W22_Fv compared to W22_Cont, which confirms previous work by Vaughan et al. (2015) that showed zealexins accumulate in response to *F. verticillioides* in W22 maize root tissue. The overall average of total zealexin accumulation was far less than that of total kauralexin accumulation in W22_Fv (Figure 13) (means of 23.46 and 156. 93 $\mu g.g^{-1}$ FW, respectively). Interestingly, *an2*_Fv had significantly less zealexin accumulation compared to W22_Fv.

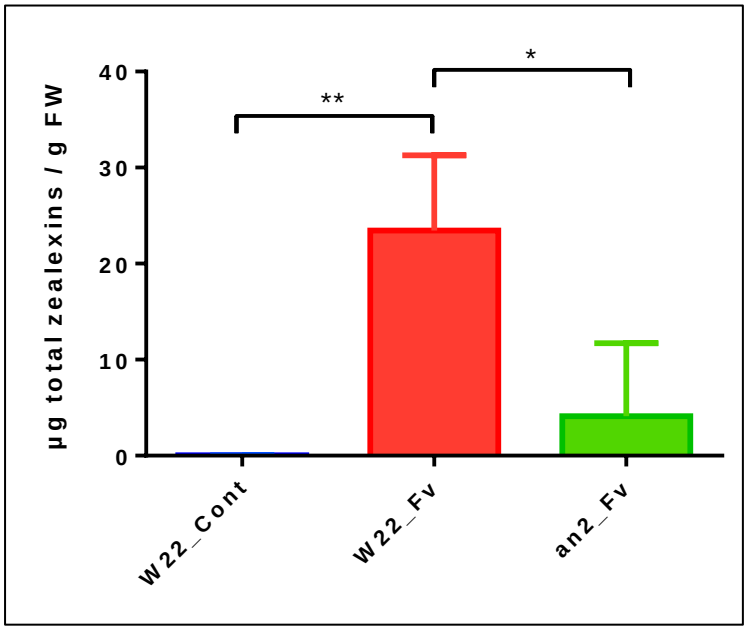

Figure 21: Total zealexin metabolites in root tissue in three sample groups (mean + s.d., n= 3-5), analysed using GC-MS. W22_Fv was significantly up-regulated compared to W22_Cont and there was significantly less accumulation in *an2*_Fv compared to W22_Fv (one-way ANOVA, $p = 0.005$). Tukey's HSD post hoc test was performed. Asterisks indicate significant differences (* $p < 0.05$, ** $p < 0.01$).

The decrease in zealexin accumulation in *an2* mutants is a novel result raising a question about how the two known maize phytoalexin pathways are linked. It has been hypothesized that there is pathway co-regulation between kauralexin and zealexins biosynthesis pathways by Ejike et al. (2013) as JA and ET synergistically act to promote kauralexin and zealexin production after fungal inoculation. A positive relationship has been shown between kauralexin and zealexins accumulation (Huffaker et al., 2011), but no studies have shown a link to indicate reducing *An2* expression and/or kauralexin accumulation would reduce zealexin accumulation as well. Vaughan et al. (2015) examined zealexin production between *an2* mutants and W22 in healthy and drought-stressed roots and found no significant decrease in zealexin accumulation in *an2* mutants in either scenario.

There was greater kauralexin accumulation in W22 in response to the hemibiotroph *F. verticillioides* than zealexin accumulation although both were significantly up-regulated. This is also in contrast to work by Vaughan et al. (2015) who showed greater zealexin accumulation in W22 roots exposed to *F. verticillioides*. This disparity could be for a few reasons, including the mode of inoculation. In that study, the roots were suspended in *F. verticillioides* whereas in this case the seeds were exposed to *F. verticillioides* and roots subsequently evaluated. There could also be a temporal component to differences in phytoalexin accumulation. These roots were analysed 14 days after planting, while in the study by Vaughan et al. (2015) the plants were 7 days old at the point of inoculation and were evaluated 21 days after that. There are also differences in growth conditions to consider. There is still much to learn about kauralexins and zealexins and what promotes their production.

Greater kauralexin than zealexin accumulation has also been found in response to another fungal pathogen, *C. zeina* (Ntuli & Murray, 2016), where kauralexins were up-regulated to a much greater extent than zealexins.

Other defence phytochemicals quantified through GC-MS profiling by Vaughan et al. (2016) and Christensen et al. (2015) were analysed in this study. One of these metabolites, 6-methxy-benzoxazolin-2-one (MBOA) is the downstream degradation product of 2,4-dihydroxy-7-methoxy-1,4-benzoxazin-3-one (DIMBOA) (Houseman et al., 1992). DIMBOA is the principal BX in maize and is considered a phytoanticipin (Meyer et al., 2016). MBOA displayed significant up-regulation in W22_Fv compared to W22_Cont, with levels of W22_Fv and *an2*_Fv remaining similar (Figure S3). This was in contrast to results shown by Vaughan et al. (2016) where MBOA accumulation appeared to display an inverse relationship to *F. verticillioides.* However, under drought conditions at normal [CO_2], MBOA accumulation appeared elevated in *F. verticillioides*-inoculated plants compared to controls (Vaughan et al., 2016). This means stressors in combination with *F. verticillioides*-inoculation have the potential to increase MBOA accumulation. MBOA may potentially have accumulated in W22_Fv for an unknown reason such as salinity, light intensity, etc. There was no difference in accumulation between W22_Fv and *an2*_Fv, indicating reduced *An2* expression has no effect on MBOA production. As MBOA is the degradation production of DIMBOA it is therefore *An2* likely has no affect on DIMBOA expression either. This is to be expected as DIMBOA is considered a phytoanticipin (Meyer et al., 2016) and has not been linked to the kauralexin biosynethic pathway.

The free fatty acid precursors of oxylipins which are involved in JA biosynthesis and have previously been shown to be increased in response to *F. verticillioides* (Vaughan et al., 2014) were also analysed (Figure S4). Significant differences between W22_Fv and *an2*_Fv were found in stearic and oleic acid accumulation (one-way ANOVA, $p < 0.01$), with significant decreases in accumulation in *an2* mutants. However, linoleic and linolenic acid showed no significant difference in accumulation between *an2*_Fv and W22_Fv (One-way ANOVA, $p > 0.05$). It is unclear why there is a difference between these four fatty acids and their role in response to kauralexin accumulation is worth further investigation, especially as previous studies have shown JA and ET induce kauralexins (Ejike et al., 2013; Schmelz et al., 2011). The other defence phytochemicals analysed in Vaughan et al. (2016) and Christensen et al. (2015) did not display any differential or vast accumulation in *an2* mutants or W22 in response to *F. verticillioides* (data not shown).

3.2.8. Discussion of *F. verticillioides*-inoculation experiments

An2 was up-regulated in response to *F. verticillioides*-inoculation in roots and in shoots (Figure 12), which was expected based on previous work (Vaughan et al., 2015). *An2* was expressed more highly in the roots than shoots, which made the roots the main focus of analysis. This was followed by *F. verticillioides*-inoculation of the segregating *an2* mutant line, which had previously not shown any reduced *An2* expression compared to W22 when only low amounts of *An2* expression was observed (Figures 7 & 10).

F. verticillioides-inoculation led to high kauralexin accumulation in W22_Fv, with significantly less kauralexins in the inoculated *an2* mutants. Although *an2:an2*_Fv had very little kauralexin accumulation (Figure 13a), the difference between it and W22_Fv was not considered significant, most likely due to the sample size of *an2:an2*_Fv (n=2). *AN2:an2*_Fv also displayed far less kauralexin accumulation than W22_Fv (means of 19.45 to 156. 93 µ/g, respectively). As *AN2:an2*_Fv mutants displayed reduced kauralexin accumulation – likely due to *Ds* insertion in one allele – they were pooled with *an2:an2*_Fv in order to increase replications in further analyses. Following this, the difference in total kauralexin accumulation between W22_Fv and *an2*_Fv was considered statistically significant (Figure 13b).

A novel and interesting find was that zealexins were also significantly reduced in *an2*_Fv (Figure 21). This seems to imply a link between *An2* and zealexin accumulation which has not been shown before. The fatty acids stearic and oleic acid also displayed significantly reduced

accumulation in *an2*_Fv compared to W22_Fv (Figure S4). This may imply *An2* plays a role in their regulation.

Gene expression analysis showed a significant up-regulation of *An2* in W22_Fv compared to W22_Cont (Figure 15). This confirms *F. verticillioides* induces *An2* accumulation in W22 roots. With the overall increase in *An2* expression, a significant difference was seen between W22_Fv and *an2*_Fv, with *an2*_Fv displaying reduced *An2* expression. This suggests *Ds*-insertions in *An2* knock-down expression rather than stopping it entirely. Although *an2*_Fv was decreased in comparison to W22_Fv, it was still significantly more than W22_cont, again indicating *An2* was still being transcribed. Our hypothesis is that *Ds* insertion does not prevent transcription but makes the gene transcript more unstable, for example by the formation of secondary structures. *An2* gene expression correlated highly with kauralexin accumulation (r = 0.94) when comparing W22_Cont, W22_Fv and *an2*_Fv. Thus, showing *An2* gene expression and kauralexin accumulation are linked.

Phenotypically, the inoculated *an2* mutants displayed greater fungal symptoms of *F. verticillioides* infection than W22_Fv (Figure 18). The difference between *an2*_Fv and W22_Fv was considered highly significant with the scoring system devised (Figure 19). The *an2* mutants also contained higher fungal load than W22_Fv (Figure 20). The difference, however, was not considered significant, likely due to vast biological variation and small sample sizes. When one takes into account the increased fungal load combined with greater phenotypic symptoms of fungal infection on *an2*_Fv there does appear to be evidence that *an2* mutants are more susceptible to *F. verticillioides*. Future work repeating fungal quantification with a greater number of samples should help confirm or deny this.

The fungal quantification in W22_Fv and *an2*_Fv had a perfect negative correlation with *An2* expression and kauralexin accumulation (r = -1.00). One can hypothesize that the increased *F. verticillioides* fungus present in *An2* mutants was a result of reduced phytoalexin accumulation which in turn was a result of reduced *An2* gene expression. Therefore, providing good evidence that *An2* plays a functional role in disease *F. verticillioides* resistance *in planta*. This all gives greater functional relevance to *An2* as a candidate gene for use in future resistance breeding and/or engineering, particularly as it may affect both kauralexin and zealexin pathways. More work is necessary to examine the role of *An2* in response to different pathogens and in different tissues.

3.3. *Cercospora zeina* inoculation

3.3.1. *C. zeina* inoculation leads to fungal growth in W22

An2 has been shown to be up-regulated in B73 in response to *C. zeina* (Christie et al., 2017). In order to determine whether *An2* is also up-regulated in W22, a *C. zeina*-inoculation was carried out. W22 samples were inoculated with *C. zeina* to determine the resistance phenotype. The W22 inbred line has been shown to be susceptible to the biologically similar *C. zeae-maydis* (Wisser et al., 2011), thus susceptibility to *C. zeina*-inoculation was expected also. A *C. zeina*-inoculation using 3×10^4 conidiospores.ml^{-1} has previously been successfully performed on maize lines (Meisel et al., 2009), however, when this dilution was attempted on W22 it did not lead to GLS infection (data not shown). A number of inoculation attempts were unsuccessfully performed with varying spore counts and environmental conditions.

It was noticed that the leaves of W22 plants produced spots or 'flecking', a mild lesion phenotype that was displayed on the older leaves (appearing approximately 10 days after the leaf had fully formed) in all plants in the W22 background (pictured in Figure 22). Despite attempts at optimising growth conditions (changing growth media and fertiliser regimes), this flecking phenotype persisted in both the plant growth chamber and growth room at UCT. The flecking was determined to be genetically regulated (Vontimitta et al., 2015).

Figure 22: Example of leaf flecking phenotype on a W22 plant at the V3 stage. This phenotype is under genetic controls and was common in the older leaves of all W22 plants.

Optimisation of *C. zeina*-inoculation of W22 was eventually obtained by increased humidity as high as possible and obtaining a spore count of 5×10^5 conidiospores.ml^{-1}. Six W22 seeds had been planted in pots in a plant growth chamber with controlled conditions and five germinated. Three of these plants were inoculated with the 5×10^5 conidiospores.ml^{-1} *C. zeina* suspension in the whorls of the forming third leaves. The two controls were mock-inoculated with water. All plants were at the late V2 stage (14 days) at the time of inoculation.

C. zeina is slow growing, with GLS symptoms usually only appearing after a week (Ward et al., 1999). Initial chlorosis symptoms, indicating GLS disease, appeared on the third leaf of inoculated plants at 7 dpi. At 14 dpi the disease symptoms were clearly apparent (Figure 23). Elongating lesions symptomatic of GLS (Latterell & Rossi, 1983) can be seen and a vast stress response was mounted in response to *C. zeina*, indicated by the red streaks (due to anthocyanin accumulation). Old conidiospores from the initial *C. zeina* inoculum can be seen on the leaves of inoculated plants (Figure 23b).

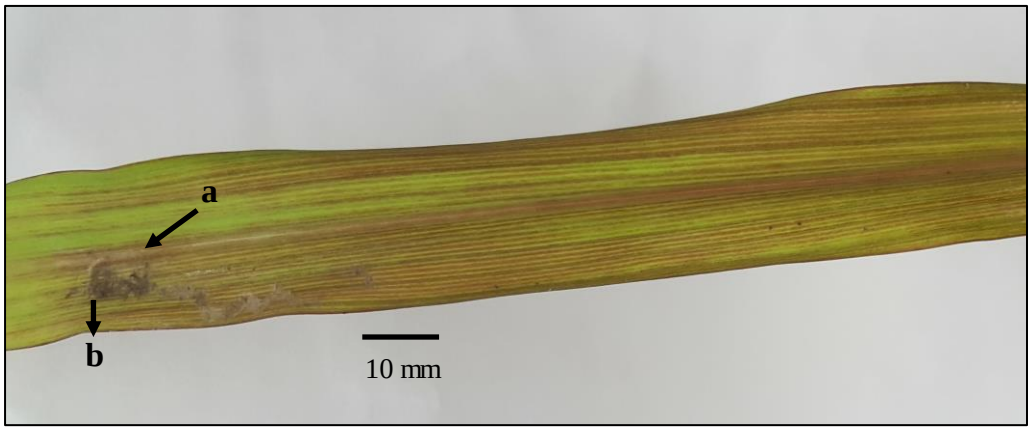

Figure 23: *C. zeina*-inoculated W22 leaf three at 14 dpi
a) Elongating lesion
b) Old *C. zeina* conidiospores from inoculation

In contrast, the third leaf of the control plants looked healthier with no evidence of elongated GLS lesions (Figure 24). There was a slight stress response with some red streaking apparent near the bottom of the leaf, most likely due to environmental conditions. Stress was far less than seen in *C. zeina*-inoculated leaves, however.

Figure 24: Mock-inoculated W22 leaf three at 14 dpi. The leaf appeared much healthier than those inoculated with *C. zeina*

The presence of elongating lesions in GLS symptom development has previously been shown to lead to high *An2* upregulation (Ntuli & Murray, 2016). The third leaf of the *C. zeina*-inoculated W22 plants displaying *C. zeina*-induced lesion elongations was harvested from each plant at 14 dpi. A 12 cm section surrounding the point of inoculation was harvested, excluding the tips of leaves which displayed signs of flecking and cell death. Matching leaf material was harvested from control plants.

DNA was extracted and qPCR performed to determine the fungal load of *C. zeina*, relative to plant DNA (Korsman et al., 2012). Fungal DNA was detected in inoculated W22 (W22_Cz) in comparison to the mock-inoculated control (W22_Cont), which displayed no fungus (Figure 25). However, this was not considered significant using a student's t test ($p > 0.05$). The non-significance was most likely due to the high variation present in W22_Cz and the small sample size of n = 2 and n = 3.

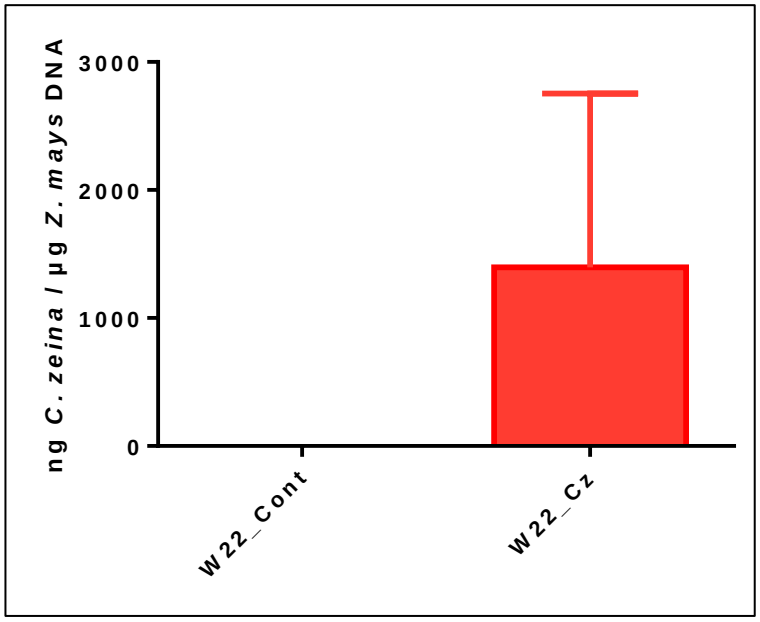

Figure 25: Fungal quantification using *C. zeina* fungal DNA (*CPR1* primers specific to *C. zeina*) relative to plant DNA (*MEP* primers) for W22_Cont and W22_Cz (mean + s.d.; n = 2 – 3). No fungus is in W22_Cont and a large amount is present in W22_Cz, albeit with high variation. The difference between W22_Cont and W22_Cz was not considered significant (student's t test, $p = 0.26$).

A very high amount of fungal DNA was detected. This was not surprising considering the high spore count used and the clear disease symptoms (Figure 23). Although the difference was not statistically significant, fungus was quantified in each inoculated sample with none present in controls. This gave confidence that *C. zeina*-inoculation increased fungal load in W22 lines

and can be detected through qPCR. The *CPR1* primers (Table 2) used in fungal quantification had previously been designed for, and confirmed to detect, *C. zeina* in leaves of an inbred maize line (Korsman et al., 2012), giving confidence in the primers' specificity.

3.3.2. *An2* showed low expression in response to *C. zeina* inoculation in W22

GLS resistance, caused by *C. zeae-maydis*, has previously been evaluated in W22 (Wisser et al., 2011), but neither kauralexin accumulation nor *An2* expression was analysed. *C. zeina* inoculation leads to high *An2* upregulation (and upregulation of two putative kauralexin biosynthesis genes, *KS2* and *KO)* in the inbred maize line B73 (Christie et al., 2017). *An2* is upregulated in W22 in response to *F. verticillioides* (this study; Vaughan et al., 2015). Based on the above, we expected *C. zeina* to induce high *An2* expression in W22.

An2 expression was analysed on the cDNA of the W22 leaf samples described in section 3.3.1. There was a very slight increase in W22_Cz in comparison to W22_Cont, however, this was not significant (student's t test, $p > 0.05$) and expression was low throughout all the samples (Figure 26).

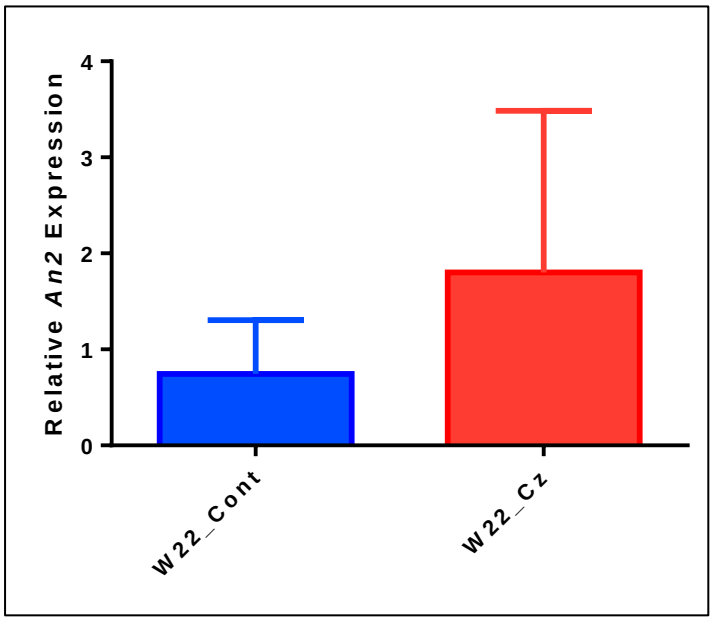

Figure 26: RT-qPCR using *An2* primers to detect expression in the third leaf of W22 samples, either mock-inoculated or inoculated with *C. zeina* (mean + s.d.; n = 2 – 3). Gene expression was normalised to *LUG* and *MEP*. There was no significant difference in *An2* expression between W22_Cont and W22_Cz (student's t test, $p = 0.47$).

Based on these results, *An2* does not appear to be upregulated in response to *C. zeina* in W22 at the lesion elongation symptom stage at 14 dpi. There was a small non-significant increase in

An2 expression in W22_Cz compared to W22_Cont. Repeating the experiment with more samples would give greater confidence in the results, but gene expression appears too low for it to make a significant difference.

High up-regulation in response to *C. zeina* was expected based on previous work (Christie et al., 2017). However, this was not seen in the W22 plants. This could be for a number of reasons. Firstly, it could be a characteristic of the W22 genotype. *An2* expression has not been determined in *C. zeina*-inoculated W22 plants previously. There is also a chance the period when *An2* was expressed was missed. However, *An2* is usually highly expressed when GLS lesions are extended (Ntuli & Murray, 2016). The reason we propose as being most likely to be responsible for low *An2* expression is the flecking phenotype seen on the older leaves (Figure 22).

Flecking has been characterised as a mild constitutive defence response observed on many maize inbred lines that is correlated with and might confer broad-spectrum disease resistance. (Vontimitta et al., 2015). It is generally agreed that flecking is genetically determined and not due to environmental conditions (Olukolu et al., 2016; Vontimitta et al., 2015). The severity of flecking has been correlated with higher levels of resistance to a number of diseases, including GLS (Olukolu et al., 2016). This would explain why a higher *C. zeina* spore count was required to induce GLS symptoms in W22 plants in comparison to previous studies using GLS susceptible lines (Meisel et al., 2009), despite W22 expected to be susceptible to GLS (Wisser et al., 2011). *C. zeina* was still able to infect leaves, based on the inoculated phenotype (Figure 23) and fungal quantification results (Figure 25). Therefore, W22 plants could still be infected by *C. zeina*. However, it is believed that genes involved in flecking may also be involved in regulating JA levels (Olukolu et al., 2016). As JA is involved in *An2* regulation (Schmelz et al., 2011), this likely has an effect on inducing basal levels of *An2* expression.

Despite these results, it was decided to proceed with *C. zeina* inoculation in order to determine if knocking down *An2* has any noticeable effect on kauralexin accumulation, *An2* expression, and fungal quantification.

3.3.3. *an2* Mutant lines were screened in response to *C. zeina*-inoculation

In order to try to remove sample size as a limiting factor, the last remaining 31 seeds of the chosen cross-pollinated cob were used in the final *C. zeina*-inoculation. Three W22 seeds were also included as controls. The seeds were planted and after 16 days a 1 x 3cm section of leaf

one was harvested from each plant when they were at the mid to late V2 stage, including the W22 controls. DNA was extracted from this material and genotyped using the *Ds*-specific PCR (Figure 4a). Of the 31 segregating plants, 27 were positive for *Ds*. Six *Ds*-positive plants were mock-inoculated to serve as future controls (*an2*_Cont). Three *Ds*-negative were also mock-inoculated. Due to low spore count when the time came, the third leaf was not able to be inoculated as was done in the W22 experiment described previously. The samples were inoculated with 1×10^5 conidispores ml^{-1} of *C. zeina* in the forming whorl of the fifth leaf instead, when the plants were 35 days old. A 12cm section of each fifth leaf, surrounding the point of inoculation, was harvested at 10 dpi. No clear symptoms of GLS were apparent then, but tissue was harvested earlier so as to avoid the leaf flecking phenotype which had not yet developed on the fifth leaf.

Genotyping was performed again on the DNA of each sample with both primers to confirm presence of *Ds* and determine which were *an2:an2*. The results of the genotyping and list of plants (inoculated and mock-inoculated controls) is shown under Table 5.

Table 5: Genotyping of 31 samples from the segregating line and 3 known W22. Samples were either inoculated (I) or mock-inoculated controls (C) as indicated.

Sample	**I / C**	***Ds***	***An2***	**Genotype**	**Sample**	**I / C**	***Ds***	***An2***	**Genotype**
1	I	✓	✓	*AN2:an2*	**18**	I	✓	✓	*AN2:an2*
2	I	✓	✓	*AN2:an2*	**19**	C	×	✓	W22
3	I	✓	✓	*AN2:an2*	**20**	C	✓	✓	*an2:an2*
4	I	✓	✓	*AN2:an2*	**21**	I	✓	✓	*an2:an2*
5	C	✓	✓	*AN2:an2*	**22**	I	✓	✓	*AN2:an2*
6	I	✓	✓	*AN2:an2*	**23**	C	✓	✓	*AN2:an2*
7	C	✓	×	*an2:an2*	**24**	C	✓	✓	*AN2:an2*
8	I	×	✓	W22	**25**	I	✓	✓	*AN2:an2*
9	I	✓	×	*an2:an2*	**26**	I	×	✓	W22
10	I	✓	×	*an2:an2*	**27**	I	✓	✓	*AN2:an2*
11	I	×	✓	W22	**28**	C	✓	✓	*AN2:an2*
12	I	✓	✓	*AN2:an2*	**29**	I	✓	✓	*AN2:an2*
13	I	✓	✓	*AN2:an2*	**30**	I	✓	✓	*AN2:an2*
14	I	✓	✓	*AN2:an2*	**31**	I	✓	✓	*AN2:an2*
15	C	✓	×	*an2:an2*	**W22 1**	C	×	✓	W22
16	I	✓	×	*an2:an2*	**W22 2**	C	×	✓	W22
17	C	✓	×	*an2:an2*	**W22 3**	C	×	✓	W22

Presence or absence of a PCR product using *Ds* primers and *An2*-specific primers is indicated by a tick or a cross.

At least three each of inoculated W22 (W22_Cz), control W22 (W22_Cont), inoculated *an2:an2* (*an2*_Cz) and control *an2:an2* (*an2*_Cont) were obtained and used in subsequent analyses.

3.3.4. Kauralexins did not significantly accumulate in W22 or *an2*

Kauralexin production was determined through GC-MS profiling. The total kauralexins are shown in Figure 27. Kauralexin accumulation was very low throughout with no significant differences between the sample groups (one-way ANOVA, $p > 0.05$). In addition, there were no significant differences between the kauralexin A and B series in any of the sample groups (data not shown).

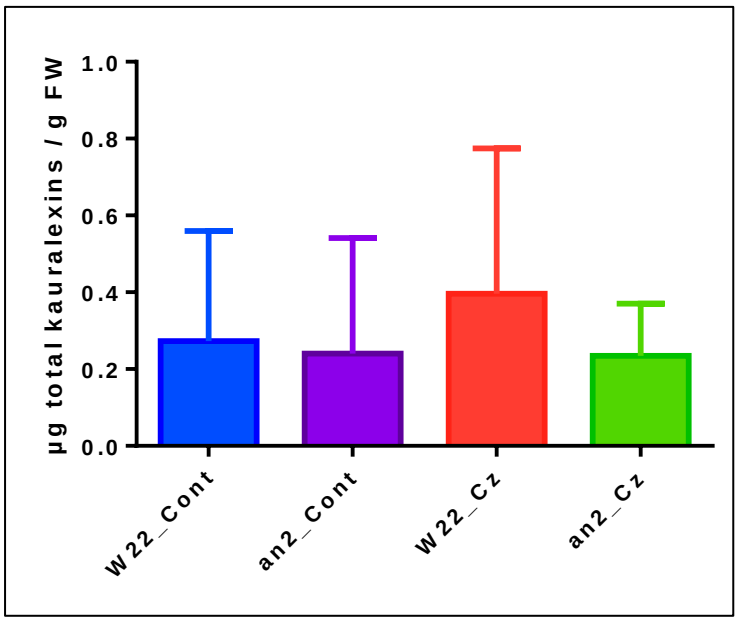

Figure 27: The sum of the mean of all six kauralexins was determined through GC-MS profiling and normalised to the internal control to get $\mu g.g^{-1}$ FW. No significant differences were found (one-way ANOVA, $p = 0.54$)

Kauralexin accumulation was very low, particularly when compared to the amount produced in response to *F. verticillioides* (Figure 13). The mean of total kauralexins in inoculated W22 with *F. verticillioides* was 156 932 compared to 497 $\mu g.g^{-1}$ FW here. Kauralexin accumulation was greatest for W22_Cz and there was a slight decrease in *an2*_Cz, but variation was too high for there to be a significant difference. The trend of decreased accumulation in *an2*_Cz was what we expected based on the initial hypothesis and the trend seen in *F. verticillioides*. However, in order to see a significant difference, more kauralexins most likely need to be produced in the inoculated W22 samples.

Zealexin accumulation was also examined, with only zealexins A1 and B1 detected. Total zealexin accumulation showed no significant differences between sample groups (one-way ANOVA, $p > 0.05$) and low overall accumulation (Figure S5). The trend was similar to total kauralexins, with a slight decrease in *an2*_Cz compared to W22_Cz, but not significant.

3.3.5. *An2* was not knocked down in *an2* mutants

Gene expression was analysed, with no significant up-regulation in *An2* expression in W22_Cz compared to W22_Cont. *An2* was also not knocked down in *an2*_Cz (Figure 28). Expression levels were low throughout with no significant differences (one-way ANOVA, $p > 0.05$).

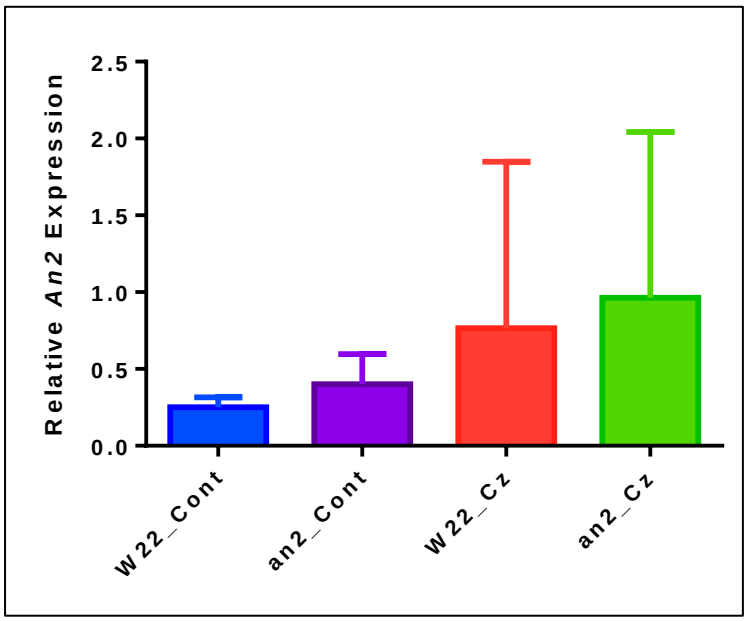

Figure 28: RT-qPCR showing *An2* expression in leaves of mock- and *C. zeina*-inoculated W22 (mean + s.d.; n = 3). Reactions were normalised to the reference genes *LUG* and *MEP*. No significant differences were found (one-way ANOVA, $p = 0.67$).

The most important thing to note is that *An2* was lowly expressed in W22_Cz with no significant upregulation compared to W22_Cont. This was expected based on the low kauralexin accumulation (Figure 27) as it's been shown that *An2* expression and kauralexin accumulation are highly correlated (this study; Ntuli & Murray, 2016). It also ties in with the preliminary *C. zeina*-inoculation gene expression results (Figure 26) where *An2* was also shown to be low. As previously hypothesized, this is most probably due to the leaf flecking phenotype observed in W22. Although newer tissue was harvested for this experiment to avoid the flecking, the older leaves had flecking which would have conferred resistance throughout the plant. *KS2* and *KO* were also analysed and displayed low expression levels, with no significant differences found between *an2*_Cz and W22_Cz (data not shown).

The gene expression results are similar to those found in the healthy seedling analysis (Figures 7 & 10) where no knock-down of *An2* was detected in mutants when *An2* expression levels were low. This again confirms that in order to see a knock-down of *An2* expression in the *an2* mutant, *An2* expression must be highly induced in inoculated W22. Interestingly, there was again slightly more expression in *an2* mutants than in respective W22 sample, although this was not significant. It does however tie in with the seedling analysis where this trend of slightly increased *An2* expression in mutants compared to W22 was seen at very low expression levels

3.3.6. Inoculated *an2* mutants have greater fungal load than controls

The leaves were harvested at 10 dpi to have tissue from an earlier leaf stage than was studied previously, before necrosis and/or leaf flecking. However, this meant GLS had not yet become fully symptomatic as shown in Figure 29 where a leaf from each of the genotypes studied is pictured.

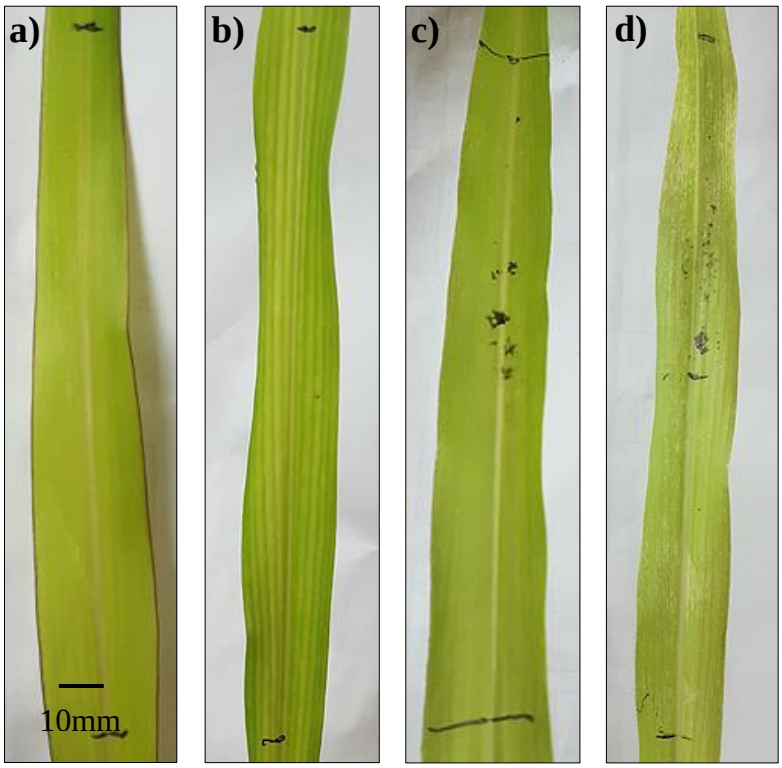

Figure 29: The fifth leaf of mock- and *C. zeina*-inoculated samples was harvested from **a)** W22_Cont **b)** *an2*_Cont **c)** W22_Cz and **d)** *an2*_Cz The black marker lines indicate the 12 cm section that was harvested. Note that the dark grey markings in the middle of the leaves in **c** and **d** are the leftover conidia from the *C. zeina*-inoculation in the whorl prior to emergence of the leaf. A scale is shown on the bottom left.

It can be seen that the *an2*_Cz sample (Figure 29d) displayed chlorotic spots which were not present in the other samples. This is one of the first symptoms of GLS (Ward et al., 1999). This seems to indicate that *an2*_Cz may be more susceptible than W22_Cz if symptoms are starting earlier. Overall, the *an2*_Cz samples showed slightly more visual chlorosis than W22_Cz, but the differences were not extreme.

In order to determine if *an2_Cz* was more susceptible in comparison to W22_Cz, fungal quantification of *C. zeina* relative to maize DNA was performed. Although not fully symptomatic, *C. zeina* would still be present and detectable in the leaves after 10 days. *C. zeina* fungal load was quantified through qPCR as shown in Figure 30. There was no fungus present in the W22_Cont or *an2*_Cont, confirming that contamination did not take place.

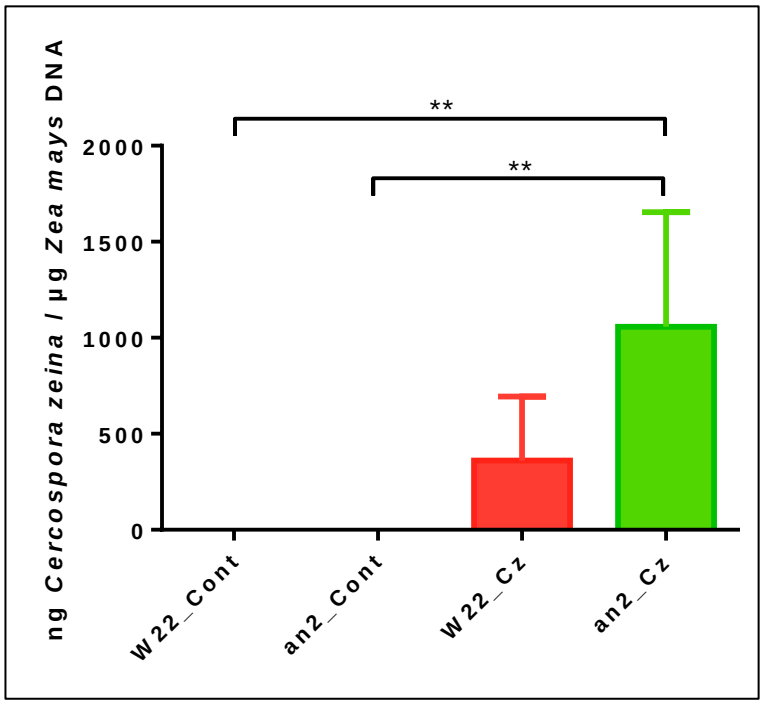

Figure 30: Fungal biomass in leaves was calculated through qPCR with *CPR1* primers specific to *C. zeina*, relative to maize DNA (determined through *MEP* primers) (mean + s.d.; n = 3). Significant differences were found (one-way ANOVA, $p = 0.003$). Post hoc Tukey's HSD test was performed for multiple comparisons. Asterisks indicate significant differences (** $p < 0.01$).

C. zeina-inoculation led to greater fungus present in inoculated leaves, although fungal biomass was low throughout. *C. zeina* was detected in W22_Cz and significantly more in *an2*_Cz compared to mock-inoculated controls. In addition, there was more fungus present in *an2*_Cz compared to W22_Cz although this difference was not significant. The fungal quantification results together with the leaf phenotypes seem to indicate that *an2*_Cz may be more susceptible

to *C. zeina* inoculation than the W22 control, but differences are not extreme. This is most likely due to the low *An2* expression and therefore low kauralexin accumulation. The fungal load was much lower than in the preliminary experiment (Figure 25), as the high spore count used in that experiment was not able to be obtained again, particularly with the need to inoculate a much larger number of samples. However, the fungal load does not appear to have made a difference in *An2* expression as it was low in both cases (Figures 26 & 28).

3.3.7. Discussion of *C. zeina* inoculation

Inoculation of *C. zeina* in the whorls of young W22 plants led to increased fungal DNA accumulation in both W22 (Figure 25) and *an2* mutants (Figure 30). Unfortunately, we were not able to obtain as high a spore count in the inoculation on the *an2* mutants. However, as *An2* was not significantly increased in W22_Cz in either experiment (Figures 26 & 28), this is unlikely to have made a big difference to the outcome. Low induction of *An2* was unexpected based on work done by Christie et al. (2017) where *C. zeina*-inoculation led to high *An2* upregulation in B73.

We hypothesize that the reason for low *An2* expression was due to the phenotype of leaf flecking (Figure 22) which was detected on the older leaves of all W22 plants, both control and mutant. Leaf flecking has been correlated with increased disease resistance, with a specific correlation shown in response to GLS (Olukolu et al., 2016). Due to this, *C. zeina*-inoculation was tested a number of times on W22 using much higher spore counts than previously used (Meisel et al., 2009). Thus, under these conditions *C. zeina* was still capable of causing infection as shown in Figure 23. Although *C. zeina*-inoculation was eventually successful, leaf flecking leads to an enhanced broad-spectrum disease response (Vontimitta et al., 2015). This would likely interfere with the phytoalexin pathway if SAR has been activated in the plant. In fact, candidate genes associated with flecking are potentially involved in the JA-dependent pathway (Olukolu et al., 2016). JA has been shown to regulate *An2* levels along with ET (Schmelz et al., 2011) and is induced in response to necrotrophs (such as *C. zeina*) (Bary, 2012). In the *F. verticillioides* metabolite analysis, *an2* mutants had differential expression of free fatty acid precursors involved in JA biosynthesis compared to W22 (Figure S4). If flecking modulates JA as hypothesized, this would most likely have an effect on *An2* expression and subsequent kauralexin accumulation.

Flecking was not apparent on the newer leaves (immediately post emergence from the whorl) which were harvested for analysis (Figure 29), but as flecking is purported to lead to broad

spectrum resistance throughout the plant, flecking on the older leaves would have led to increased resistance on the new ones too.

Despite all this, there did appear to be a slight increase in disease symptoms (Figure 29) and fungal DNA (Figure 30) in *an2*_Cz compared to W22_Cz. These differences were too small to be significant, but there is promise that knocking down *an2* could increase susceptibility to *C. zeina*. For future work, in terms of examining the response of *an2* mutants to *C. zeina* inoculation, we suggest using a different method in a different maize line to avoid the flecking phenotype. For example, gene silencing through RNAi (van der Linde et al., 2011), or CRISPR-Cas9 (Svitashev et al., 2016) are other methods to knock-down *An2* expression without having to use the W22 line. Another way of characterising *An2* would be to clone and overexpress it in a different plant system and examine the response.

3.4. Cloning *An2* towards *A. thaliana* transformation for overexpression

3.4.1. Overview of cloning

An alternative method of determining the benefit of *An2* is to overexpress it and determine if this leads to improved resistance to fungal pathogens. It was decided to clone *An2* into the dicoytledon, *A. thaliana*, which does not contain a kauralexin biosynthesis pathway and for which the turnover time to get mutant progeny is far shorter than maize. As *A. thaliana* is a model system, the tools and vectors required for cloning and overexpressing are readily available. As *A. thaliana* has an *An1* gene involved in gibberellic acid (GA) synthesis (http://www.plantcyc.org/), the *An2* precursors would be produced and *An2* can be screened in transgenic lines.

Diterpenoid phytoalexins are only found in monocots (Ahuja et al., 2012; Huffaker et al., 2011; Schmelz et al., 2011). By overexpressing *An2* in a transgenic Arabidopsis line, one evaluates if kauralexins could be produced in a different plant system. If so, it would enable more potential uses of *An2* and show its use in a biotechnology role. The aim towards overexpression of *An2* in *A. thaliana* was to establish if kauralexins could be produced in dicotyledons, and play a role in resistance through analysis of response to the fungal pathogen *Botrytis cinerea*. The Gateway pENTR-1A (Invitrogen) cloning vector (Figure 3a) was used as the initial entry vector. Restriction cloning the gene of interest, *An2*, into pENTR-1A would generate an entry clone. A recombination reaction between this and the Gateway destination vector pFAST-G02

(Shimada et al., 2010) would generate an expression clone. This expression clone would be introduced into *A. thaliana* via *Agrobacterium tumefaciens* transformation using the floral-dip method. *An2* would be driven by CaMV35S promoter.

3.4.2. Restriction digest of *An2* and pENTR-1A

As a large gene, the cDNA of *An2* alone spans 2.76 kb. Primers were designed that amplified the full length cDNA (Table 2), with restriction sites at both ends, designed to fit in-frame into pENTR-1A for directional cloning. XhoI and BamHI were the respective restriction sites used initially. These primers were used in a PCR to amplify *An2* using cDNA of B73 maize tissue that had been inoculated with *C. zeina*, and in which *An2* expression had previously been shown to be very high (Christie et al., 2017). PCR conditions were optimised, with PCR products of the expected sizes being produced (Figure 31). The resulting PCR products were subsequently gel extracted and purified.

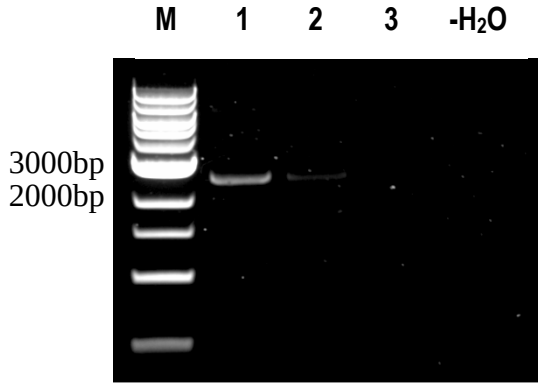

Figure 31: *An2* primers produced a clear 2.76 kb PCR product using 1) 100 ng and 2) 10 ng cDNA. No clear product was seen in 3) 1ng cDNA. M indicates 1 kb DNA ladder (NEB).

A double restriction digest was performed on the insert and pENTR-1A vector with BamHI and XhoI. In pENTR-1A the restriction sites frame the toxic *ccdB* gene (Gateway™ pENTR™ Vectors Instruction Manual, Invitrogen, 2002). The *ccdb* gene allows negative selection of non-recombinant clones. Vectors containing this gene would be unable to be propagated in *E. coli* DH5α cells due to the toxic *ccdB* gene product. Through successful double digestion of pENTR-1A and extraction of the larger backbone, the *ccdB* gene would be removed. Digested pENTR-1A was run on a gel and two DNA products of the expected sizes were present: The larger ~2.3 kb product that formed the backbone of the vector and smaller ~750bp product

which contained the *ccdB* gene (Figure 32). The larger product was excised and purified through gel extraction.

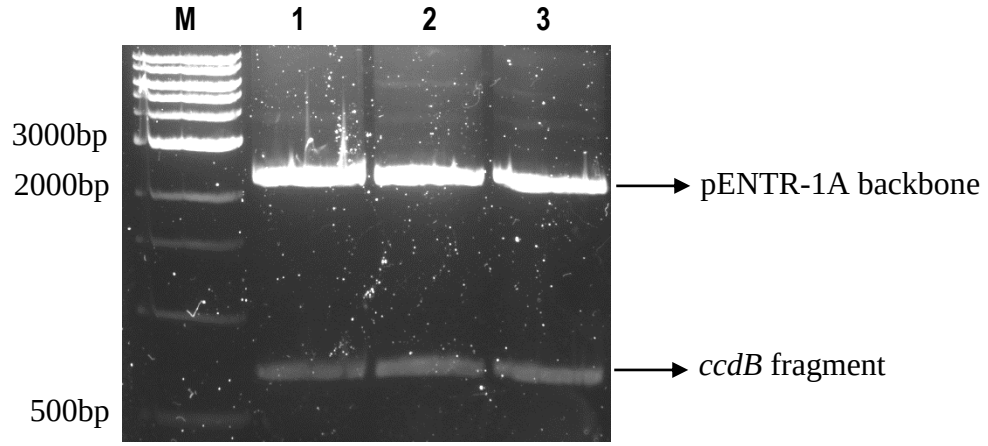

Figure 32: Agarose gel image of pENTR-1A products after BamHI and XhoI double digestion. Three samples were run in lanes 1 – 3.

3.4.3. Ligation of *An2*-pENTR-1A produced colonies

A ligation and heat-shock transformation was performed using the double digested *An2* insert and the purified pENTR-1A backbone, with the aim of inserting the gene of interest into the vector. Undigested pENTR-1A DNA and *E.coli* DH5α competent cells were used as negative controls. In total, 22 colonies were obtained. As the vector containing the *ccdB* gene should not be able to grow without insert, one expects any colonies to contain the insert of interest. No colonies grew on the negative control plates.

A colony PCR was performed on eight selected colonies with pENTR-1A primers that flank the point of expected insertion. Thus, one would expect products of approximately 2.76 kb if the gene was inserted correctly. Instead, each colony produced products of approximately 700bp (Figure 33). The product sizes were equal for all colonies.

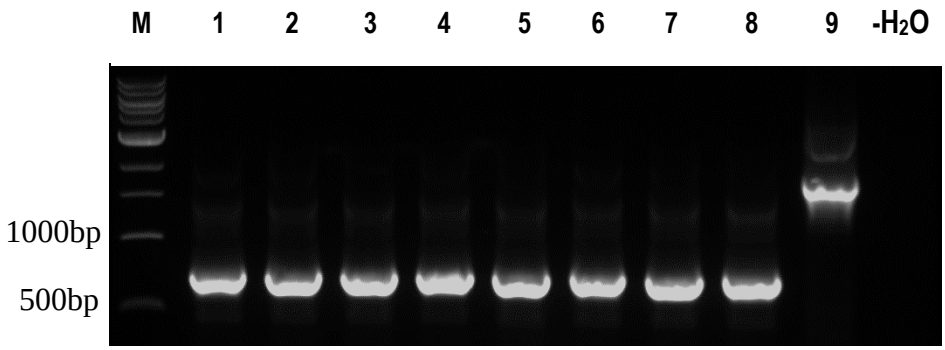

Figure 33: Colony PCR using pENTR- 1A primers on candidate *An2*-pENTR- 1A clones (samples 1 – 8). pENTR- 1A plasmid DNA was used as a point of comparison (sample 9). All candidate clones were shorter than expected.

The flanking *An2* primers - initially used to amplify the cDNA - were also used in the colony PCR and produced no products (data not shown). Colony PCRs were repeated with the same results.

Plasmid DNA was obtained from one of the colonies and this was sequenced using the pENTR-1A and the *An2* forward and reverse primers. Good sequence results were obtained using pENTR-1A primers, but nothing was obtained using the *An2* primers. The sequence results are summarised in Table 6, with the description, query cover, identity match and E value are all indicated. A nucleotide NCBI BLAST search (https://blast.ncbi.nlm.nih.gov/Blast.cgi) on the sequence results had top matches of 100% identity with *An2*.

Table 6: Top five BLAST results for pENTR-1A forward and reverse primers sequenced on plasmid DNA of a potential *An2*-pENTR-1A clone.

	Description	**Query Cover**	**Sequence Identity**	**E Value**
pENTR-1A fwd primer	*Zea mays kaurene synthase 2 (**an2**)*, mRNA	75%	100%	7^{-157}
	Zea mays full-length cDNA clone ZM_BFc0088O06 mRNA, complete cds	75%	100%	7^{-157}
	*Zea mays ent-copalyl diphosphate synthase (**An2**)* mRNA, complete cds	75%	100%	7^{-157}
	*Zea mays ent-copalyl diphosphate synthase (**An2**)* gene, complete cds	75%	100%	9^{-96}
	Vector **pENTR-1A**-NLS-LacZ, complete sequence	26%	94%	4^{-40}
pENTR-1A rvs primer	*Zea mays kaurene synthase 2 (**an2**)*, mRNA	81%	100%	0.0
	Zea mays full-length cDNA clone ZM_BFc0088O06 mRNA, complete cds	81%	100%	0.0
	*Zea mays ent-copalyl diphosphate synthase (**An2**)* mRNA, complete cds	81%	100%	0.0
	*Zea mays ent-copalyl diphosphate synthase (**An2**)* gene, complete cds	80%	100%	4^{-120}
	Cloning vector **pE6c***, complete sequence	15%	100%	4^{-25}

*pE6c is a Gateway vector and shares sequence homology with pENTR-1A

The sequence produced using the pENTR-1A forward and reverse primers aligned, indicating that only a small fragment of *An2* was inserted. A segment from 2090 – 2522bp of the *An2* sequence was shown to be inserted into the clone (433 bp). This fragment was near the 3' end

of *An2* cDNA (2.76 kb). Thus, the *An2* primers had nothing to hybridise to which explains why no products were produced in the colony PCR. pENTR-1A primers, meanwhile, match to the vector and span the point of insertion, so were able to produce a product. The fifth BLAST result for the forward and reverse primers matched to pENTR-1A and another Gateway vector, respectively (Table 6). Identity match was high, but query cover was low indicating the primers amplified a small region of pENTR-1A before the *An2* insert sequence.

The pENTR-1A were also used to generate sequence from pENTR-1A DNA that had not been digested. The pENTR-1A primers matched with 100% identity to the known pENTR-1A sequence. The *ccdB* gene was also present in the pENTR-1A sequenced DNA (data not shown) but was not detected in the sequences generated from *An2*-pENTR-1A. These results confirmed the pENTR-1A primers could be used to generate sequence, that *ccdB* gene was not present in the colonies, that a truncated version of *An2* had been inserted into Pentr-1A and that this was a fragment near the 3' end of the *An2* gene.

3.4.4. Attempted cloning produced truncated products despite troubleshooting

The cloning was repeated a number of times with several modifications, including different restriction enzymes, a different vector and various kits. A summary of the multiple attempts of cloning *An2* is shown under Table 7.

Table 7: Attempts to generate an entry clone of *An2* are shown, with the vector, restriction enzymes used, modification, number of colonies and the resulting PCR product size all indicated.

Attempt	Gateway Vector	Restriction enzymes	Modifications	Colonies	Colony PCR product size
1	pENTR-1A	XhoI, BamHI		22	-700bp (pENTR-1A primers) -no product (*An2* primers)
2	pENTR-1A	XhoI, BamHI	1. Dephosphorylated vector (using rSAP) 2. Increased *An2* insert DNA 3. Left ligation overnight	> 600 from 8 plates	-700bp (pENTR-1A primers)
3	pENTR-1A	XhoI, BamHI	1. Different PCR buffer including DMSO 2. Fresh pENTR-1A vector from glycerol stock 3. Column purification of insert instead of gel extraction	40	-700bp (pENTR-1A primers)
4	pENTR-1A	EcoR1 (on both sides of *ccdB*)	1. New primer pairs 2. New cDNA 3. New PCR reagents	20	-700bp (pENTR-1A primers)
5	TOPO TA	none	1. Different vector 2. No restriction digest 3. Forward primer with overhang designed for directional cloning	35	700bp (*An2* primers)
6	TOPO TA	none	1. Left out shaking step in transformation	9	700bp (GW1 and GW2 sequencing primers)

The pCR™8 TOPO® TA vector (Figure 3b) was also used, as indicated in Table 7. These vectors use topoisomerase activity to insert the gene of interest and therefore do not require restriction sites for cloning, eliminating a few variables. However, the colony PCR again showed products of the incorrect size. Some of the *An2* PCR product that had been gel extracted was run on a gel to determine if shearing had taken place, however, the product was of the expected 2.76kb size (data not shown).

3.4.5. Discussion of *An2* cloning

It was confirmed that only a small fragment of approximately 430bp of *An2* was inserted in the cloning vector. No negative plates produced colonies and all colonies always produced PCR products, albeit shorter-than-expected. Different restriction enzymes were used as well as a completely different vector, with the same result of truncated products. A potential reason for *An2* truncation could be due to degradation, however, it is unusual for each insert to degrade to the same size.

We hypothesize that it is extremely hard to clone the full cDNA of such large genes successfully. It is possible there are potential "weak" points in the genome with sequences that are prone to sheathing – which would explain why the truncated products were always the same size. Future work in terms of cloning *An2* could involve synthesizing the entire cDNA, or cloning the cDNA in two segments with restriction enzymes sites engineered so they can be ligated back together. It may also be useful to clone the putative kauralexin genes, *KS2* and *KO,* along with *An2* and transiently express them together as Fu et al. (2016) did in *Nicotiana benthamiana.* A comparison between transient single-gene expression and expression of all three genes may help clarify the relationship between the three kauralexin biosynthesis genes.

Chapter 4: Final Conclusion

The utility of *Ds*-transposon insertions was examined in this study and were found to knock-down, but not completely knock-out, gene expression when inserted into the fourth exon of *An2*. Significant differences in gene expression between *an2* mutants and wild type W22 were only found when *An2* was highly up-regulated, such as after *F. verticillioides*-inoculation (Figure 15). When overall *An2* expression was low, gene expression in *an2* mutants was not reduced at all as shown in the seedling and *C. zeina*-inoculation analyses (Figures 7, 10 & 28).

The effects of the *Ds*-insertions in *An2* were only determined after *F. verticillioides*-inoculation. It was shown that kauralexin accumulation was significantly reduced in *an2* mutants compared to W22 (Figure 13). The same trend was seen when analysing *An2* gene expression, with reduced expression in mutants again (Figure 15). Kauralexin accumulation and *An2* gene expression were highly correlated (r = 0.94). This all indicates that knocking down *An2* gene expression reduced kauralexin accumulation significantly, thereby indicating *An2* gene expression and kauralexin accumulation are positively linked. This validates the work of Harris et al. (2005) and Schmelz et al. (2011) who hypothesized that *An2* regulates kauralexin production. It also gives greater confidence in the currently utilised pathway of kauralexin biosynthesis (Figure 1).

Disease symptoms were analysed from each sample, with large noticeable differences in plant susceptibility across all samples despite the seeds being suspended in the same *F. verticillioides* inoculum. The inoculated *an2* mutants had less root and shoot tissue growth and more severe fungal symptoms than inoculated W22 (Figure 18). A scoring system was devised based on the phenotypic symptoms and significant differences were calculated, with *an2* mutants scoring the highest (Figure 19). Fungal load was also quantified by calculating fungal and plant DNA through qPCR. The amount of *F. verticillioides* DNA was greatest in the *an2* mutants, with a marked increase in comparison to inoculated W22 (means of 113.5 and 11.2 ng *F. verticillioides*/µg plant DNA, respectively) (Figure 20). However, the difference was not considered statistically significant due to the variability within the sample groups. The fungal load in inoculated *an2* mutant and W22 lines was correlated with kauralexin accumulation and *An2* expression and was found to have a perfect negative correlation (r = -1.00) in both cases.

Our initial hypothesis was that knocking down *An2* would decrease kauralexin accumulation and *An2* expression, which would lead to increased susceptibility to *F. verticillioides*. There is

a lot of support for this hypothesis. Decreased kauralexin accumulation and *An2* expression was confirmed in *an2* mutants compared to wild type. The mutants also appeared more susceptible to *F. verticillioides* using our scoring system and had vastly more fungus. Due to the non-significance of the fungal load results we cannot confirm that the mutants were more susceptible, however, the results do provide promising evidence that the reduction of antifungal kauralexin activity makes mutants more susceptible to fungi. We believe that significance will be found with a larger sample size. Unfortunately, only two *an2:an2* mutants were obtained for our study and therefore had to be combined with the knocked-down *AN2:an2*. A larger number of replicates would give greater statistical power.

The expression of *KS2* and *KO,* which have been shown to be co-regulated with *An2* (Christie et al., 2017), was also examined, with no significant differences between *an2* mutants and W22 (Figure 16). This suggests that knocking down *An2* has no impact on *KS2* and *KO*. It is possible a full knock-out of *An2* is required for *KS2* and *KO* expression to be impaired. Or, alternatively, *An2*, *KS2* and *KO* are co-expressed due to their sharing of common transcription factor binding sites rather than due to their positions in the kauralexin pathway (Figure 1a). Further gene paralogues of *KS2* and *KO* should also be examined to see whether they are effected by reduced *An2* expression.

A novel find was that total zealexin accumulation was significantly reduced in *an2* mutants compared to W22 following *F. verticillioides* inoculation (Figure 21). This has not been shown before and suggests some pathway conservation between kauralexins and zealexins, which has previously been proposed (Ejike et al., 2013). *TPS11* expression is thought to potentially induce zealexins accumulation (Huffaker et al., 2011), but no reduction of *TPS11* was seen in the mutants (Figure 17).

The free fatty acid precursors of oxylipins involved in JA biosynthesis were found to have differential accumulation in *F. verticillioides*-inoculated *an2* mutants (Figure S4). This provides evidence that the JA and *An2* signalling pathways are linked. JA, along with ET, has been shown to induce *An2* and kauralexins (Ejike et al., 2013; Schmelz et al., 2011). However, these results suggest that *An2* may also affect JA signalling, indicating the relationship may be reciprocal.

C. zeina-inoculation of *an2* mutants was also examined as an example of an alternative foliar pathogen. Leaf instead of root tissue was analysed in slightly older plants. Unfortunately, *An2* was not significantly induced in response to *C. zeina* in W22 at 14 (Figure 26) and 10 (Figure

28) dpi. This is despite fungus accumulating in inoculated *an2* mutants (Figures 30). We hypothesize the reason for this was due to the leaf flecking phenotype seen in W22 plants which may have induced SAR. W22 plants were grown under a number of environmental conditions in order to try prevent it, but this was unsuccessful as it is likely flecking is under genetic determination. Leaf flecking is thought to potentially modulate the JA pathway (Olukolu et al., 2016). As JA and *An2* appear to be linked, we believe this is a likely reason for low *An2* levels. The vast array of other signalling pathways induced after the broad-spectrum resistance conferred by leaf flecking may also affect *An2* expression. With regards to *F. verticillioides,* we inadvertently got around this via seed-inoculations and were able to inoculate the pathogen before the plant was able to produce a leaf flecking phenotype. Seed-inoculation was attempted with *C. zeina*, but was unsuccessful. This is unsurprising as *C. zeina* causes a foliar disease.

Our initial hypothesis that kauralexin accumulation would be reduced in mutants after *C. zeina*-inoculation was therefore not confirmed as kauralexin accumulation was too low, likely due to low *An2* expression. However, there was a small non-significant decrease in mutants (Figure 27). This trend was also apparent in zealexins (Figure S5). Fungal accumulation was greater in mutants compared to W22, but again not significant (Figure 30). Leaves also had more chlorotic spots than W22 (Figure 29), but no extreme difference. Overall, the *C. zeina*-inoculation show slight promise that *An2* knock-downs in maize may lead to decreased kauralexin accumulation and increased susceptibility, however, a different maize line should be used to examine this to avoid the effects of leaf flecking.

In order to further characterise *An2*, an attempt was made to clone it towards *A. thaliana* transformation for overexpression. This, along with future work cloning other genes in the kauralexin pathway, would have enabled us to examine if kauralexins could be produced in dicotyledons and confer increased resistance. Unfortunately, cloning was unsuccessful despite numerous attempts. Only a small segment of *An2* was able to be inserted into the expression vector. Thus, our initial hypothesis that kauralexins would be expressed and resistance conferred could not be proven or rejected.

For future work we suggest knocking out *An2* through RNAi gene silencing or CRISPR-Cas9. It would also be revealing to do a knock-out of the three putative kauralexin biosynthetic genes and examine kauralexin accumulation and susceptibility to both W22 and single *An2* knock-outs. This would help us further characterise *KS2* and *KO*, as well as their relationship with *An2*. We also suggest transiently co-expressing the three putative kauralexin biosynthesis genes

in *N. benthamiana*, as done by Fu et al. (2016) and examining if the transient clones display increased kauralexin accumulation.

Overall, this study looked to further characterise *An2* and its relationship with the putative kauralexin genes, *KS2* and *KO*, in different tissues and in response to two different fungal pathogens. The positive relationship between *An2* expression and kauralexin accumulation was shown. No differences in accumulation were found between kauralexin As and Bs. Accumulation of zealexins and JA-related phytochemicals in response to *F. verticillioides* were shown to be impacted by knocking-down *An2* which may be an area of further research. The loss in antifungal kauralexin activity did appear to make mutants more susceptible to *F. verticillioides* but more samples are needed to confirm this. Sample size was a limiting factor throughout this study. Despite this, there was promising evidence that *An2* plays an important and functional role in disease resistance, as reducing just the single gene had such a notable effect. Therefore, *An2* remains a promising avenue of research for the long-term goal of potentially utilising *An2* or other components of the kauralexin pathway in future resistance breeding.

References

Agrios, G. (2005). Plant Pathology. San Diego: Academic Press. p: 63 http://doi.org/10.1016/j.plantsci.2005.02.019

Ahern, K. R., Deewatthanawong, P., Schares, J., Muszynski, M., Weeks, R., Vollbrecht, E., Duvick, J., Brendel, V.P. Brutnell, T. P. (2009). Regional mutagenesis using Dissociation in maize. Methods, 49(3), 248–254. http://doi.org/10.1016/j.ymeth.2009.04.009

Ahuja, I., Kissen, R., & Bones, A. M. (2012). Phytoalexins in defense against pathogens. Trends in Plant Science, 17(2), 73–90. http://doi.org/10.1016/j.tplants.2011.11.002

Bacon, C. W., & Hinton, D. M. (1996). Symptomless endophytic colonization of maize by *Fusarium moniliforme*. Canadian Journal of Botany, 74(8), 1195–1202. http://doi.org/10.1139/b96-144

Bary, A. De. (2012). Fighting for their lives: Plants and pathogens. The Plant Cell, 24(6), tpc.112.tt0612. http://doi.org/10.1105/tpc.112.tt0612

E. Becker, C. Herrfurth, S. Irmisch, T.G. Ko, I. Feussner, P. Karlovsky, et al., Infection of corn ears by Fusarium spp. induces the emission of volatile sesquiterpenes, J. Agric. Food Chem. (2014), http://dx.doi.org/10.1021/ jf500560f.

Boutigny, A.L., Beukes, I., Small, I., Zühlke, S., Spiteller, M., Van Rensburg, B. J., Flett, B., Viljoen, A. (2012). Quantitative detection of Fusarium pathogens and their mycotoxins in South African maize. Plant Pathology, 61(3), 522–531. http://doi.org/10.1111/j.1365-3059.2011.02544.x

Candolara, A. N. S., Ertuzzi, T. E. B., & Arocco, A. D. M. (2008). Logistic Regression Modeling of Cropping Systems To Predict Fumonisin Contamination in Maize, 10433–10438.

Cartwright, D., Langcake, L., Pryce, R. J., Leworthy, D. P., & Ride, J. P. (1977). Chemical activation of host defence mechanisms as a basis for crop protection. Nature, 267(5611), 511–513. http://doi.org/10.1038/267511a0

Chakraborty, S., & Newton, a. C. (2011). Climate change, plant diseases and food security: an overview. Plant Pathology, 60(1), 2–14. http://doi.org/10.1111/j.1365-3059.2010.02411.x

Christensen, S. A., Huffaker, A., Kaplan, F., Sims, J., Ziemann, S., Doehlemann, G., Ji, L., Schmitz, R. J., Kolomiets, M. V., Alborn, H. T., Mori, N., Jander, G., Ni, X., Sartor, R. C., Byers, S., Abdo, Z., & Schmelz, E. A. (2015). Maize death acids, 9-lipoxygenase-derived cyclopente(a)nones, display activity as cytotoxic phytoalexins and transcriptional mediators. Proceedings of the National Academy of Sciences of the United States of America, 112(36), 11407–11412. http://doi.org/10.1073/pnas.1511131112

Christie, N., Myburg, A. A., Joubert, F., Murray, S. L., Carstens, M., Lin, Y.-C., Meyer, J., Crampton, B. G., Christensen, S. A., Ntuli, J. F., Wighard, S. S., Van de Peer, Y., & Berger, D. K. (2017). Systems genetics reveals a transcriptional network associated with susceptibility in the maize-grey leaf spot pathosystem. The Plant Journal, 89(4), 746–763. http://doi.org/10.1111/tpj.13419

Dangl, J. L., & Jones, J. D. G. (2001). Plant pathogens and integrated defence responses to infection. Nature, 411(June), 826–833.

Dash, S., Van Hemert, J., Hong, L., Wise, R. P., & Dickerson, J. a. (2012). PLEXdb: gene expression resources for plants and plant pathogens. Nucleic Acids Research, 40 (Database issue), D1194-201. http://doi.org/10.1093/nar/gkr938

Dicke, M., Van Beek, T. A., Posthumus, M. A., Ben Dom, N., Van Bokhoven, H., & De Groot, A. (1990). Isolation and identification of volatile kairomone that affects acarine predator-prey interactions. Journal of Chemical Ecology, 16(2), 381–396. http://doi.org/10.1007/BF01021772

Dooner, H. K., & He, L. (2008). Maize Genome Structure Variation: Interplay between Retrotransposon Polymorphisms and Genic Recombination. The Plant Cell, 20(February), 249–258. http://doi.org/10.1105/tpc.107.057596

Dorner, J. W., Cole, R. J., Sanders, T. H., & Blankenship, P. D. (1989). Interrelationship of kernel water activity, soil temperature, maturity, and phytoalexin production in preharvest aflatoxin contamination of drought-stressed peanuts. Mycopathologia, 105(2), 117–128. http://doi.org/10.1007/BF00444034

Ejike, C. E. C. C., Gong, M., & Udenigwe, C. C. (2013). Phytoalexins from the Poaceae: Biosynthesis, function and prospects in food preservation. Food Research International, 52(1), 167–177. http://doi.org/10.1016/j.foodres.2013.03.012

European Commission (EC), 2007. Commission Regulation (EC) No 1126/2007 of 28 September 2007 amending Regulation (EC) No 1881/2006 setting maximum levels for certain contaminants in foodstuffs as regards Fusarium toxins in maize and maize products. Official Journal of the European Union L255: 14-17.

Felix, G., Duran, J. D., Volko, S., & Boller, T. (1999). Plants have a sensitive perception system for the most conserved domain of bacterial flagellin. The Plant Journal, 18(3), 265–276. http://doi.org/10.1046/j.1365-313X.1999.00265.x

Felix, G., Regenass, M., & Boller, T. (1993). Specific perception of subnanomolar concentrations of chitin fragments by tomato cells: induction of extracellular alkalinization, changes in protein phosphorylation, and establishment of a refractory state. The Plant Journal, 4(2), 307–316. http://doi.org/10.1046/j.1365-313X.1993.04020307.x

Flett, B. C., McLaren, N. W., & Wehner, F. C. (1998). Incidence of Ear Rot Pathogens Under Alternating Corn Tillage Practices. Plant Disease, 82(7), 781–784. http://doi.org/10.1094/PDIS.1998.82.7.781

Fu, J., Ren, F., Lu, X., Mao, H., Xu, M., Degenhardt, J., Peters, R. J., & Wang, Q. (2016). A Tandem Array of ent -Kaurene Synthases in Maize with Roles in Gibberellin and More Specialized Metabolism. Plant Physiology, 170(2), 742–751. http://doi.org/10.1104/pp.15.01727

Gelderblom, W. C. A., Kriek, N. P. J., Marasas, W. F. O., & Thiel, P. G. (1991). Toxicity and carcinogenicity of the *Fusarium monilioforme* metabolite, fumonisin B1, in rats. Carcinogenesis, 12(7), 1247–1251. Retrieved from

http://www.scopus.com/inward/record.url?eid=2-s2.0-0025878789%7B&%7DpartnerID=tZOtx3y1

Gershenzon, J., & Dudareva, N. (2007). The function of terpene natural products in the natural world. Nature Chemical Biology, 3(7), 408–414. http://doi.org/10.1038/nchembio.2007.5

Hall, T. (1999). BioEdit: a user-friendly biological sequence alignment editor and analysis program for Windows 95/98/NT. Nucleic Acids Symposium Series. http://doi.org/citeulike-article-id:691774

Harris, L. J., Saparno, A., Johnston, A., Prisic, S., Xu, M., Allard, S., Kathiresan, A., Ouellet, T., & Peters, R. J. (2005). The maize *An2* gene is induced by *Fusarium* attack and encodes an ent-copalyl diphosphate synthase. Plant Molecular Biology, 59(6), 881–94. http://doi.org/10.1007/s11103-005-1674-8

Heisey, P. W., & Edmeades, G. O. (1998). World Maize Facts and Trends 1997 / 98 Maize Production in Drought-Stressed Environments: Technical Options and Research Resource Allocation. Agricultural Economics, CIMMYT. Retrieved from (www.cimmyt.mx)

Hellin, J., Shiferaw, B., Cairns, J. E., Reynolds, M. P., Ortiz-monasterio, I., Banziger, M., Sonder, K., & Rovere, R. La. (2012). Climate Change and Food Security in the Developing World: Potential of Maize and Wheat Research to Expand Options for Adaptation and Mitigation. Journal of Development and Agricultural Economics, 4(October), 311–321. http://doi.org/10.5897/JDAE11.112

Houseman, J. G., Campos, F., Thie, N. M. R., Philogene, B. J. R., Atkinson, J., Morand, P., & Arnason, J. T. (1992). Effect of the Maize-Derived Compounds DIMBOA and MBOA on Growth and Digestive Processes of European Corn Borer (Lepidoptera: Pyralidae). Journal of Economic Entomology, 85(3), 669–674. http://doi.org/10.1093/jee/85.3.669

Huffaker, A., Kaplan, F., Vaughan, M. M., Dafoe, N. J., Ni, X., Rocca, J. R., Alborn, H. T., Teal, P. E-A., & Schmelz, E. a. (2011). Novel acidic sesquiterpenoids constitute a dominant class of pathogen-induced phytoalexins in maize. Plant Physiology, 156(4), 2082–97. http://doi.org/10.1104/pp.111.179457

Jones, J. D. G., & Dangl, J. L. (2006). The plant immune system. Nature, 444(7117), 323–9. http://doi.org/10.1038/nature05286

J. Korsman, B. Meisel, F.J. Kloppers, B.G. Crampton, D.K. Berger, Quantitative phenotyping of grey leaf spot disease in maize using real-time PCR, Eur. J. Plant Pathol. 133 (2012) 461e471, http://dx.doi.org/10.1007/s10658-011- 9920-1.

Langenheim, J. H. (1994). Higher plant terpenoids: A phytocentric overview of their ecological roles. Journal of Chemical Ecology, 20(6), 1223–1280. http://doi.org/10.1007/BF02059809

Lanubile, A., Ferrarini, A., Maschietto, V., Delledonne, M., Marocco, A., & Bellin, D. (2014). Functional genomic analysis of constitutive and inducible defense responses to *Fusarium verticillioides* infection in maize genotypes with contrasting ear rot resistance. BMC Genomics, 15(1), 710. http://doi.org/10.1186/1471-2164-15-710

Latterell, F. M., & Rossi, A. E. (1983). Gray Leaf Spot of Corn: A Disease on the Move.

Lobell, D. B., Bänziger, M., Magorokosho, C., & Vivek, B. (2011). Nonlinear heat effects on African maize as evidenced by historical yield trials. Nature Climate Change, 1(1), 42–45. http://doi.org/10.1038/nclimate1043

Manoli, A., Sturaro, A., Trevisan, S., Quaggiotti, S., & Nonis, A. (2012). Evaluation of candidate reference genes for qPCR in maize. Journal of Plant Physiology, 169(8), 807–815. http://doi.org/10.1016/j.jplph.2012.01.019

Marasas, W. F. O., Riley, R. T., Hendricks, K. A., Stevens, V. L., Sadler, T. W., Gelineau-van Waes, J., Missmer, S. A., Cabrera, J., Torres, O., Gelderblom, W. C. A., Allegood, J., Martinez, C., Maddox, J., Miller, J. D., Starr, L., Sullards, M. C., Roman, A. V., Voss, K. A., Wang, E., & Merrill, A. H. (2004). Fumonisins disrupt sphingolipid metabolism, folate transport, and neural tube development in embryo culture and in vivo: a potential risk factor for human neural tube defects among populations consuming fumonisin-contaminated maize. The Journal of Nutrition, 134(4), 711–6. http://doi.org/10.1104/pp.103.029694.quality

Martin, D. M., Gershenzon, J., & Bohlmann, J. (2003). Induction of Volatile Terpene Biosynthesis and Diurnal Emission by Methyl Jasmonate in Foliage of Norway Spruce 1, 132, 1586–1599. http://doi.org/10.1104/pp.103.021196.some

Meisel, B., Korsman, J., Kloppers, F. J., & Berger, D. K. (2009). *Cercospora zeina* is the causal agent of grey leaf spot disease of maize in southern Africa. European Journal of Plant Pathology, 124(4), 577–583. http://doi.org/10.1007/s10658-009-9443-1

Mellon, J. A. Y. E., & West, C. A. (1979). Diterpene Biosynthesis in Maize Seedlings in Response to Fungal Infection, Plant Physiology, 406–410.

Meyer, J., Murray, S. L., & Berger, D. K. (2016). Signals that stop the rot: Regulation of secondary metabolite defences in cereals. Physiological and Molecular Plant Pathology, 94, 156–166. http://doi.org/10.1016/j.pmpp.2015.05.011

Miller, J. D. (2014). Factors That Affect the Occurrence of Fumonisin. Environmental Health Perspectives, 109(2), 321–324.

Murashige, T., & Skoog, F. (1962). A Revised Medium for Rapid Growth and Bio Agsays with Tohaoco Tissue Cultures. Physiol. Plant, 15(3), 473–497. http://doi.org/10.1111/j.1399-3054.1962.tb08052.x

Ncube, E., Flett, B. C., Waalwijk, C., & Viljoen, A. (2011). *Fusarium spp*. and levels of fumonisins in maize produced by subsistence farmers in South Africa. South African Journal of Science, 107(1/2), 1–7. http://doi.org/10.4102/sajs.v107i1/2.367

Ntuli, J., Murray, S.L. (2016). Characterisation of Phytoalexin Accumulation in Maize Inoculated with *Cercospora Zeina*, the Causal Organism of Grey Leaf Spot Disease. M.Sc Dissertation. University of Cape Town.

Nicolaisen, M., Suproniene, S., Nielsen, L. K., Lazzaro, I., Spliid, N. H., & Justesen, A. F. (2009). Real-time PCR for quantification of eleven individual Fusarium species in cereals. Journal of Microbiological Methods, 76(3), 234–240. http://doi.org/10.1016/j.mimet.2008.10.016

Oerke, E.-C. (2006). Crop losses to pests. The Journal of Agricultural Science, 144(1), 31. http://doi.org/10.1017/S0021859605005708

Olukolu, B. A., Bian, Y., De Vries, B., Tracy, W. F., Wisser, R. J., Holland, J. B., & Balint-Kurti, P. J. (2016). The Genetics of Leaf Flecking in Maize and Its Relationship to Plant Defense and Disease Resistance. Plant Physiology, 172(3), 1787–1803. http://doi.org/10.1104/pp.15.01870

Oren, L., Ezrati, S., Cohen, D., Sharon, A. (2003). Early Events in the *Fusarium verticillioides* -Maize Interaction Characterized by Using a Green Fluorescent Protein-Expressing Transgenic Isolate. Applied and environmental microbiology, 69(3), 1695–1701. http://doi.org/10.1128/AEM.69.3.1695

Poland, J. A., Balint-Kurti, P. J., Wisser, R. J., Pratt, R. C., & Nelson, R. J. (2009). Shades of gray: the world of quantitative disease resistance. Trends in Plant Science, 14(1), 21–29. http://doi.org/10.1016/j.tplants.2008.10.006

Rasmann, S., Köllner, T. G., Degenhardt, J., Hiltpold, I., Toepfer, S., Kuhlmann, U., Gershenzon, J., & Turlings, T. C. (2005). Recruitment of entomopathogenic nematodes by insect-damaged maize roots. Nature, 434(7034), 732–737. http://doi.org/nature03451 [pii]\r10.1038/nature03451

Rheeder, J. P., Marasas, W. F. O., Thiel, P. G., W, S. E., Shephard, G. S., & Van Schalkwyk, D. J. (1992). Fusarium moniliforme and Fumonisins in Corn in Relation to Human Esophageal Cancer in Transkei. Phytopathology, 82(3), 353. http://doi.org/10.1094/Phyto-82-353

Ryals, J. A, Neuenschwander, U. H., Willits, M. G., Molina, A., Steiner, H. Y., & Hunt, M. D. (1996). Systemic Acquired Resistance. The Plant Cell, 8(10), 1809–1819. http://doi.org/10.1105/tpc.8.10.1809

Sambrook, J., Fritsch, E. F., & Maniatis, T. (1989). Molecular Cloning: A Laboratory Manual. Cold Spring Harbor laboratory press. New York.

Schmelz, E. a, Kaplan, F., Huffaker, A., Dafoe, N. J., Vaughan, M. M., Ni, X., Rocca, J. R. Alborn, H. T., & Teal, P. E. (2011). Identity, regulation, and activity of inducible diterpenoid phytoalexins in maize. Proceedings of the National Academy of Sciences of the United States of America, 108(13), 5455–60. http://doi.org/10.1073/pnas.1014714108

Sekhon, R. S., Lin, H., Childs, K. L., Hansey, C. N., Buell, C. R., de Leon, N., & Kaeppler, S. M. (2011). Genome-wide atlas of transcription during maize development. The Plant Journal : For Cell and Molecular Biology, 66(4), 553–63. http://doi.org/10.1111/j.1365-313X.2011.04527.x

Shephard, G. S., Marasas, W. F. O., Burger, H.-M., Somdyala, N. I. M., Rheeder, J. P., Van der Westhuizen, L., … Van Schalkwyk, D. J. (2007). Exposure assessment for fumonisins in the former Transkei region of South Africa. Food Additives and Contaminants, 24(June), 621–629. http://doi.org/10.1080/02652030601101136

Shiferaw, B., Prasanna, B. M., Hellin, J., & Bänziger, M. (2011). Crops that feed the world 6. Past successes and future challenges to the role played by maize in global food security. Food Security. http://doi.org/10.1007/s12571-011-0140-5

Shimada, T. L., Shimada, T., & Hara-Nishimura, I. (2010). A rapid and non-destructive screenable marker, FAST, for identifying transformed seeds of Arabidopsis thaliana. The Plant Journal, 61(3), 519–528. http://doi.org/10.1111/j.1365-313X.2009.04060.x

Singh, R. P., Hodson, D. P., Huerta-Espino, J., Jin, Y., Bhavani, S., Njau, P., Herrera-Foessel, S., Singh P. K., Singh, S., & Govindan, V. (2011). The Emergence of Ug99 Races of the Stem Rust Fungus is a Threat to World Wheat Production. Annual Review of Phytopathology, 49(1), 465–481. http://doi.org/10.1146/annurev-phyto-072910-095423

Small, I. M., Flett, B. C., Marasas, W. F. O., McLeod, A., & Viljoen, A. (2012). Use of resistance elicitors to reduce Fusarium ear rot and fumonisin accumulation in maize. Crop Protection, 41, 10–16. http://doi.org/10.1016/j.cropro.2012.05.016

Sobolev, V. S. (2008). Localized Production of Phytoalexins by Peanut (*Arachis hypogaea*) Kernels in Response to Invasion by *Aspergillus* Species. Journal of Agricultural and Food Chemistry, 56(6), 1949–1954. http://doi.org/10.1021/jf703595w

South Africa Yearbook 2015/2016: Agriculture, Forestry and Fisheries. Government Communication and Information System. (2016)

Svitashev, S., Schwartz, C., Lenderts, B., Young, J. K., & Mark Cigan, A. (2016). Genome editing in maize directed by CRISPR–Cas9 ribonucleoprotein complexes. Nature Communications, 7, 13274. http://doi.org/10.1038/ncomms13274

Ueno, Y., Iijima, K., Wang, S.-D., Sugiura, Y., Sekijima, M., Tanaka, T., Chen, C., & Yu, S.-Z. (1997). Fumonisins as a possible contributory risk factor for primary liver cancer: A 3-year study of corn harvested in Haimen, China, by HPLC and ELISA. Food and Chemical Toxicology, 35(12), 1143–1150. http://doi.org/10.1016/S0278-6915(97)00113-0

van der Linde, K., Kastner, C., Kumlehn, J., Kahmann, R., & Doehlemann, G. (2011). Systemic virus-induced gene silencing allows functional characterization of maize genes during biotrophic interaction with *Ustilago maydis*. New Phytologist, 189(2), 471–483. http://doi.org/10.1111/j.1469-8137.2010.03474.x

Van Etten, H. D., Mansfield, J. W., Bailey, J. A., & Farmer, E. E. (1994). Two Classes of Plant Antibiotics: Phytoalexins versus "Phytoanticipins." The Plant Cell, 6(9), 1191–1192. http://doi.org/10.1105/tpc.6.9.1191

Vandesompele, J., Preter, K. De, Poppe, B., Roy, N. Van, & Paepe, A. De. (2002). Accurate normalization of real-time quantitative RT -PCR data by geometric averaging of multiple internal control genes, Genome Biology 3 (7)

Vaughan, M. M., Huffaker, A., Schmelz, E. A., Dafoe, N. J., Christensen, S., Sims, J., Martins, V. F., Swerbilow, J. Romero, M., Alborn, H. T., Allen, L.H., & Teal, P. E. A. (2014). Effects of elevated [CO2] on maize defence against mycotoxigenic Fusarium verticillioides. Plant, Cell and Environment, 37(12), 2691–2706. http://doi.org/10.1111/pce.12337

Vaughan, M. M., Christensen, S., Schmelz, E. A., Huffaker, A., Mcauslane, H. J., Alborn, H. T., Romero, M., Allen, L.H., & Teal, P. E. A. (2015). Accumulation of terpenoid phytoalexins in maize roots is associated with drought tolerance. Plant, Cell & Environment, 38(11), 2195–2207. http://doi.org/10.1111/pce.12482

Vaughan, M. M., Huffaker, A., Schmelz, E. A., Dafoe, N. J., Christensen, S. A., McAuslane, H. J., Alborn, H. T., Allen, L.H., & Teal, P. E. A. (2016). Interactive Effects of Elevated [CO2] and Drought on the Maize Phytochemical Defense Response against Mycotoxigenic Fusarium verticillioides. PLOS ONE, 11(7), e0159270. http://doi.org/10.1371/journal.pone.0159270

Vollbrecht, E., Duvick, J., Schares, J. P., Ahern, K. R., Deewatthanawong, P., Xu, L., Conrad, L. J., Kikuchi, K., Kubinec, T. A., Hall, B. D., Weeks, R., Unger-Wallace, E., Muszynski, M., Brendel V. P., & Brutnell, T. P. (2010). Genome-Wide Distribution of Transposed Dissociation Elements in Maize. The Plant Cell, 22(6), 1667–1685. http://doi.org/10.1105/tpc.109.073452

Vontimitta, V., Olukolu, B. A., Penning, B. W., Johal, G., & Balint-Kurti, P. J. (2015). The genetic basis of flecking and its relationship to disease resistance in the IBM maize mapping population. Theoretical and Applied Genetics, 128(11), 2331–2339. http://doi.org/10.1007/s00122-015-2588-8

Ward, J. M. J., Laing, M. D., & Cairns, A. L. P. (1997). Management Practices to Reduce Gray Leaf Spot of Maize. Crop Science, 37(4), 1257. http://doi.org/10.2135/cropsci1997.0011183X003700040038x

Ward, J. M. J., Stromberg, E. L., & Nowell, D. C. (1999). Gray Leaf Spot: A Disease of Global Importance in Maize Production. Plant Disease, 83(10).

Wighard, S.S., Murray, S.L. (2014). Characterisation of phytoalexin accumulation in maize: an investigation into key kauralexin biosynthetic genes. BSc (Hons) Thesis. University of Cape Town.

Wisser, R. J., Kolkman, J. M., Patzoldt, M. E., Holland, J. B., Yu, J., Krakowsky, M., Nelson, R. J., & Balint-Kurti, P. J. (2011). Multivariate analysis of maize disease resistances suggests a pleiotropic genetic basis and implicates a GST gene. Proceedings of the National Academy of Sciences, 108(18), 7339–7344. http://doi.org/10.1073/pnas.1011739108

Wotton, H. R., & Strange, R. N. (1987). Increased susceptibility and reduced phytoalexin accumulation in drought-stressed peanut kernels challenged with *Aspergillus flavus*. Applied and Environmental Microbiology, 53(2), 270–3. Retrieved from http://www.ncbi.nlm.nih.gov/pubmed/3105455

Wu, Z., Song, L., & Huang, D. (2011). Food Grade Fungal Stress on Germinating Peanut Seeds Induced Phytoalexins and Enhanced Polyphenolic Antioxidants. Journal of Agricultural and Food Chemistry, 59(11), 5993–6003. http://doi.org/10.1021/jf200776w

Supplementary Data

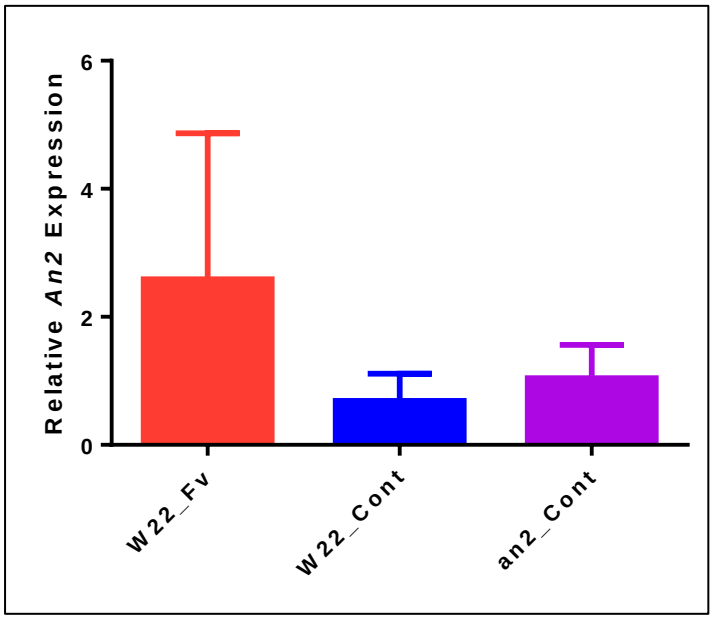

Figure S1: RT-qPCR showing *An2* expression in the roots of W22_Fv, W22_Cont and *an2*_Cont (mean + s.d., n = 2-5). Reactions run in triplicate. Gene expression was normalised to *LUG*, *MEP* and *UBCP*. W22_Cont and *an2*_Cont displayed similar expression levels, indicating healthy mock-inoculated *an2* mutants did not have knocked down *An2* expression in roots at low levels. There was no significant difference between samples (one-way ANOVA, p = 0.16).

Table S1: The corkscrew root appearance and root redness was quantified by measuring the length of the corkscrew root and the diameter of roots that were red. Values were given as; **0**: none; **1**: 0 – 1 cm; **2**: 1 – 2cm; **3**: 2 – 3cm. Values of 1 were given for overall root truncation, overall shoot truncation, leaf one truncation and leaf senescence. All sample selected for further analysis are indicated in bold, including the three *AN2:an2* mutants.

Genotype	Sample no.	Corkscrew Root	Root redness	Root truncation	Shoot truncation	Leaf one truncation	Leaf senescence	Total
W22	**3**	**1**	**1**	**1**	**0**	**0**	**1**	**4**
W22	**6**	**0**	**1**	**1**	**0**	**0**	**1**	**3**
W22	**13**	**0**	**1**	**0**	**1**	**1**	**1**	**4**
AN2:an2	**5**	**2**	**2**	**1**	**1**	**1**	**0**	**7**
AN2:an2	**7**	**2**	**3**	**1**	**1**	**1**	**0**	**8**
AN2:an2	**10**	**3**	**3**	**1**	**1**	**1**	**1**	**10**
an2:an2	**8**	**3**	**3**	**1**	**1**	**1**	**1**	**10**
an2:an2	**15**	**2**	**3**	**1**	**1**	**1**	**1**	**9**
AN2:an2	2	2	1	1	0	0	1	5
AN2:an2	4	1	2	1	1	0	0	5
AN2:an2	9	1	1	1	1	1	1	6
AN2:an2	11	2	2	1	1	1	1	8
AN2:an2	12	2	2	1	1	0	1	7
AN2:an2	14	0	2	1	0	1	1	5
AN2:an2	16	1	0	1	1	1	1	5
AN2:an2	17	2	1	1	0	1	0	5
AN2:an2	18	3	0	1	0	0	0	4

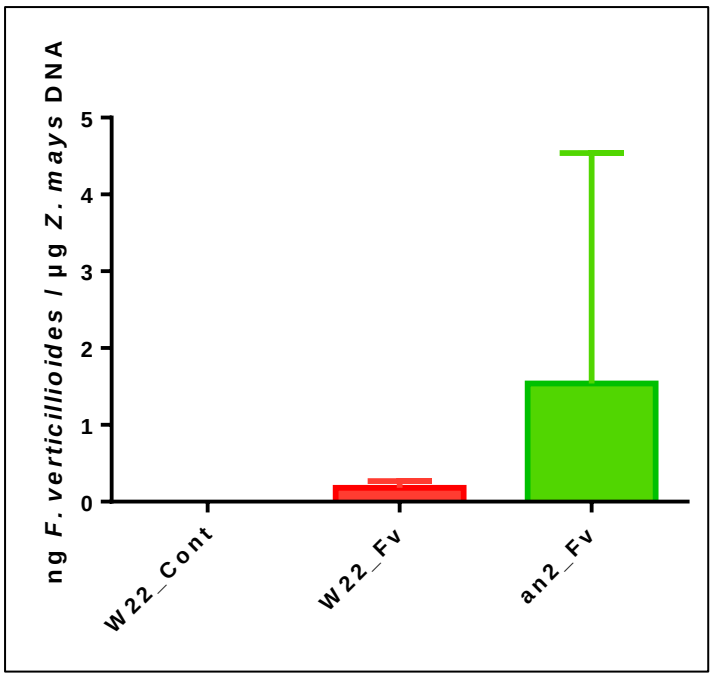

Figure S2: Fungal biomass in shoots was calculated through qPCR with the ratio of *F. verticillioides* fungal DNA (*EF1α*) to maize DNA (*LUG*) displayed (mean + s.d.; n = 3 – 5). No fungus was detected in W22_Cont. There was a low amount present in W22_Fv and more in *an2*_Fv, however, variation was extremely large. Overall fungal levels were far lower than in roots with no significant differences found (one-way ANOVA, p = 0.55).

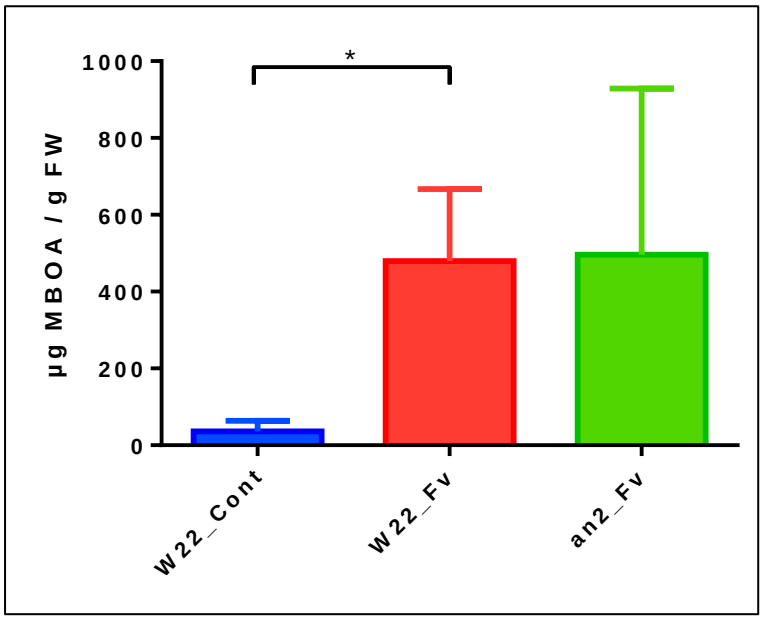

Figure S3: GC-MS profiling detected accumulation of 6-mthoxy-benzoxazolin-2-one (MBOA). Normalised to the internal control ^{13}C-linolenic acid. W22_Fv displayed significant accumulation of MBOA compared to W22_Cont (student's t test, p = 0.02). There was no difference between W22_Fv and *an2*_Fv.

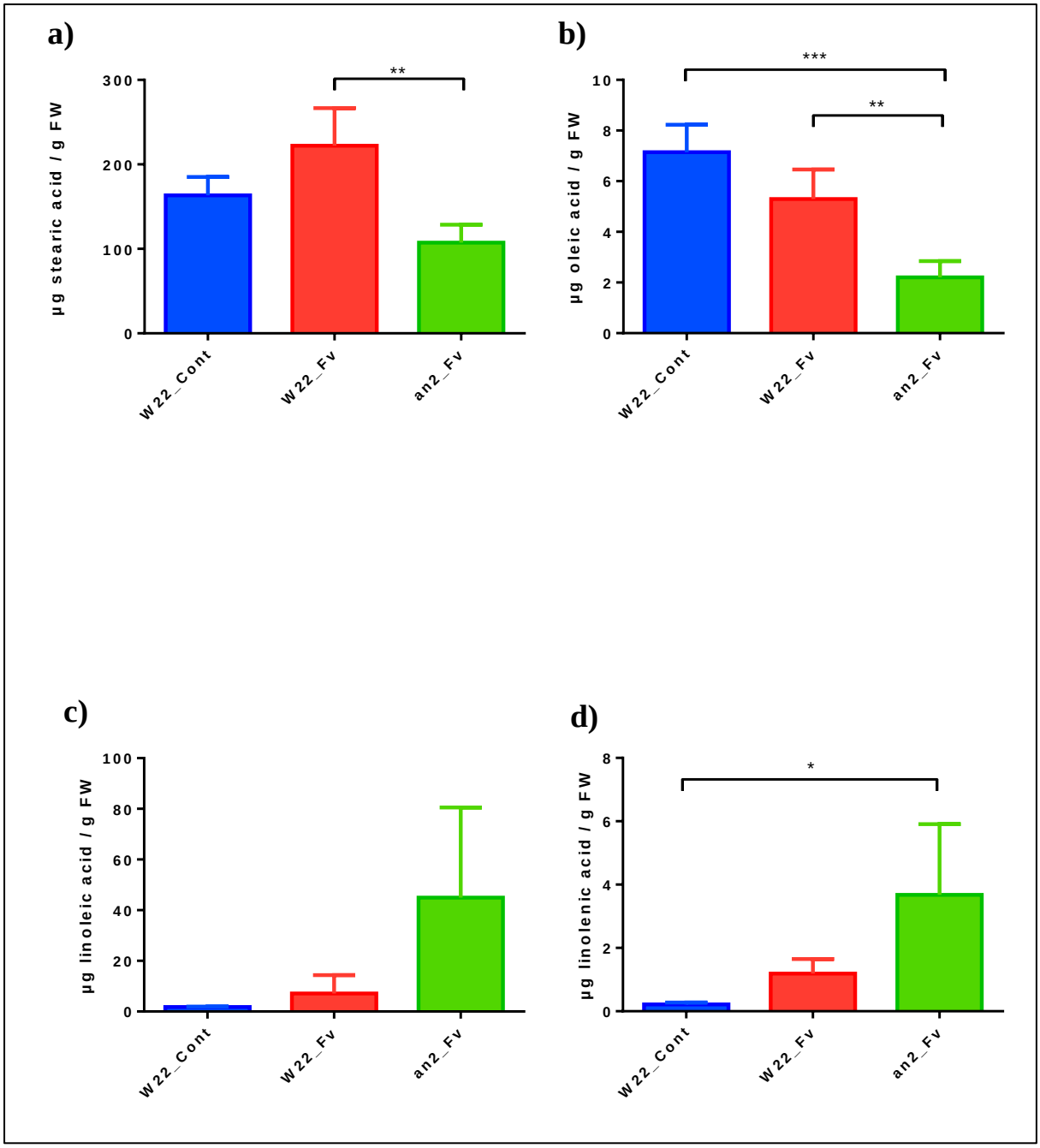

Figure S4: Metabolic profiling of the free fatty acid precursors of oxylipins, stearic, oleic, linoleic and linolenic acid through GC-MS profiling. There are significant decreases in *an2*_Fv in **a)** stearic and **b)** oleic acid, while there are notable increased in *an2*_Fv in **c)** linoleic and **d)** linolenic acid. One-way ANOVA illustrated significant differences between groups in stearic, oleic and linolenic acid. Tukey's HSD post hoc test was performed. Asterisks indicate significant differences (* $p < 0.05$, ** $p < 0.01$, *** $p < 0.001$).

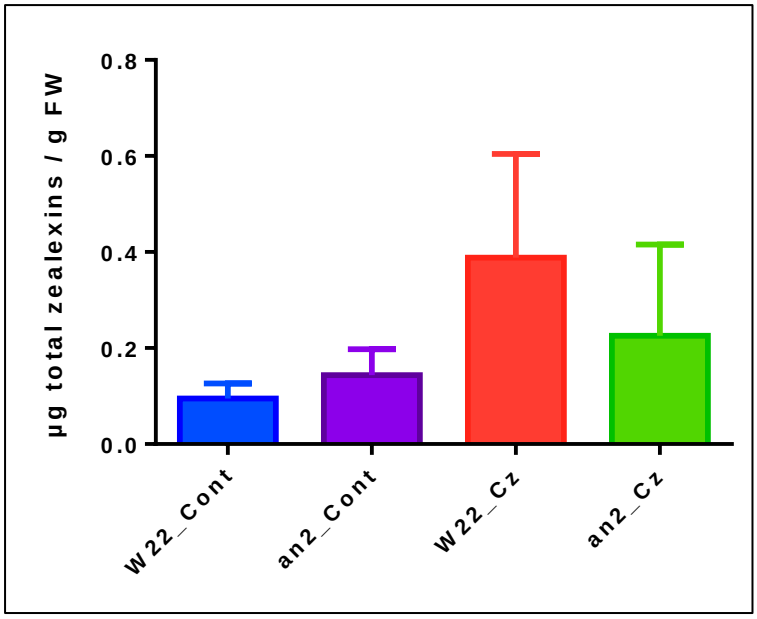

Figure S5: The sum of the mean of zealexins A1 and B1. Determined through GC-MS profiling and normalised to the internal control to get µg.g^{-1} FW. No significant differences were found (one-way ANOVA, p = 0.34). There was a small decrease in *an2*_Cz compared to W22_Cz.